Supramolecular self-associating amphiphiles as aqueous pollutant scavengers

Rebecca J. Ellaby, Lisa J. White, Jessica E. Boles, Sena Ozturk and Jennifer R. Hiscock*

Table of contents

Chemical structures

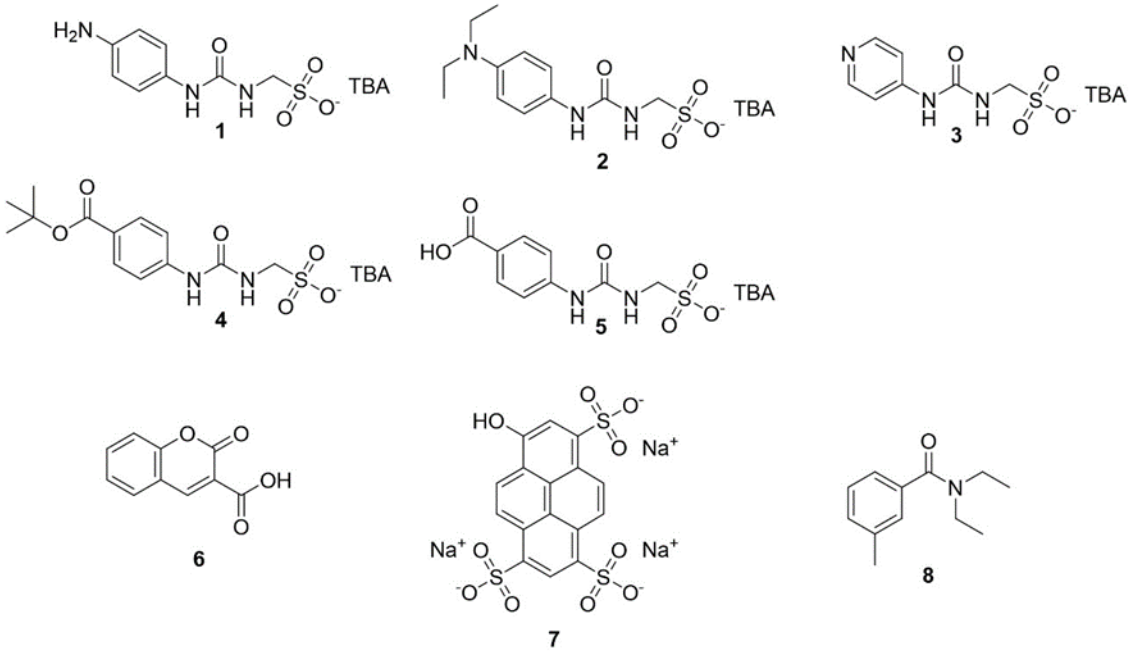

Figure S1: Chemical structures of compounds **1**-**8**.

Table S1 – Molecular components of the co-formulations ***a***-***l***.

Co-formulation	SSA	Co-formulant
a	**1**	**6**
b	**2**	**6**
c	**3**	**6**
d	**5**	**6**
e	**1**	**7**
f	**2**	**7**
g	**3**	**7**
h	**5**	**7**
i	**1**	**8**
j	**2**	**8**
k	**3**	**8**
l	**5**	**8**

Experimental

General experimental

A positive pressure of nitrogen and oven dried glassware were used for all reactions. All solvents and starting materials were purchased from known chemical suppliers or available stores and used without any further purification unless specifically stipulated. The NMR spectra were obtained using a Burker AV2 400 MHz or AVNEO 400 MHz spectrometer. The data was processed using Topspin

software. NMR Chemical shift values are reported in parts per million (ppm) and calibrated to the centre of the residual solvent peak set (s = singlet, br = broad, d = doublet, t = triplet, q = quartet, m = multiplet). Tensiometry measurements were undertaken using the Biolin Scientific Theta Attension optical tensiometer. The data was processed using Biolin OneAttension software. A Hamilton (309) syringe was used for the measurements. The melting point for each compound was measured using Stuart SMP10 melting point apparatus. High resolution mass spectrometry was performed using a Bruker microTOF-Q mass spectrometer and spectra recorded and processed using Bruker's Compass Data Analysis software. Infrared spectra were obtained using a Shimadzu IR-Affinity-1 model Infrared spectrometer. The data are analysed in wavenumbers (cm^{-1}) using IRsolution software. Dynamic Light Scattering (DLS) and Zeta Potential studies were obtained using an Anton Paar Litesizer™ 500 and processed using KalliopeTM Professional or using a Malvern Zetasizer Nano ZS. Fluorescence intensity measurements were obtained using a Clariostar plus plater reader using MARS data analysis software.

Tensiometry studies

All the samples were prepared in a EtOH:H_2O (1:19) solution. All samples underwent an annealing process in which the various solutions were heated to approximately 40 °C before being allowed to cool to room temperature, allowing each sample to reach a thermodynamic minimum. All samples were prepared through serial dilution of the most concentrated sample. Three surface tension measurements were obtained for each sample at a given concentration, using the pendant drop method. These average values were then used to calculate the critical aggregation concentration (CAC).

DLS studies

All the samples were prepared in series with an aliquot of the most concentrated solution undergoing serial dilution. Sample sizes were kept to 1 mL. All solvents used for DLS studies were filtered to remove particulates from the solvents. Samples were heated to approximately 40 °C before being allowed to equilibrate for 1 hour at room temperature. A series of 10 'runs' were performed with each sample at 25 °C to give enough data to derive an appropriate average. In some instances, the raw correlation data indicated that a greater amount of time may be needed for the samples to reach a stable state. For this reason, only the last 9 or 8 'runs' were included in the average size distribution calculations.

Zeta potential studies

All solvents used for Zeta potential studies were filtered to remove particulates from the solvents. Samples were heated to approximately 40 °C, before being allowed equilibrate at room temperature for 1 hour. A series of 10 'runs' were performed with each sample at 25 °C to give enough data to derive an appropriate average. In some instances, the raw correlation data indicated that a greater amount of time may be needed for the samples to reach a stable state. For this reason, only the last 9 'runs' were included in the average size distribution calculations.

High-resolution mass spectrometry studies

Chemical samples were dissolved in HPLC-grade methanol at a concentration of 1 mg/mL before being further diluted 1 in 100 in methanol. 10 µL of the sample was injected into a flowing stream of 10 mM ammonium acetate in 95% methanol in water (flow rate: 0.02 mL/min) and the flow directed into the electrospray source of the mass spectrometer. Mass spectra were acquired in the negative ion mode and data processed in Bruker's Compass Data Analysis software.

Quantitative ^{1}H NMR studies

Initially, to enable characterisation of those SSA self-associated species present within the solution state, quantitative ^{1}H NMR techniques are used to confirm the presence of larger self-associated species, after an annealing process in which the sample was heated to approximately 40 °C before being allowed to cool to room temperature. Here comparative integration against an

internal standard is used to calculate the proportion of a molecular component visible using standard solution state NMR techniques. The proportion of a molecular component that appears 'lost' from a solution is assumed to form larger higher-order self-associated structures with solid-like properties, thus rendering them NMR inactive. These studies enable the elucidation of the proportion of any secondary molecular substituents involved in the construction of these larger higher order species.

Co-formulation preparation

The appropriate aliquot of SSA (**1**-**5**) or co-formulant (**6**-**8**) were weighed out into a vial, the appropriate solvent mixture added, the vial sealed and the resultant solution subjected to an annealing process in which the sample was heated up to approximately 40 °C before being allowed to cool to room temperature.

Co-formulant uptake studies

A series of quantitative ^{1}H NMR studies were conducted over a time period of 24 hours after the addition of one equivalent of the co-formulant to the SSA. With the first time point being 20 minutes post the addition of the co-formulant solution, the subsequent time points are 12 hours and 24 hours. These time points were chosen to identify if there is any loss of signal which would indicate the uptake of the co-formulant by the SSAs into the larger self-associated aggregates that they are known to form. These experiments were conducted in a 5% EtOH/D_2O solution, with the exception of **co-formulations *i*-*l*** which were conducted in a D_2O/ 1% acetonitrile solution, this was to allow for accurate comparative integration of both internal standard and compound peaks. All co-formulants were also studied individually in the same solvent system to ensure that they themselves do not exhibit the formation of larger self-associated species, and that any 'loss' of signal is due to the uptake of the co-formulant by the SSA. These studies showed no co-formulant loss of signal, indicating that there are no larger aggregated species present in solution. Here we can see that there is a loss of co-formulant in every experiment conducted. The results also show that the amount of co-formulant signal lost stays relatively the same from the first ^{1}H NMR to the ^{1}H NMR 24 hours after the solutions were mixed, this is indicative of co-formulant uptake by the SSAs.

Here the original SSA and co-formulant stock solutions was prepared individually at a concentration of 11.12 mM, in an appropriate solvent mixture. The SSA stock solution then underwent an annealing process in which the sample was heated to approximately 40 °C before being allowed to cool back to room temperature, thus ensuring the sample had reached a thermodynamic minimum. The SSA stock solution (0.5 mL) was then added to an NMR tube, followed by the addition of 0.5 mL of the appropriate co-formulant solution, this time point was taken as T=0.This experiment was conducted at a 1:1 molar ratio of SSA:co-formulant (5.56 mM).

Chemical synthesis

Compound 1: This compound was synthesized in line with our previously published method.[1] ^{1}H NMR (400 MHz, 298.15 K, DMSO-d_6): δ: 0.93 (t, *J* = 7.3 Hz, 12H), 1.26 - 1.35 (m, 8H), 1.52 - 1.60 (m, 8H), 3.14 - 3.18 (m, 8H), 3.81 (d, *J* = 5.8 Hz, 2H), 4.63 (s, 2H), 6.17 (t, *J* = 5.7 Hz, 1H), 6.45 (d, *J* = 8.7 Hz, 2H), 6.99 (d, *J* = 8.6 Hz, 2H), 8.22 (s, 1H).

Compound 2: This compound was synthesized in line with our previously published method.[2] ^{1}H NMR (400 MHz, 298.15 K, DMSO-d_6): δ: 0.92-1.06 (m, 18H), 1.29 - 1.35 (m, 8H), 1.56 - 1.59 (m, 8H), 3.15 - 3.27 (m, 12H), 3.84 (d, *J* = 5.8 Hz, 2H), 6.22 (t, *J* = 5.6 Hz, 1H), 6.59 (d, *J* = 9.0 Hz, 2H), 7.14 (d, *J* = 9.0 Hz, 2H), 8.34 (s, 1H).

Compound 3: Aminomethanesulfonic acid (0.22 g, 2.0 mM) was dissolved in tetrabutylammonium hydroxide in methanol (2.0 mL, 2.0 mM) and taken to dryness. Triphosgene (0.30 g, 1.0 mM) was added to 4-aminopyridine (0.39 g, 2.0 mM) and triethylamine (1.83 mL, 6.0 mM) in ethyl acetate (30 mL) and left to stir at RT under an inert atmosphere for 4 hours. Tetrabutylammonium aminomethanesulfonate (2.0 mM) was dissolved in ethyl acetate (10 mL) and added to a stirring solution of the isocyanate in ethyl acetate (30 mL), refluxed at 60 °C under an inert atmosphere overnight. The resultant precipitate was recrystallised with ethyl acetate to give a white solid with a yield of 63.5 % (0.60 g, 1.27 mM). Melting point: > 200 °C ; ^{1}H NMR (400 MHz, 298.15 K, DMSO-d_6): δ: 0.93 (t, *J* = 7.3 Hz, 12H), 1.26 - 1.35 (m, 8H), 1.53 - 1.61 (m, 8H), 3.14 - 3.18 (m, 8H), 3.87 (d, *J* = 5.9 Hz, 2H), 6.67 (s, 1H), 7.33 (d, *J* = 6.4 Hz, 2H), 8.27 (d, *J* = 6.2 Hz, 2H), 9.22 (s, 1H); ^{13}C{^{1}H} NMR (100 MHz, 298.15 K, DMSO-d_6): δ: 13.6 (CH_3), 19.7 (CH_2), 23.5 (CH_2), 56.3 (CH_2), 58.0 (CH_2), 112.3 (ArCH), 147.9 (ArC), 150.0 (ArCH), 154.5 (C=O); IR (film): ν = 3275 (NH stretch), 1694, 1244, 1167, 878; HRMS for the sulfonate-urea ion ($C_7H_8N_3O_4S^-$) (ESI$^-$): m/z: act: 230.8784 $[M]^-$ cal: 230.2185 $[M]^-$.

Compound 4: Aminomethanesulfonic acid (0.22 g, 2.0 mM) was dissolved in tetrabutylammonium hydroxide in methanol (2.0 mL, 2.0 mM) and taken to dryness. Triphosgene (0.30 g, 1.0 mM) was added to *tert*-butyl-4-aminobenzoate (0.39 g, 2.0 mM) in ethyl acetate (30 mL) and left to stir at 60 °C under an inert atmosphere for 4 hours. Tetrabutylammonium aminomethanesulfonate (2.0 mM) was dissolved in ethyl acetate (10 mL) and added to a stirring solution of the isocyanate in ethyl acetate (30 mL), refluxed at 60 °C under an inert atmosphere overnight. The organic phase was then twice washed with H_2O (20 mL) and the organic layer taken to dryness to give a brown oil with a yield of 80.5 % (0.92 g, 1.60 mM). Melting Point: 68 °C; ^{1}H NMR (400 MHz, 298 K, DMSO-d_6): δ: 0.94 (t, *J* = 7.3 Hz, 12H), 1.26 - 1.34 (m, 8H), 1.50 - 1.61 (m, 17H), 3.15 - 3.19 (m, 8H), 3.88 (d, *J* = 5.8 Hz, 2H), 6.63 (s, 1H), 7.47 (d, *J* = 8.8 Hz, 2H), 7.76 (d, *J* = 8.8 Hz, 2H), 9.15 (s, 1H); ^{13}C{^{1}H} NMR (100 MHz, 298 K, DMSO-d_6): δ: 13.5 (CH_3), 19.2 (CH_2), 23.06 (CH_2), 27.9 (CH_3), 55.9 (CH_2), 57.5 (CH_2), 79.8 (C), 116.5 (ArCH), 123.4 (ArC), 130.0 (ArCH), 144.9 (ArC), 154.2 (C=O), 164.8 (C=O); IR (film): ν = 3280 (NH stretch), 1695, 1219, 1157, 858; HRMS for the sulfonate-urea ion ($C_{13}H_{15}N_2O_6S^-$) (ESI$^-$): m/z: act: 164.0026 $[M - H]^{2-}$, cal: 164.0107 $[M - H]^{2-}$.

Compound 5: Trifluoroacetic acid (2 mL) was added to a stirring solution of compound **4** (0.20 g, 0.39 mM) in dichloromethane (5 mL) and left at RT for 30 minutes. Sodium hydroxide (6 M) was added dropwise until a neutral pH was reached. The resultant precipitate removed by filtration to give the pure product as a white solid with a yield of 79.5 % (0.16 g, 0.31 mM). Melting point: 90 °C ; ^{1}H NMR (400 MHz, 298 K, DMSO-d_6): δ: 0.93 (t, *J* = 7.3 Hz, 12H), 1.26 - 1.35 (m, 8H), 1.53 - 1.60 (m, 8H), 3.14 - 3.18 (m, 8H), 3.87 (d, *J* = 5.8 Hz, 2H), 6.58 (s, 1H), 7.46 (d, *J* = 8.7 Hz, 2H), 7.80 (d, *J* = 8.8 Hz, 2H), 9.15 (s, 1H), 12.49 (s, 1H); ^{13}C{^{1}H} NMR (100 MHz, 298 K, DMSO-d_6): δ: 13.6 (CH_3), 19.2 (CH_2), 23.1 (CH_2), 56.2 (CH_2), 57.5 (CH_2), 115.9 (ArCH), 129.7 (ArCH), 133.2 (ArC), 141.4 (ArC), 157.8 (C=O), 170.0 (C=O); IR (film): ν = 3278 (NH stretch), 1697, 1220, 1163, 881; HRMS for the sulfonate-urea ion ($C_9H_7N_2O_6S^-$) (ESI$^-$): m/z: act: 164.0107 $[M - H]^{2-}$ cal: 164.0370 $[M- H]^{2-}$.

NMR charicterisation

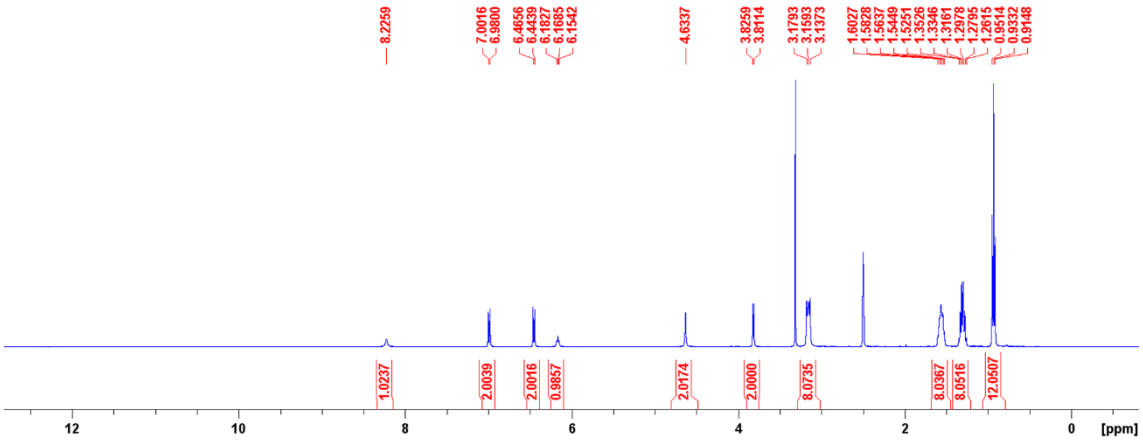

Figure S2- ^{1}H NMR of compound **1** in DMSO-d_6 conducted at 298 K.

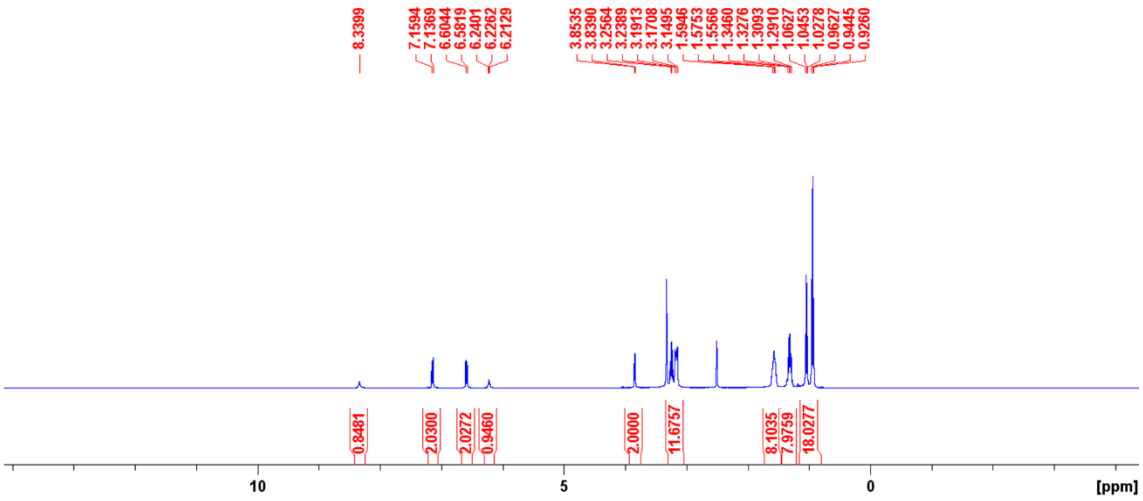

Figure S3 - ^{1}H NMR of compound **2** in DMSO-d_6 conducted at 298 K.

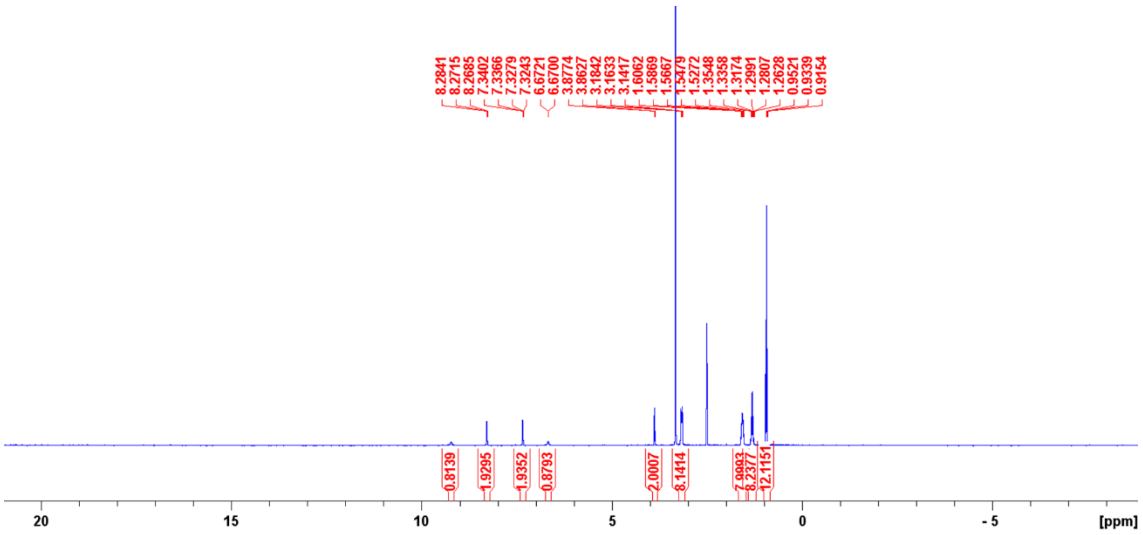

Figure S4 - ^{1}H NMR of compound **3** in DMSO-d_6 conducted at 298 K.

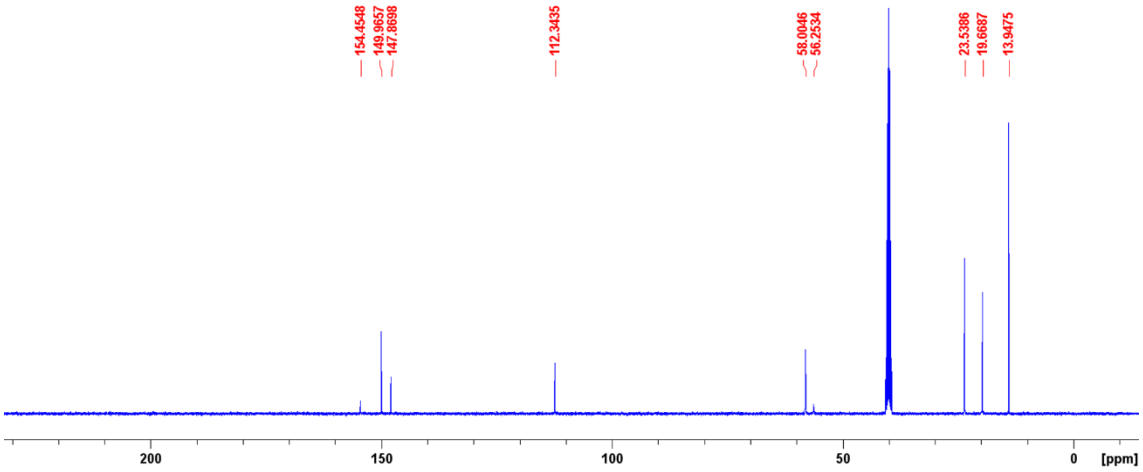

Figure S5 - ^{13}C{^{1}H} NMR of compound **3** in DMSO-d_6 conducted at 298 K

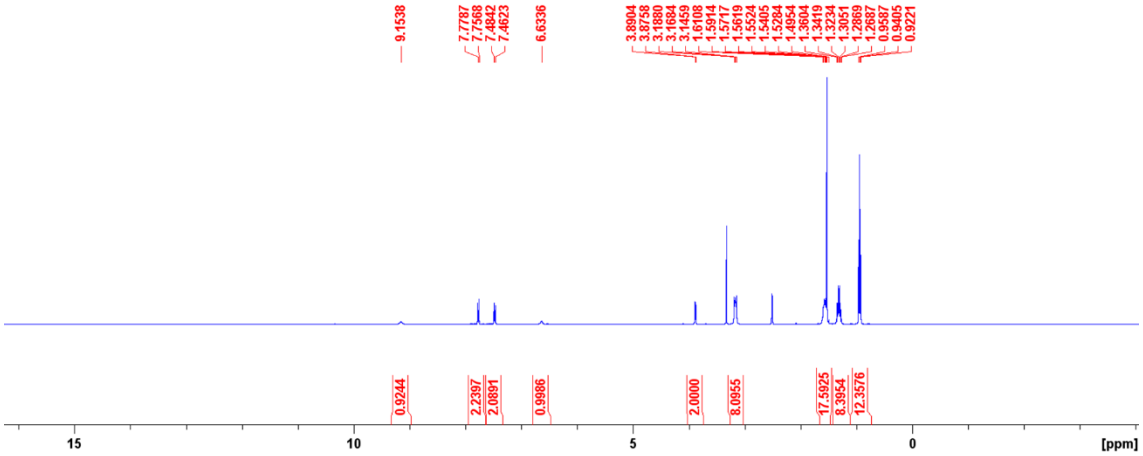

Figure S6 - ^{1}H NMR of compound **4** in DMSO-d_6 conducted at 298 K.

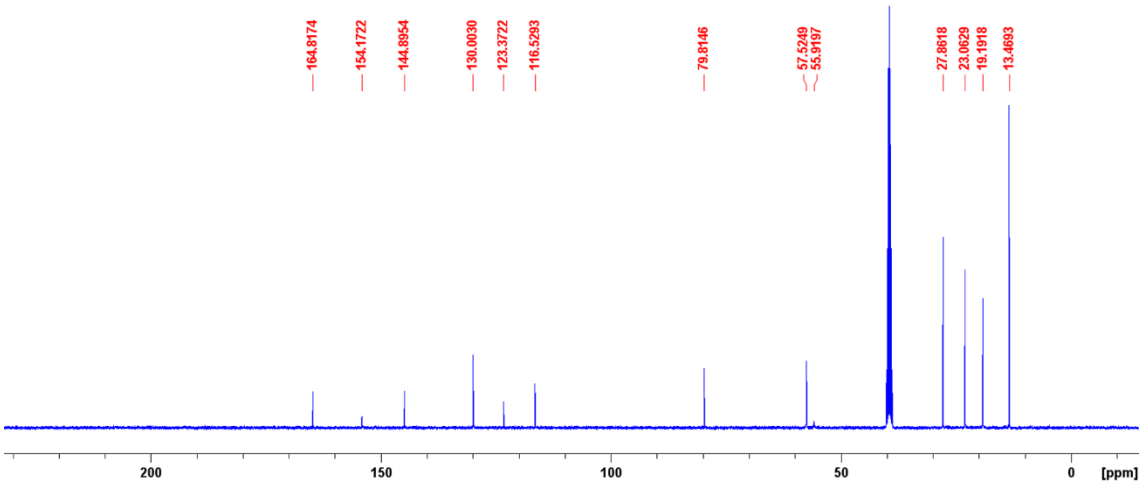

Figure S7 – ^{13}C{^{1}H} NMR of compound **4** in DMSO-d_6 conducted at 298 K

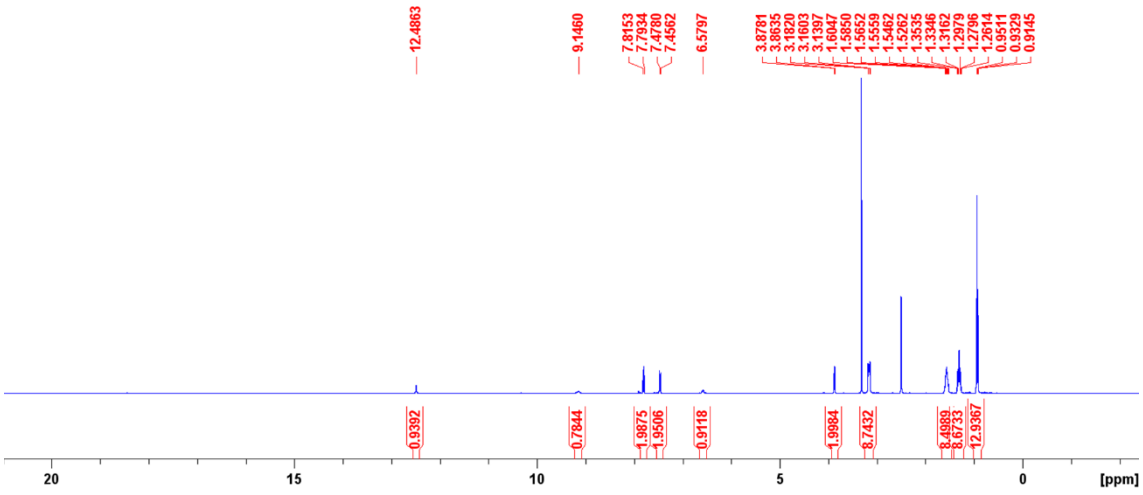

Figure S8 - ^{1}H NMR of compound **5** in DMSO-d_6 conducted at 298 K.

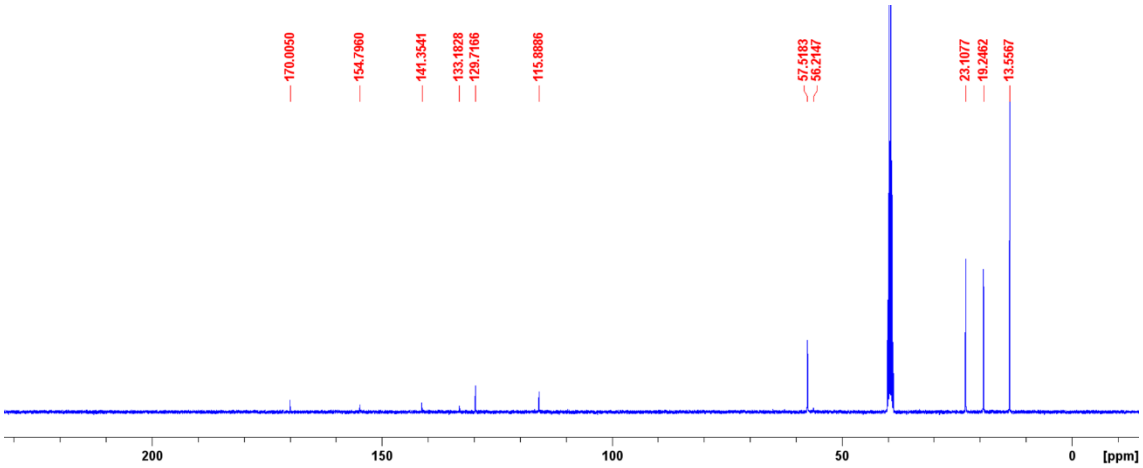

Figure S9 - ^{13}C{^{1}H} NMR of compound **5** in DMSO-d_6 conducted at 298 K

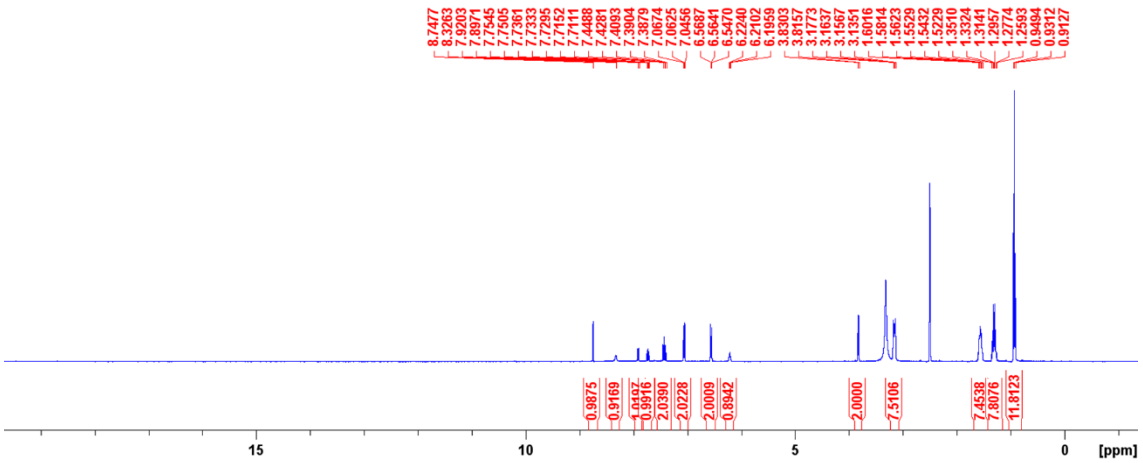

Figure S10 - ^{1}H NMR of compound **Co-formulation *a*** in DMSO-d_6 conducted at 298 K.

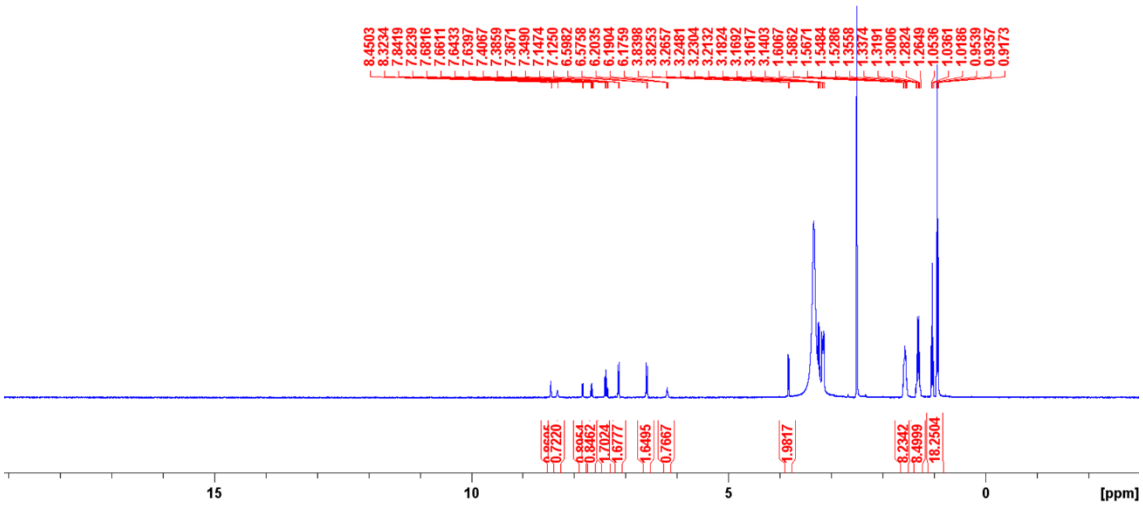

Figure S11 – ^{1}H NMR of compound **Co-formulation *b*** in DMSO-d_6 conducted at 298 K. Multiplet at 3.14-3.27 ppm could not be accurately integrated due to overlap with H_2O peak.

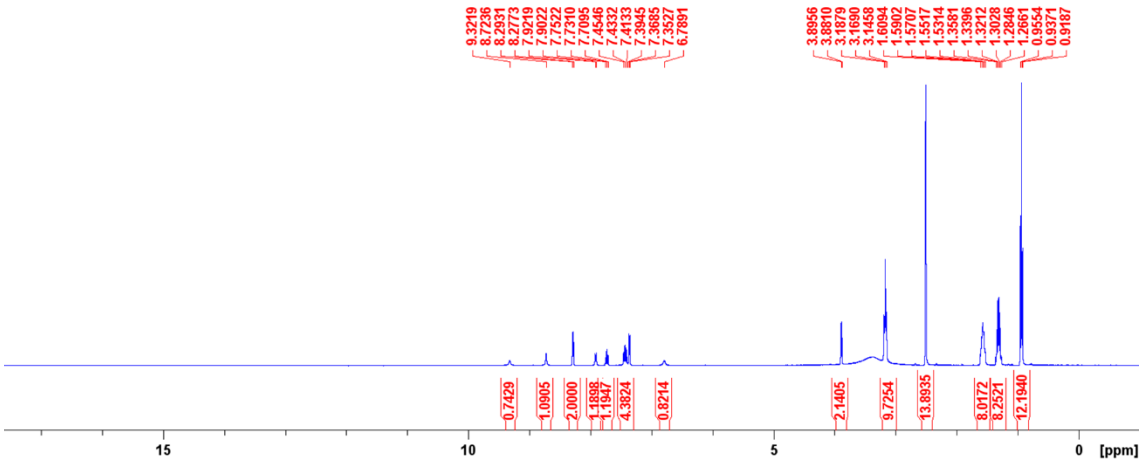

Figure S12 - ^{1}H NMR of compound **Co-formulation *c*** in DMSO-d_6 conducted at 298 K. Multiplet at 3.14-3.19 ppm integrates for 2H higher than expected due to overlap with H_2O peak.

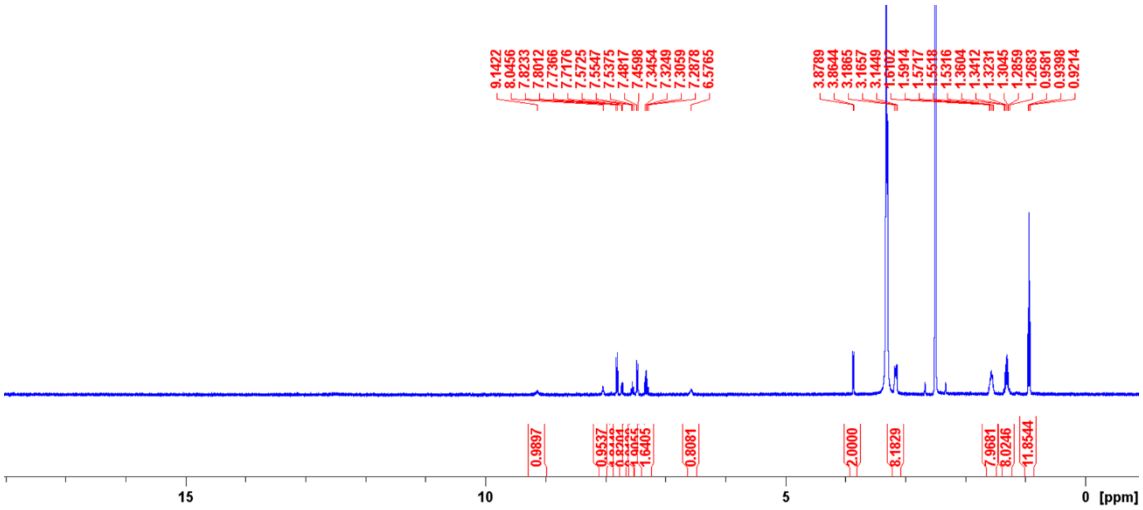

Figure S13 - ^{1}H NMR of compound **Co-formulation *d*** in DMSO-d_6 conducted at 298 K.

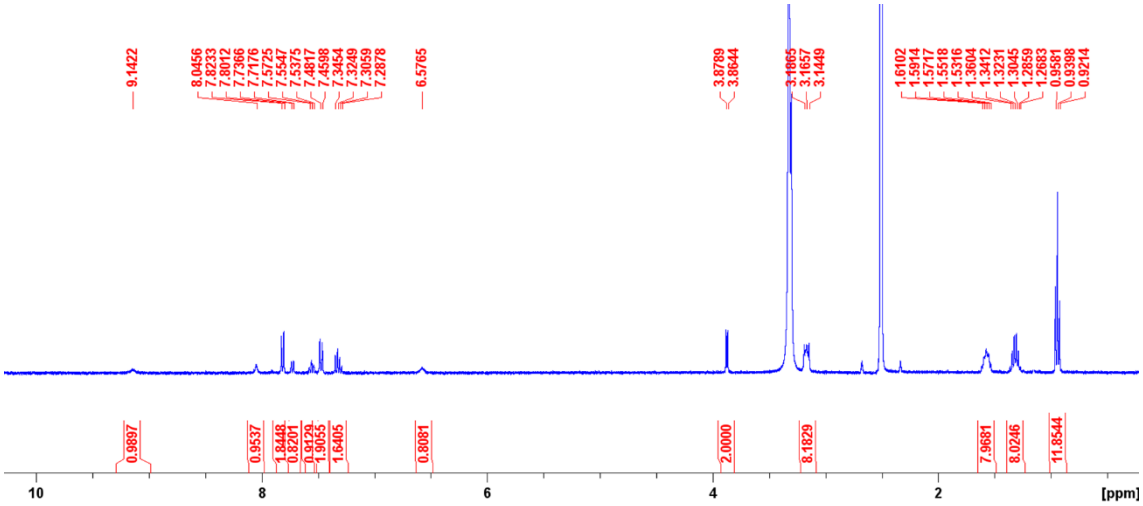

Figure S14 – Zoomed in ^{1}H NMR of compound **Co-formulation *d*** in DMSO-d_6 conducted at 298 K.

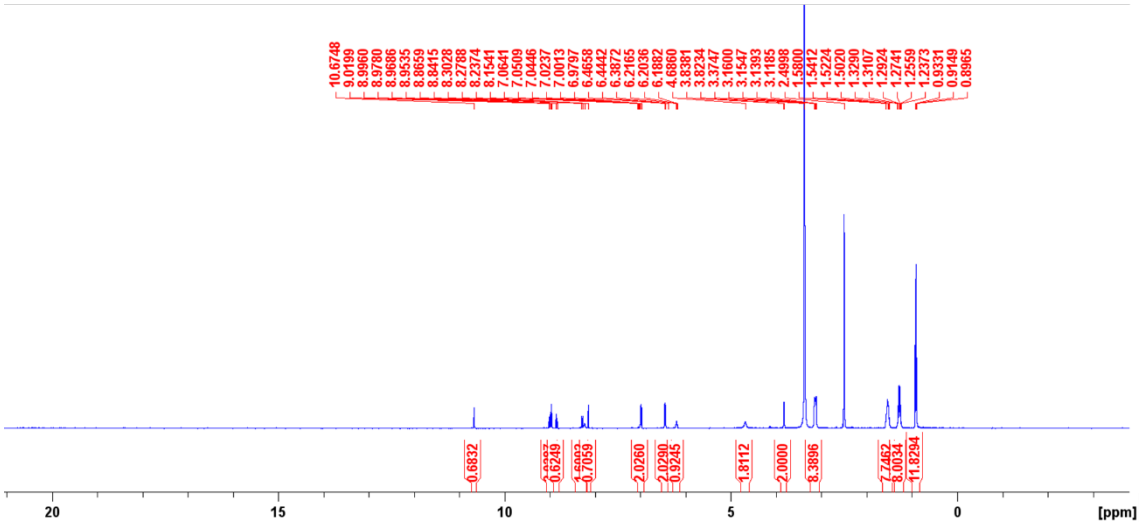

Figure S15 - ^{1}H NMR of compound **Co-formulation *e*** in DMSO-d_6 conducted at 298 K.

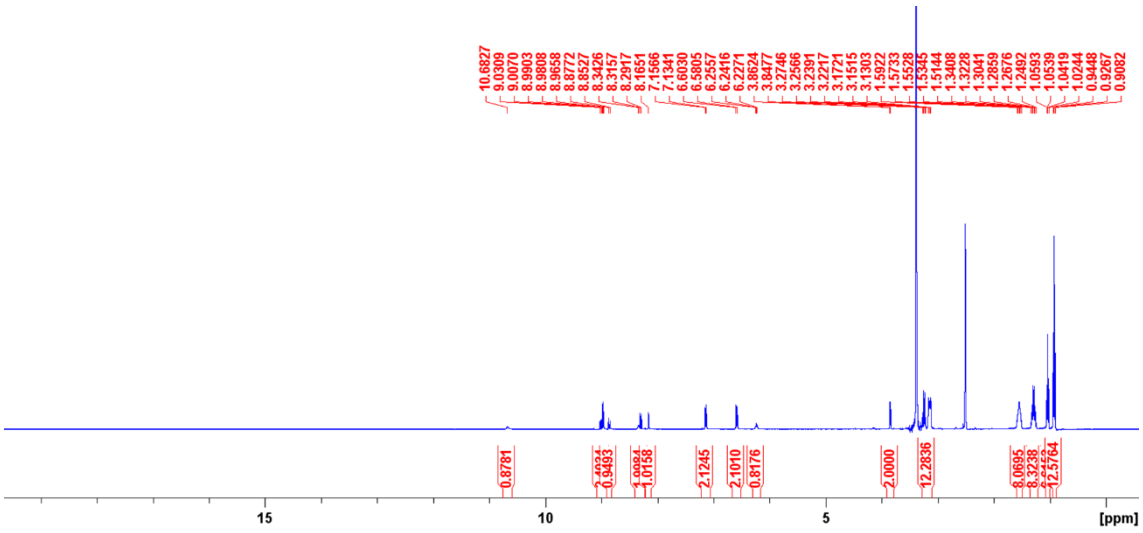

Figure S16 - ^{1}H NMR of compound **Co-formulation *f*** in DMSO-d_6 conducted at 298 K.

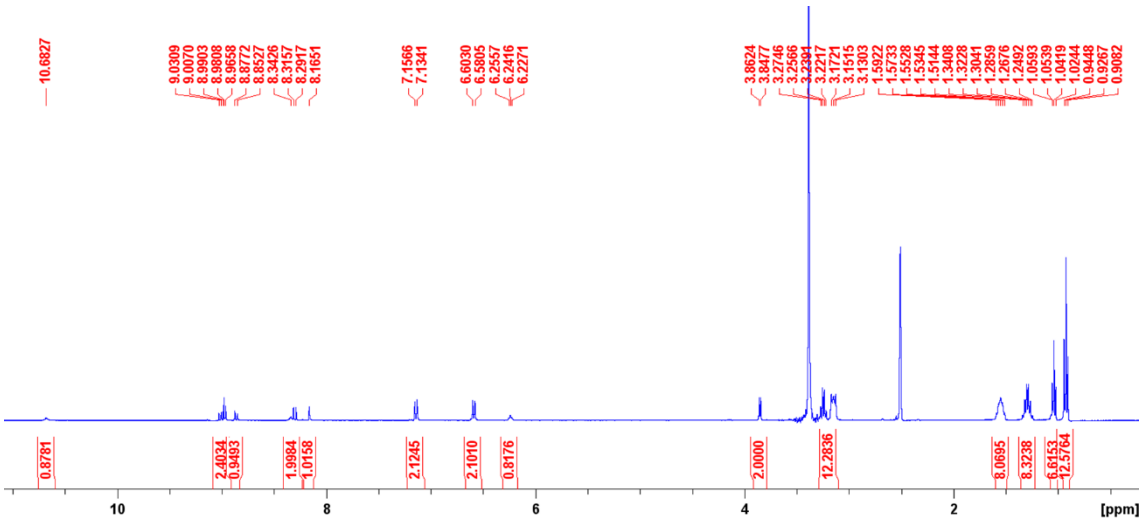

Figure S17 – Zoomed in ^{1}H NMR of compound **Co-formulation *f*** in DMSO-d_6 conducted at 298 K.

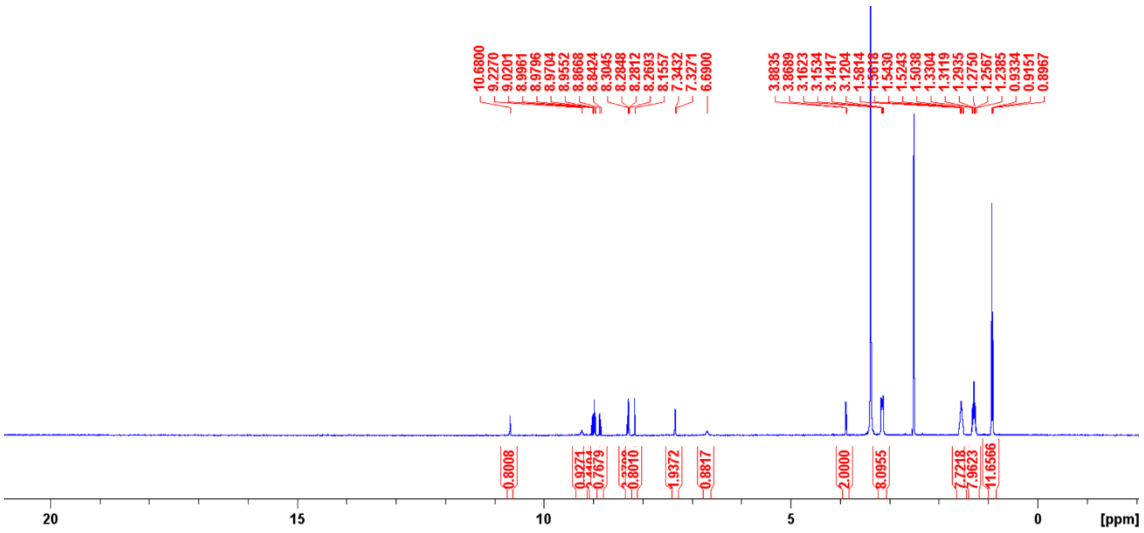

Figure S18 - ^{1}H NMR of compound **Co-formulation *g*** in DMSO-d_6 conducted at 298 K.

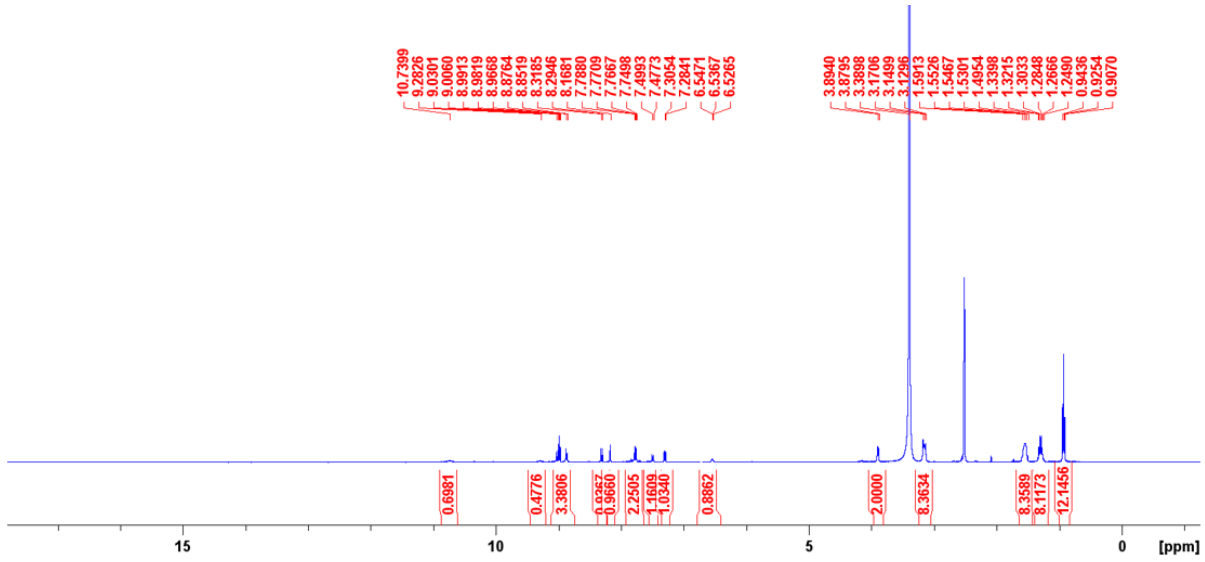

Figure S19 - ^{1}H NMR of compound **Co-formulation *h*** in DMSO-d_6 conducted at 298 K.

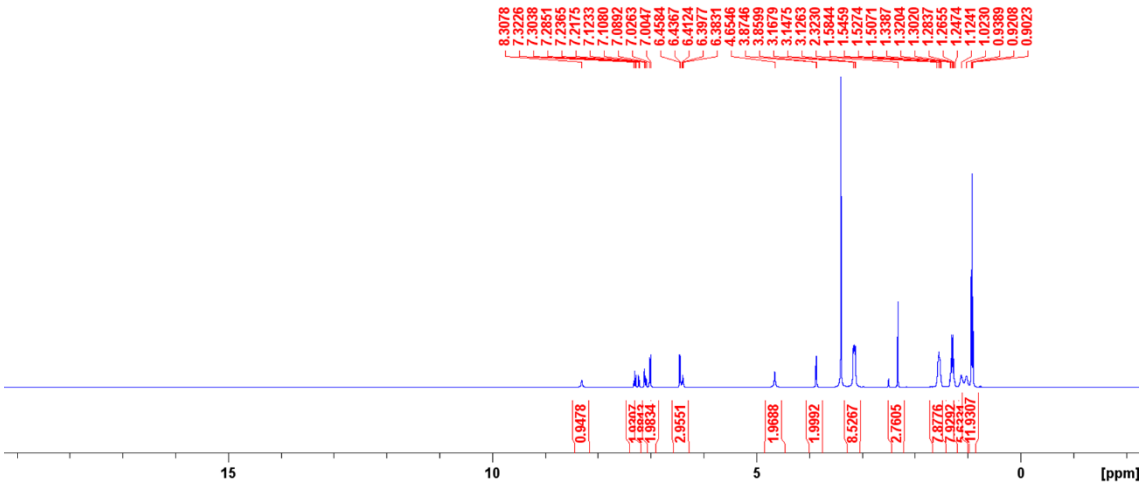

Figure S20 - ^{1}H NMR of compound **Co-formulation *i*** in DMSO-d_6 conducted at 298 K.

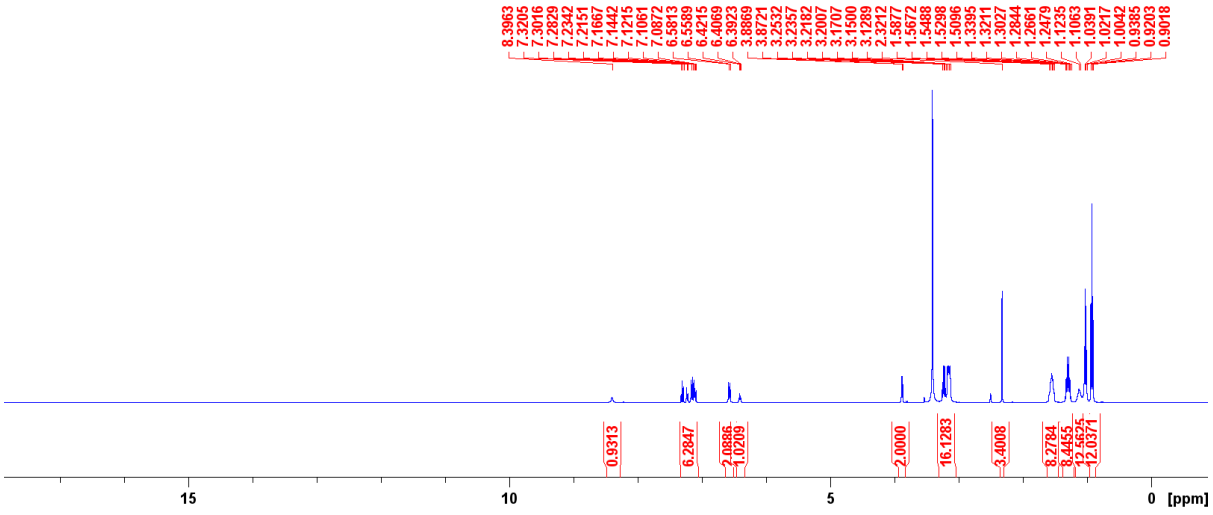

Figure S21 - ^{1}H NMR of compound **Co-formulation *j*** in DMSO-d_6 conducted at 298 K.

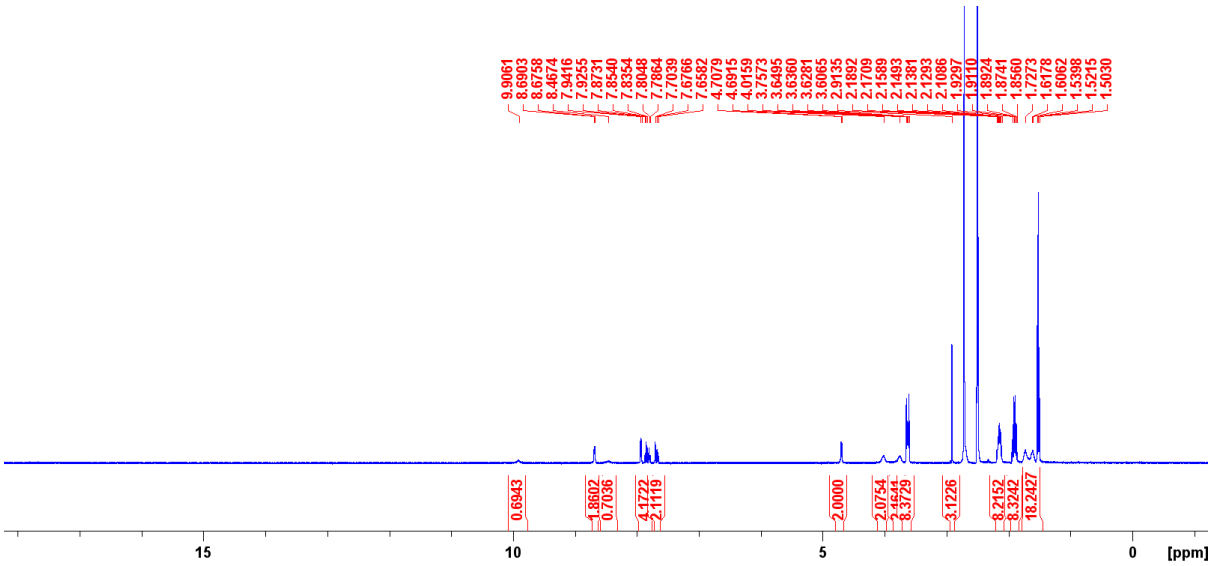

Figure S22 - ^{1}H NMR of compound **Co-formulation *k*** in DMSO-d_6 conducted at 298 K.

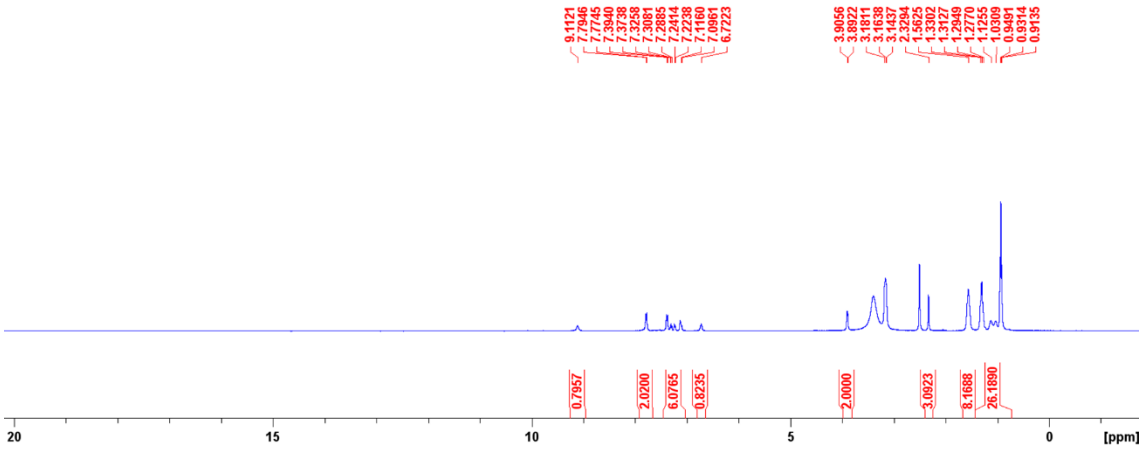

Figure S23 - ^{1}H NMR of compound **Co-formulation *l*** in DMSO-d_6 conducted at 298 K.

Quantitative ^{1}H NMR study data

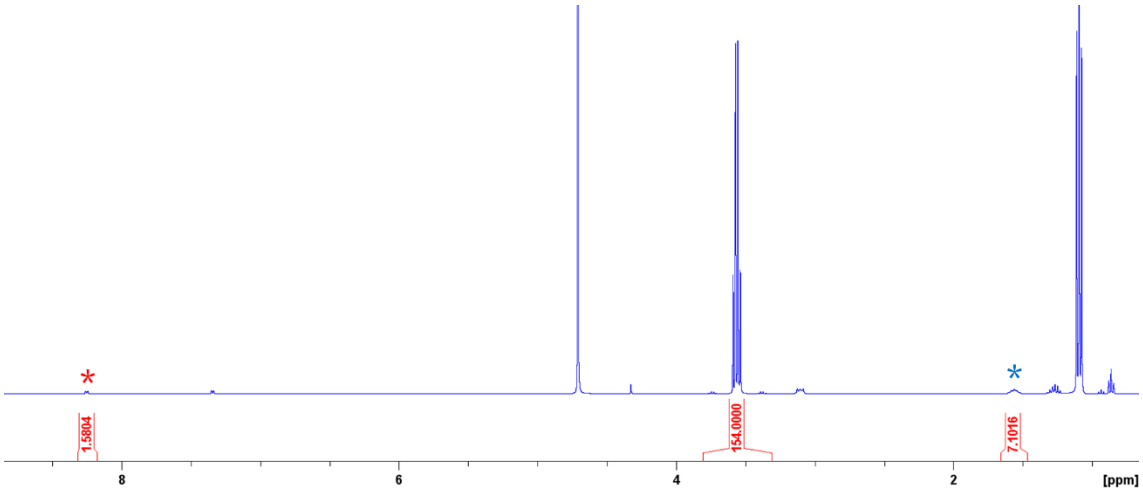

Figure S24 - ^{1}H NMR spectrum with a delay (d_1 = 60 s) of **3** (5.56 mM) in D_2O/5.0% EtOH. Comparative integration indicated 25% of the anionic component of SSA (*) and 11% of TBA (*) has become NMR silent.

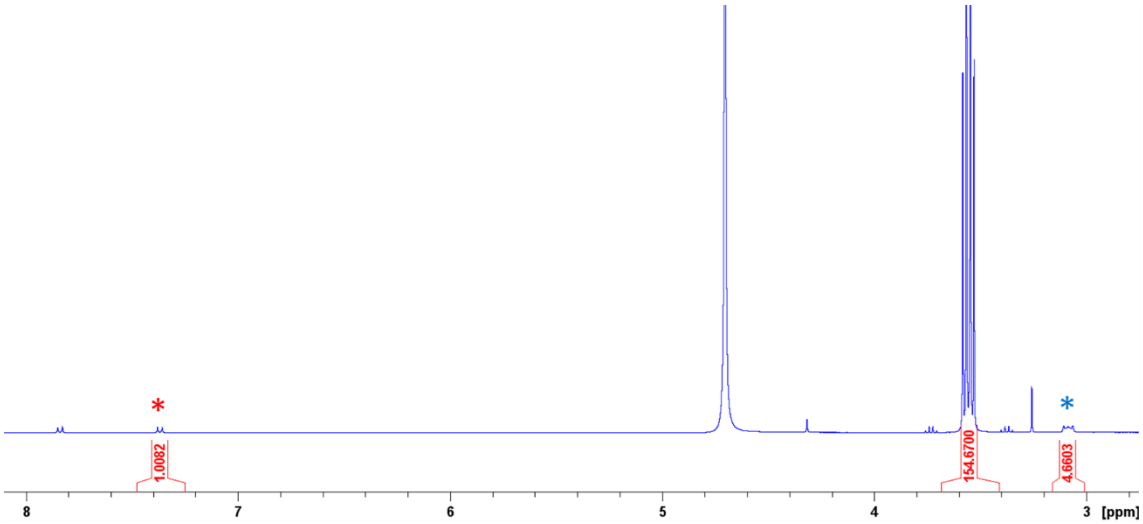

Figure S25 - ^{1}H NMR spectrum with a delay (d_1 = 60 s) of **4** (5.56 mM) in D_2O/5.0% EtOH. Comparative integration indicated 50% of the anionic component of SSA (*) and 42% of TBA (*) has become NMR silent.

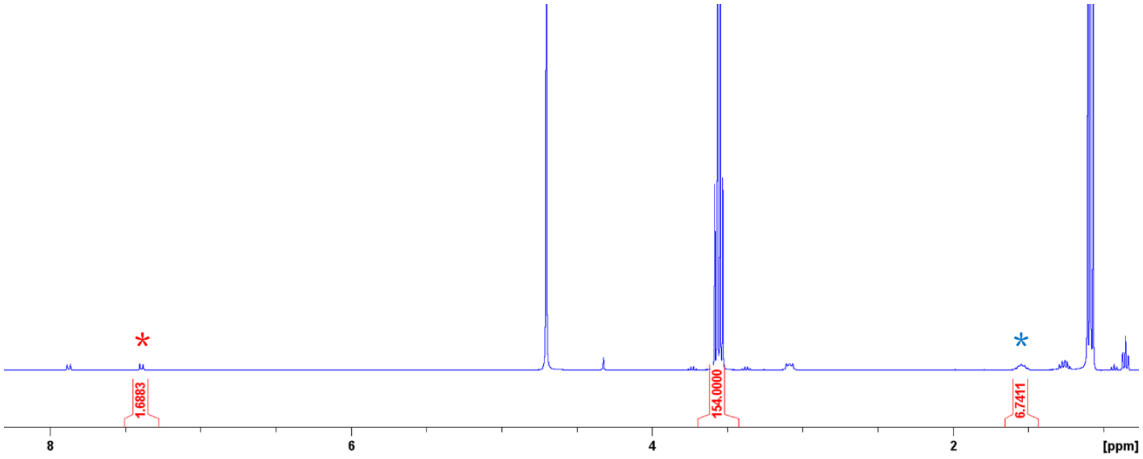

Figure S26 - ^{1}H NMR spectrum with a delay (d_1 = 60 s) of **5** (5.56 mM) in D_2O/5.0% EtOH. Comparative integration indicated 14% of the anionic component of SSA (*) and 16% of TBA (*) has become NMR silent.

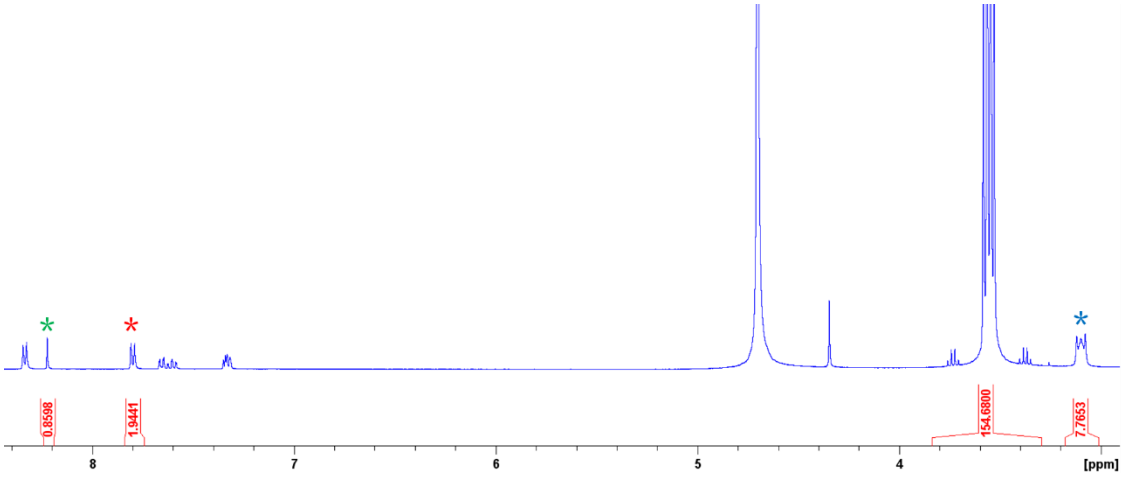

Figure S27 - ^{1}H NMR spectrum with a delay (d_1 = 60 s) of **Co-formulation *c*** (5.56 mM) in D_2O/5.0% EtOH. Comparative integration indicated 3% of the anionic component of SSA (*), 3% of TBA (*) and 14% of co-formulant **6** (*) has become NMR silent.

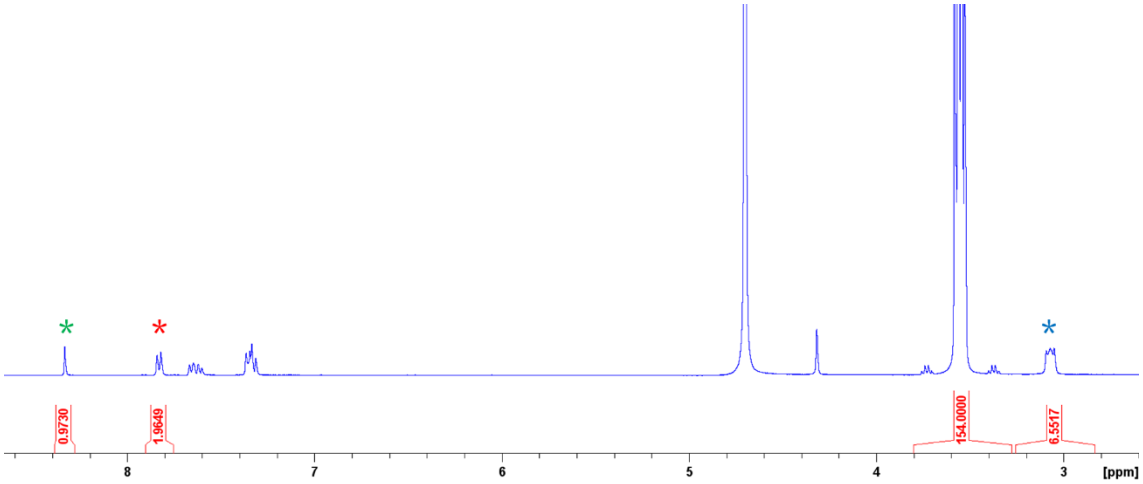

Figure S28 - ^{1}H NMR spectrum with a delay (d_1 = 60 s) of **Co-formulation *d*** (5.56 mM) in D_2O/5.0% EtOH. Comparative integration indicated 2% of the anionic component of SSA (*), 18% of TBA (*) and 3% of co-formulant **6** (*) has become NMR silent.

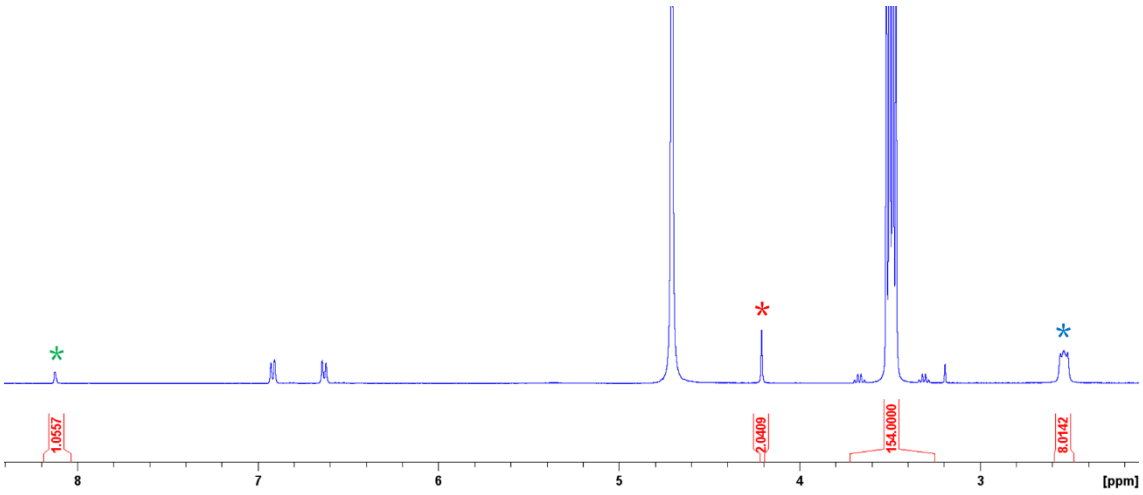

Figure S29 - ^{1}H NMR spectrum with a delay (d_1 = 60 s) of **Co-formulation *e*** (5.56 mM) in D_2O/5.0% EtOH. Comparative integration indicated 0% of the anionic component of SSA (*), 0% of TBA (*) and 0% of co-formulant **7** (*) has become NMR silent.

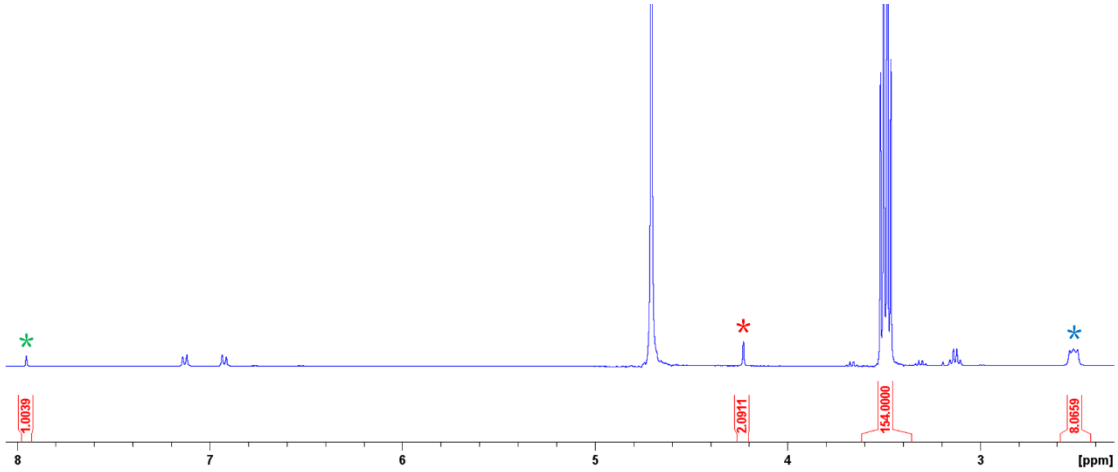

Figure S30 - ^{1}H NMR spectrum with a delay (d_1 = 60 s) of **Co-formulation *f*** (5.56 mM) in D_2O/5.0% EtOH. Comparative integration indicated 0% of the anionic component of SSA (*), 0% of TBA (*) and 0% of co-formulant **7** (*) has become NMR silent.

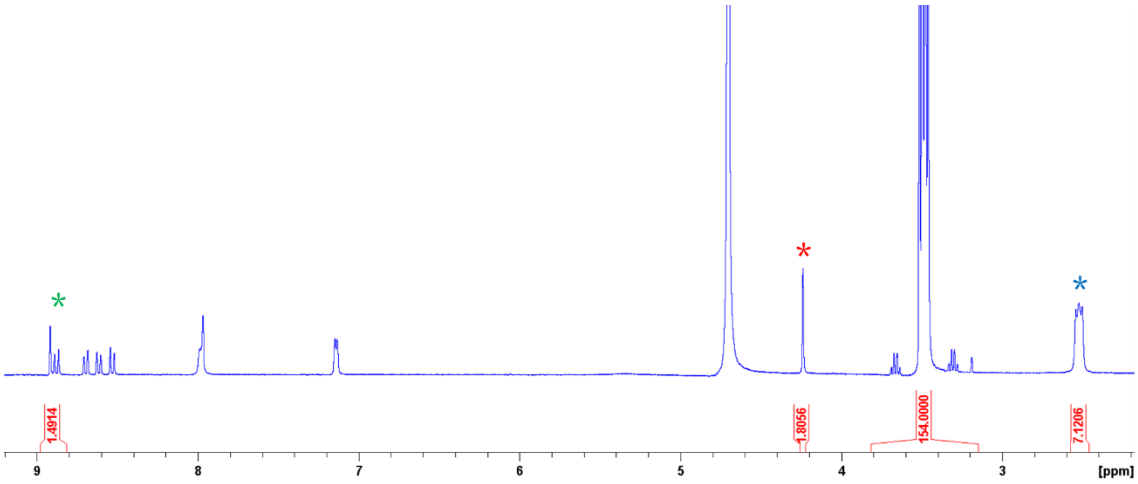

Figure S31 - ^{1}H NMR spectrum with a delay (d_1 = 60 s) of **Co-formulation *g*** (5.56 mM) in D_2O/5.0% EtOH. Comparative integration indicated 10% of the anionic component of SSA (*), 11% of TBA (*) and 25% of co-formulant **7** (*) has become NMR silent.

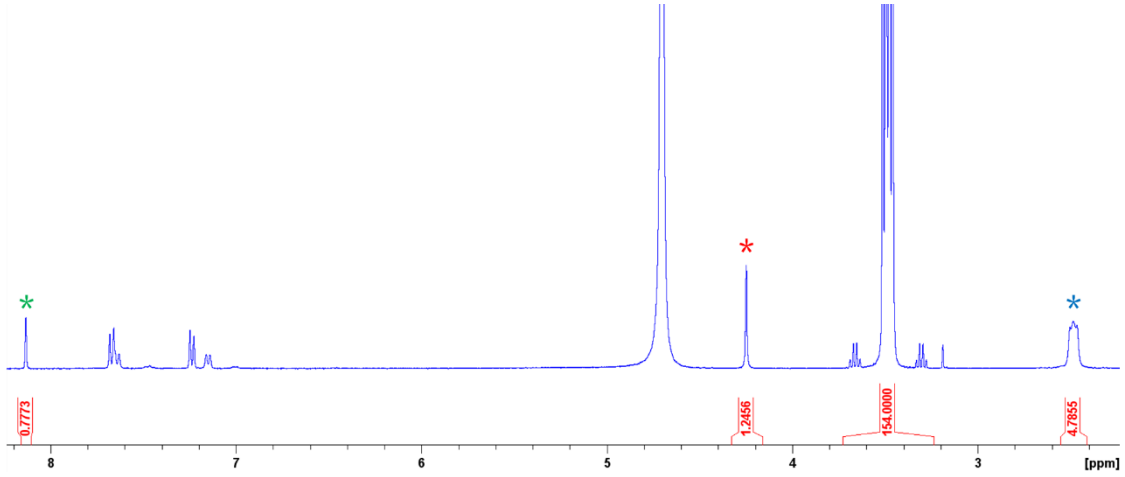

Figure S32 - ^{1}H NMR spectrum with a delay (d_1 = 60 s) of **Co-formulation *h*** (5.56 mM) in D_2O/5.0% EtOH. Comparative integration indicated 38% of the anionic component of SSA (*), 40% of TBA (*) and 22% of co-formulant **7** (*) has become NMR silent.

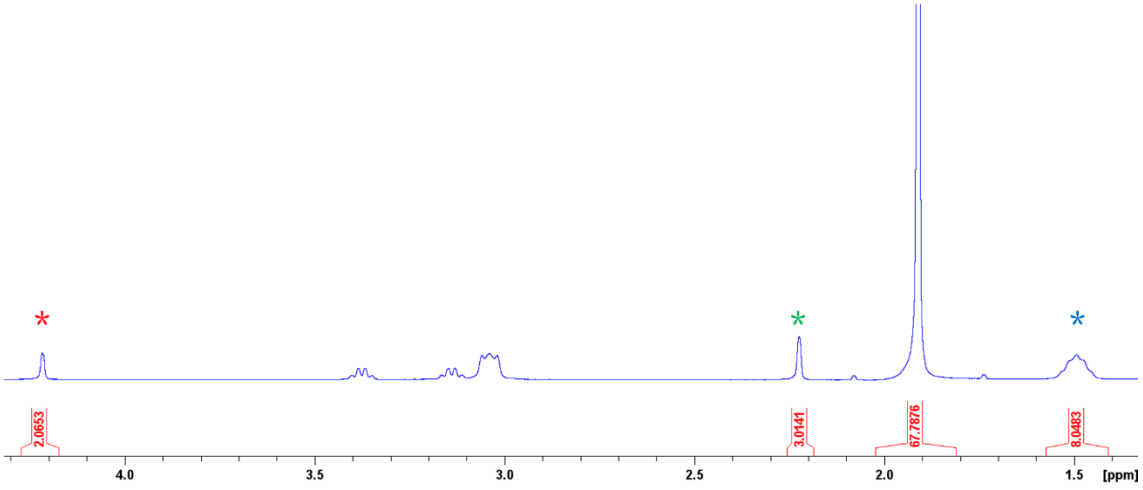

Figure S33 - ^{1}H NMR spectrum (d_1 = 60 s) of compound **Co-formulation *i*** (5.56 mM) in D_2O/1.0% CH_3CN. Comparative integration indicated 0% of sample has become NMR silent (anionic component of SSA*, TBA*, **8** *).

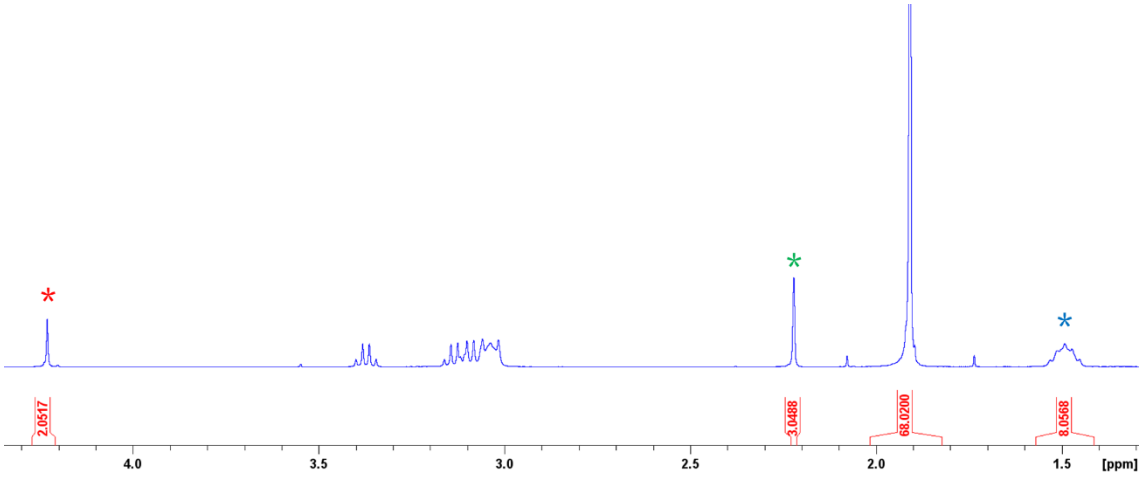

Figure S34 - ^{1}H NMR spectrum (d_1 = 60 s) of compound **Co-formulation *j*** (5.56 mM) in D_2O/1.0% CH_3CN. Comparative integration indicated 0% of sample has become NMR silent (anionic component of SSA*, TBA*, **8** *).

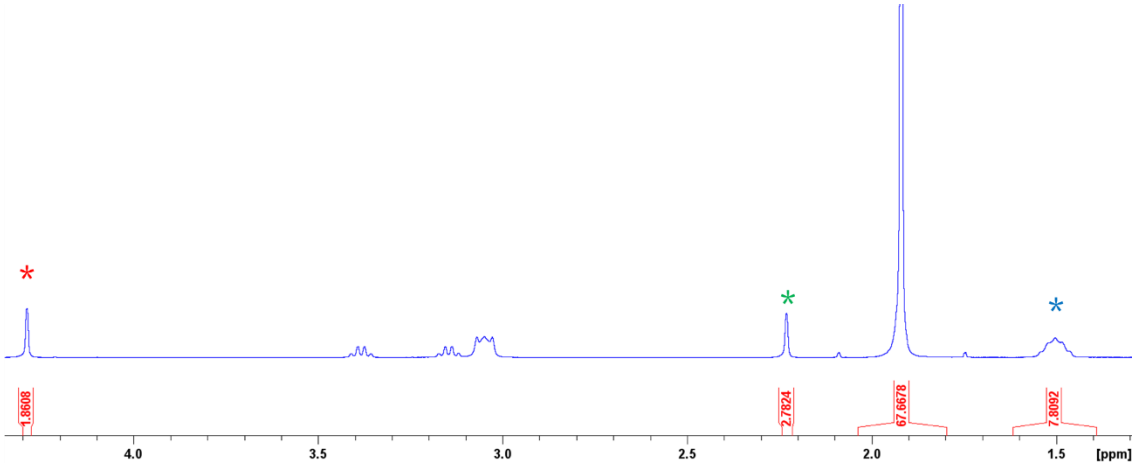

Figure S35 - ^{1}H NMR spectrum with a delay (d_1 = 60 s) of **Co-formulation *k*** (5.56 mM) in D_2O/1.0% CH_3CN. Comparative integration indicated 7% of the anionic component of SSA (*), 2% of TBA (*) and 7% of co-formulant **8** (*) has become NMR silent.

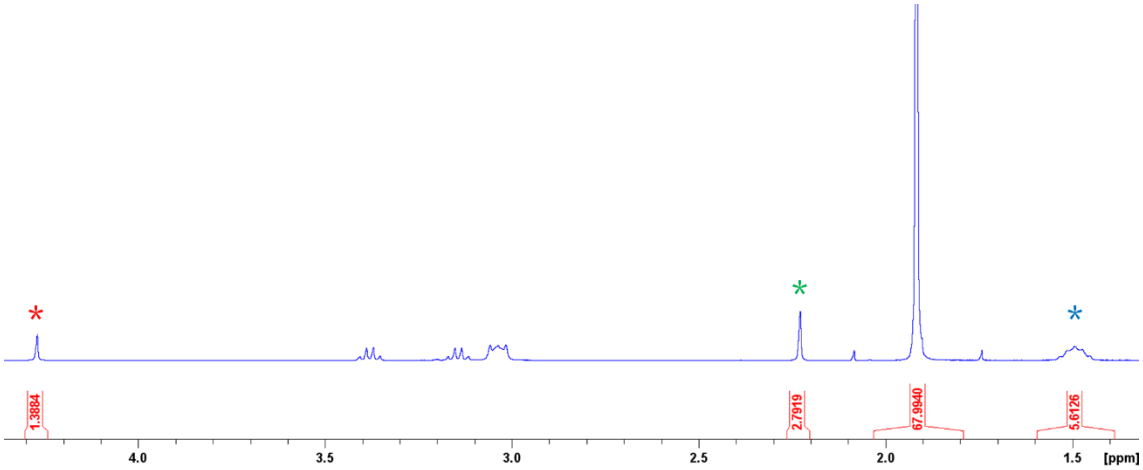

Figure S36 - ^{1}H NMR spectrum with a delay (d_1 = 60 s) of **Co-formulation *I*** (5.56 mM) in D_2O/1.0% CH_3CN. Comparative integration indicated 31% of the anionic component of SSA (*), 30% of TBA (*) and 7% of co-formulant **8** (*) has become NMR silent.

Quantitative ^{1}H NMR co-formulant uptake study data

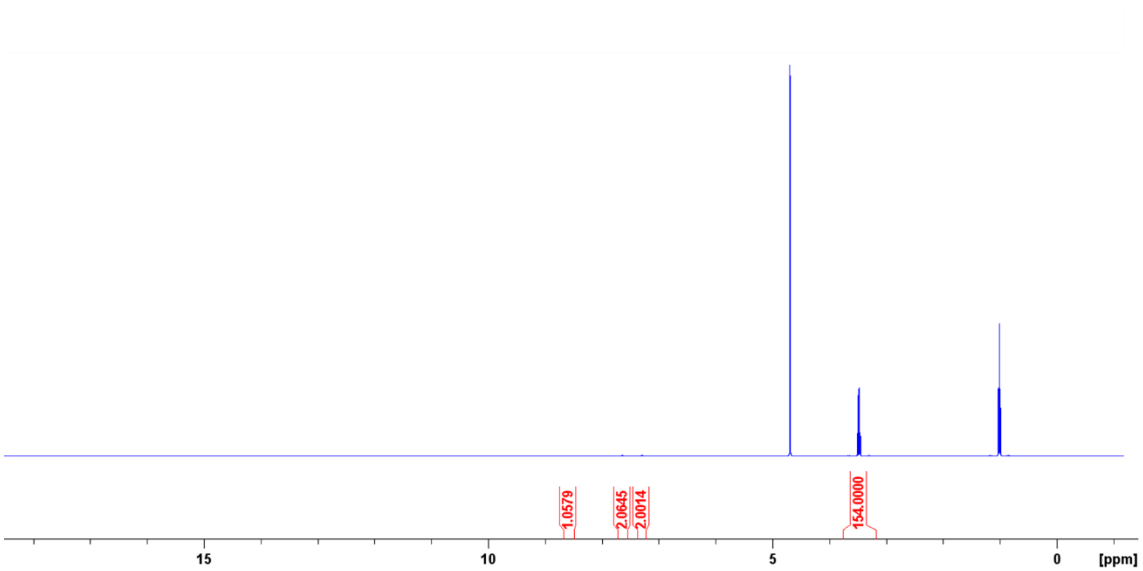

Figure S37 - ^{1}H NMR spectrum with a delay (d_1 = 60 s) of **6** (11.12 mM) in D_2O/5.0% EtOH. Comparative integration indicated 0% of sample has become NMR silent.

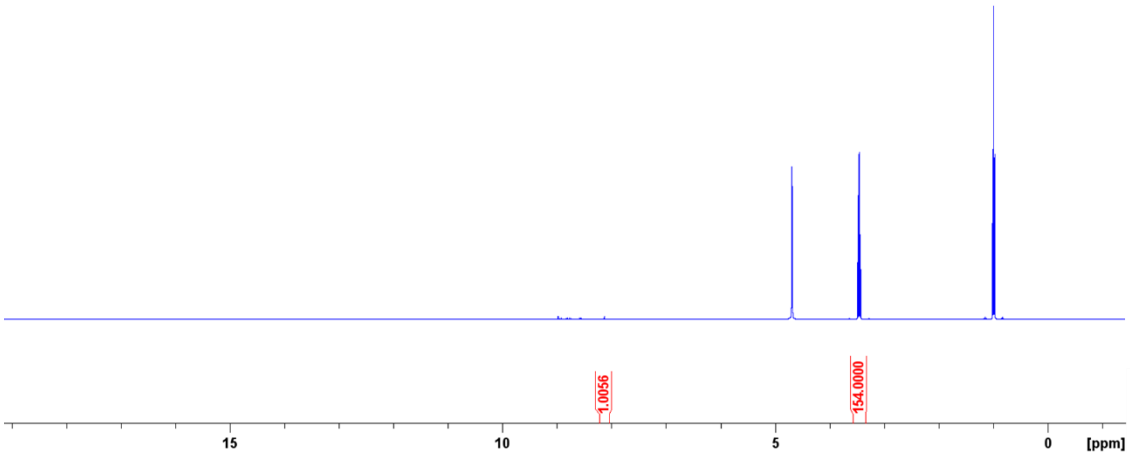

Figure S38 - ^{1}H NMR spectrum with a delay (d_1 = 60 s) of **7** (11.12 mM) in D_2O/5.0% EtOH. Comparative integration indicated 0% of sample has become NMR silent.

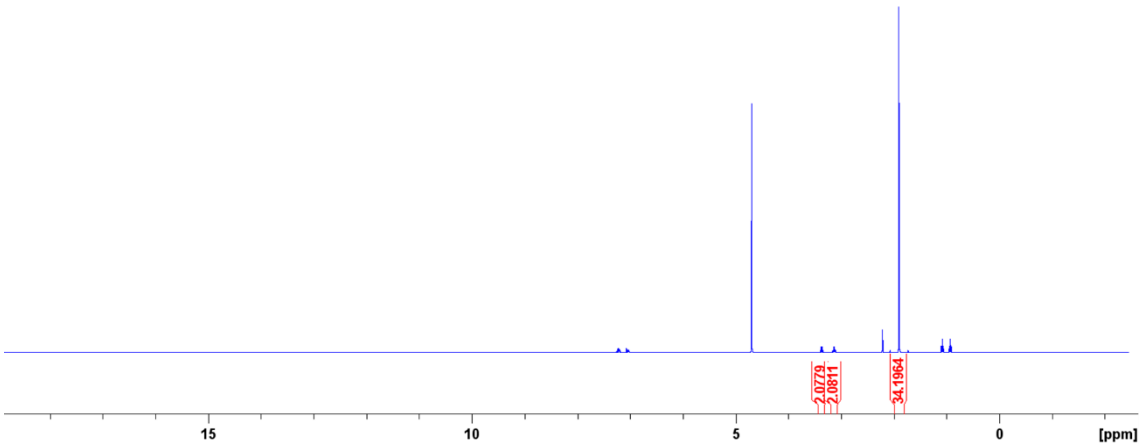

Figure S39 - ^{1}H NMR spectrum with a delay (d_1 = 60 s) of **8** (11.2 mM) in D_2O/1.0% CH_3CN. Comparative integration indicated 0% of sample has become NMR silent.

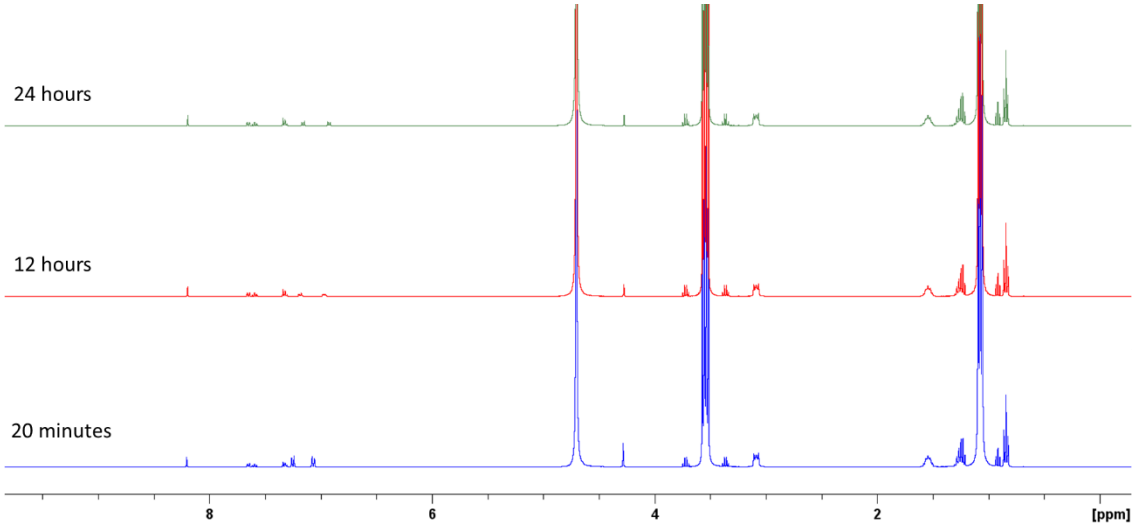

Figure S40 – Zoomed in ^{1}H NMR spectrum with a delay (d_1 = 60 s) of **Co-formulation *a*** (5.56 mM) in D_2O/5.0% EtOH. Comparative integration indicated 62% of sample has become NMR silent 20 minutes after the addition of coumarin-3-carboxylic acid, 59% of the sample has become NMR silent after 12 hours and 59% has become NMR silent after 24 hours.

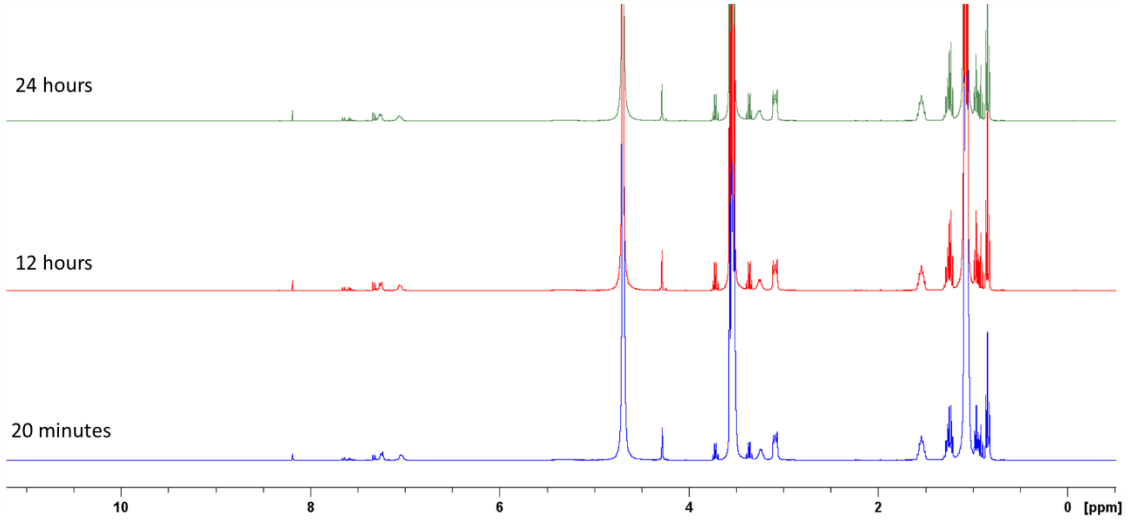

Figure S41 - Zoomed in ^{1}H NMR spectrum with a delay (d_1 = 60 s) of **Co-formulation *b*** (5.56 mM) in D_2O/5.0% EtOH. Comparative integration indicated 87% of sample has become NMR silent 20 minutes after the addition of coumarin-3-carboxylic acid, 84% of the sample has become NMR silent after 12 hours and 84% has become NMR silent after 24 hours.

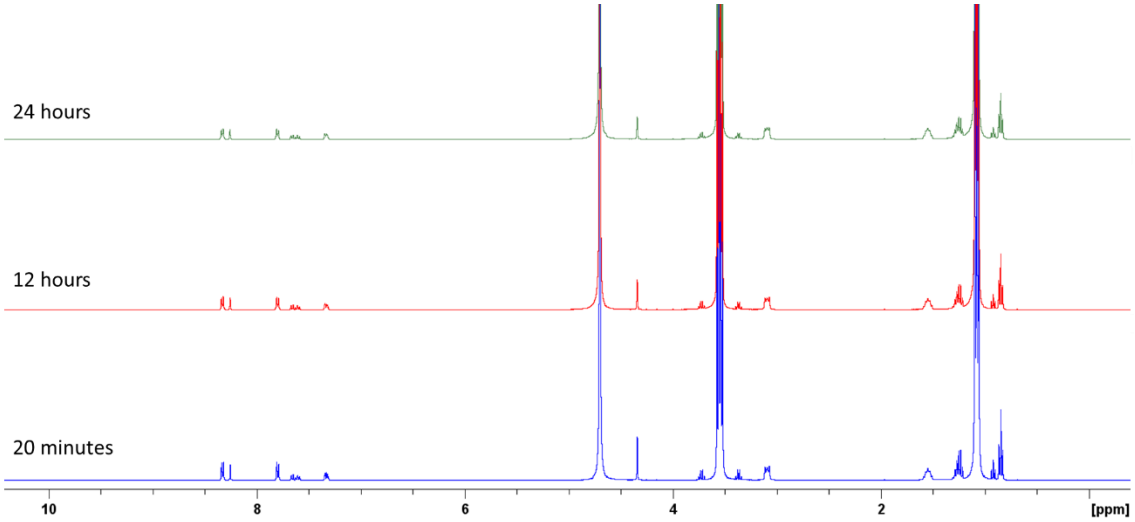

Figure S42 - Zoomed in ^{1}H NMR spectrum with a delay (d_1 = 60 s) of **Co-formulation *c*** (5.56 mM) in D_2O/5.0% EtOH. Comparative integration indicated 87% of sample has become NMR silent 20 minutes after the addition of coumarin-3-carboxylic acid, 84% of the sample has become NMR silent after 12 hours and 84% has become NMR silent after 24 hours.

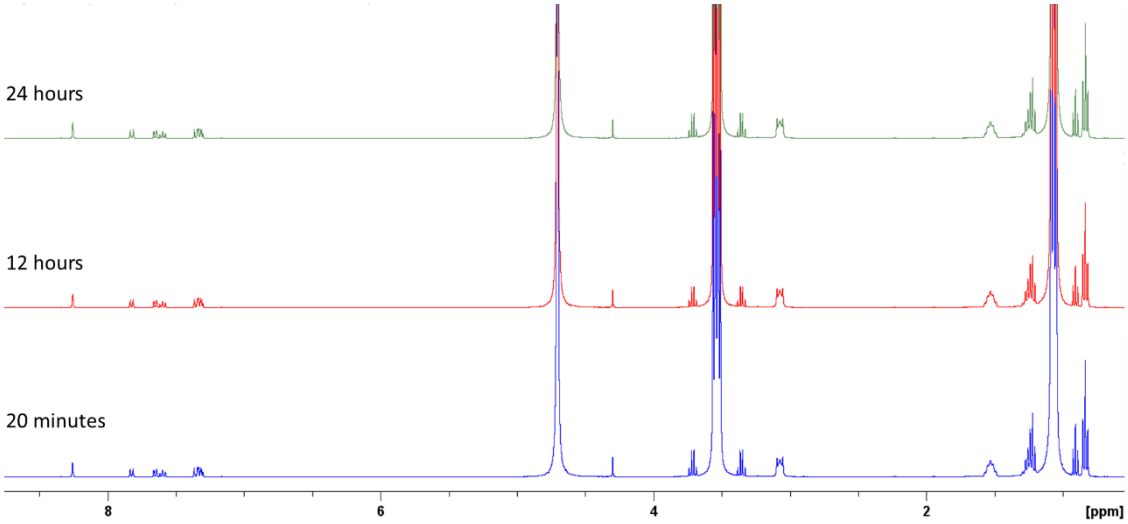

Figure S43 - Zoomed in ^{1}H NMR spectrum with a delay (d_1 = 60 s) of **Co-formulation *d*** (5.56 mM) in D_2O/5.0% EtOH. Comparative integration indicated 59% of sample has become NMR silent 20 minutes after the addition of coumarin-3-carboxylic acid, 60% of the sample has become NMR silent after 12 hours and 61% has become NMR silent after 24 hours.

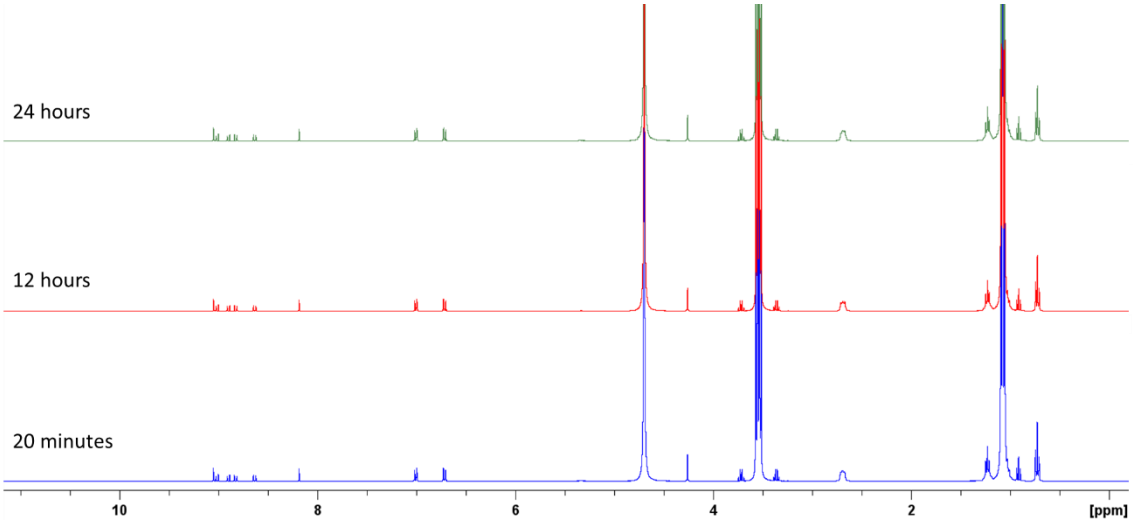

Figure S44 - Zoomed in ^{1}H NMR spectrum with a delay (d_1 = 60 s) of **Co-formulation *e*** (5.56 mM) in D_2O/5.0% EtOH. Comparative integration indicated 62% of sample has become NMR silent 20 minutes after the addition of 8-Hydroxypyrene-1,3,6-trisulfonic acid trisodium salt , 62% of the sample has become NMR silent after 12 hours and 62% has become NMR silent after 24 hours.

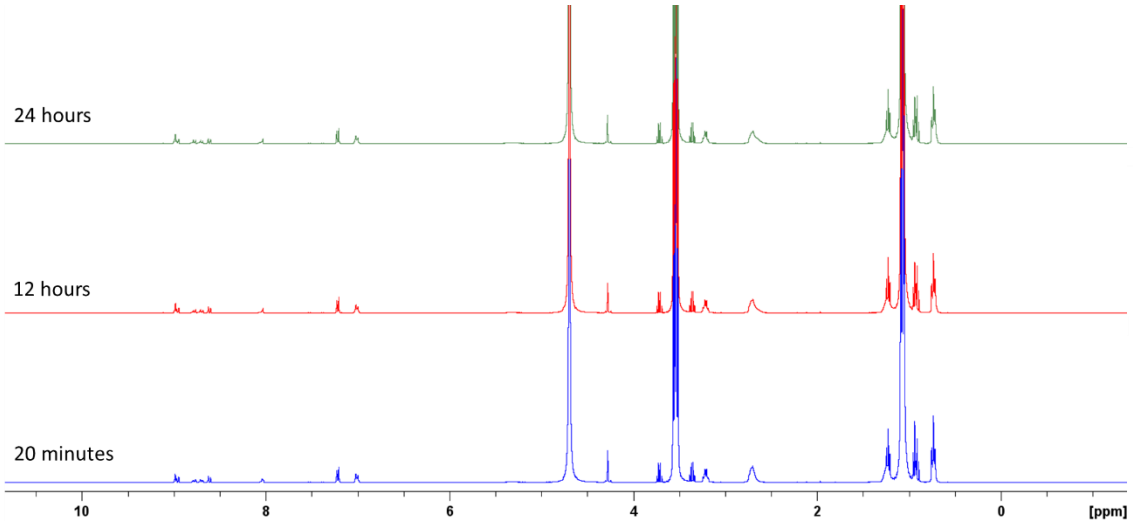

Figure S45 - Zoomed in ^{1}H NMR spectrum with a delay (d_1 = 60 s) of **Co-formulation *f*** (5.56 mM) in D_2O/5.0% EtOH. Comparative integration indicated 66% of sample has become NMR silent 20 minutes after the addition of 8-Hydroxypyrene-1,3,6-trisulfonic acid trisodium salt, 65% of the sample has become NMR silent after 12 hours and 64% has become NMR silent after 24 hours.

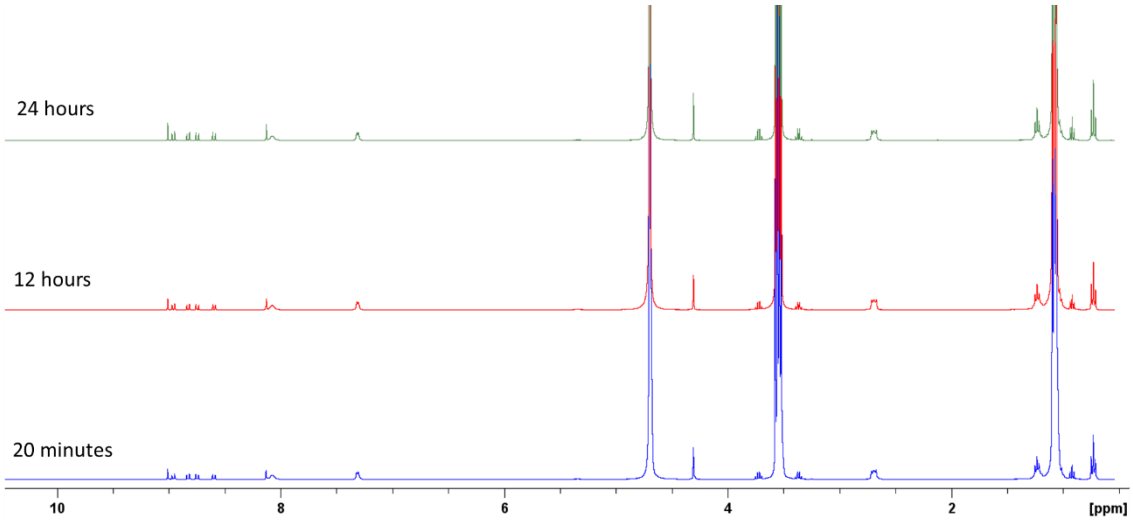

Figure S46 - Zoomed in ^{1}H NMR spectrum with a delay (d_1 = 60 s) of **Co-formulation *g*** (5.56 mM) in D_2O/5.0% EtOH. Comparative integration indicated 50% of sample has become NMR silent 20 minutes after the addition of 8-Hydroxypyrene-1,3,6-trisulfonic acid trisodium salt, 50% of the sample has become NMR silent after 12 hours and 50% has become NMR silent after 24 hours.

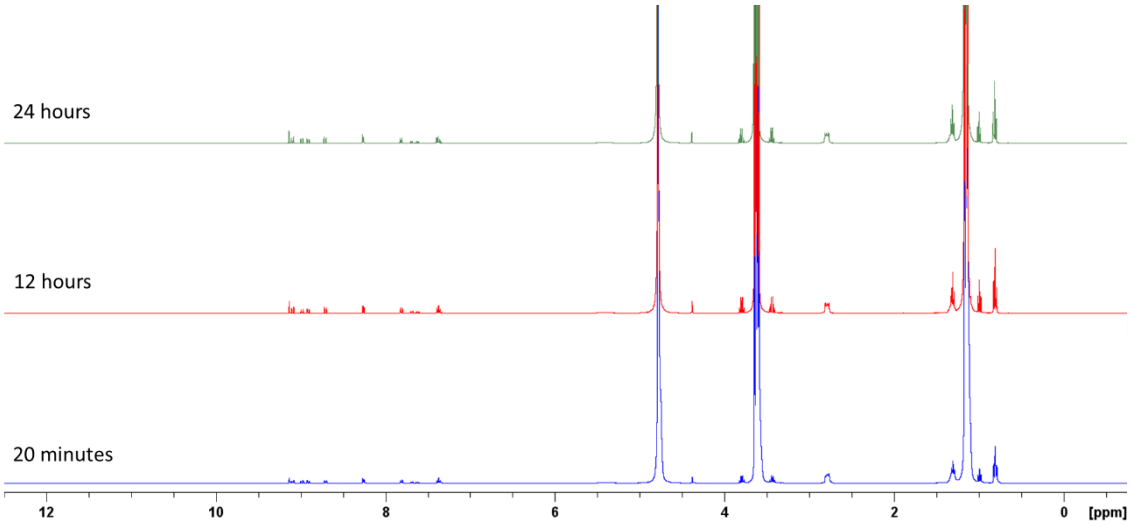

Figure S47 - Zoomed in ^{1}H NMR spectrum with a delay (d_1 = 60 s) of **Co-formulation *h*** (5.56 mM) in D_2O/5.0% EtOH. Comparative integration indicated 72% of sample has become NMR silent 20 minutes after the addition of 8-Hydroxypyrene-1,3,6-trisulfonic acid trisodium salt, 72% of the sample has become NMR silent after 12 hours and 72% has become NMR silent after 24 hours.

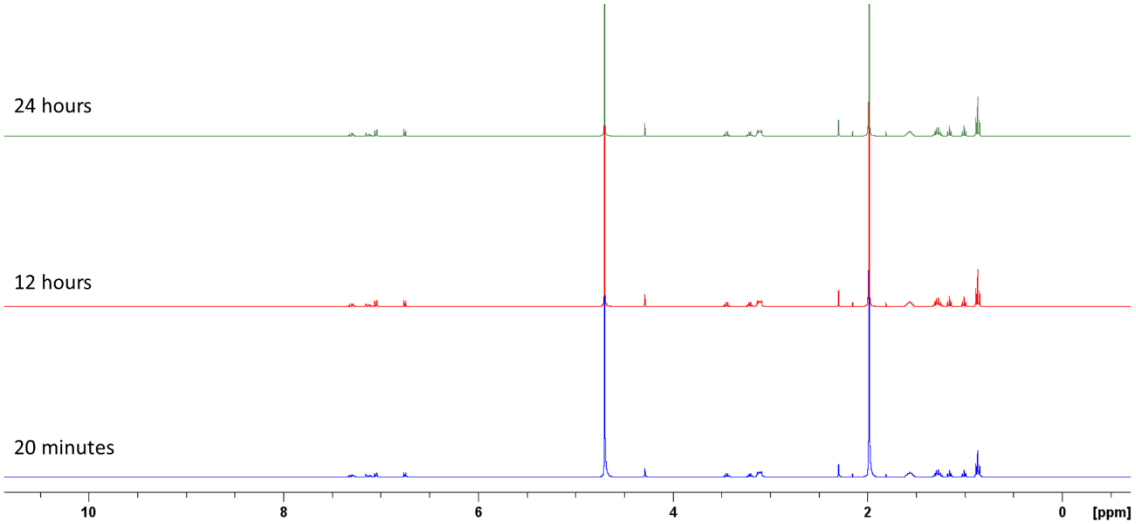

Figure S48 - Zoomed in ^{1}H NMR spectrum with a delay (d_1 = 60 s) of **Co-formulation *i*** (5.56 mM) in D_2O/1.0% CH_3CN. Comparative integration indicated 10% of sample has become NMR silent 20 minutes after the addition of N, N-diethyl-meta-toluamide, 10% of the sample has become NMR silent after 12 hours and 11% has become NMR silent after 24 hours.

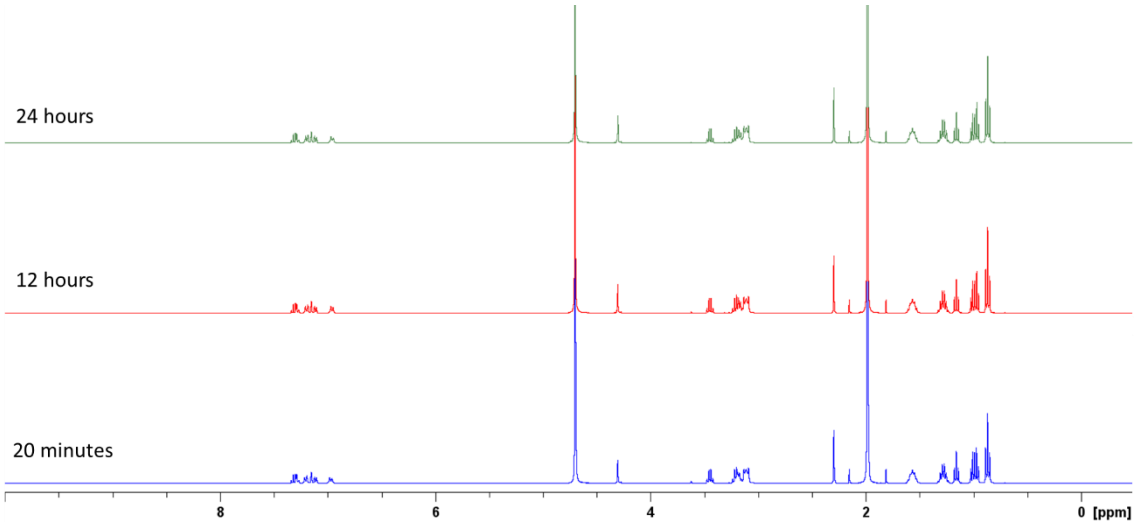

Figure S49 - Zoomed in ^{1}H NMR spectrum with a delay (d_1 = 60 s) of **Co-formulation *j*** (5.56 mM) in D_2O/1.0% CH_3CN. Comparative integration indicated 18% of sample has become NMR silent 20 minutes after the addition of N, N-Diethyl-meta-toluamide, 18% of the sample has become NMR silent after 12 hours and 18% has become NMR silent after 24 hours.

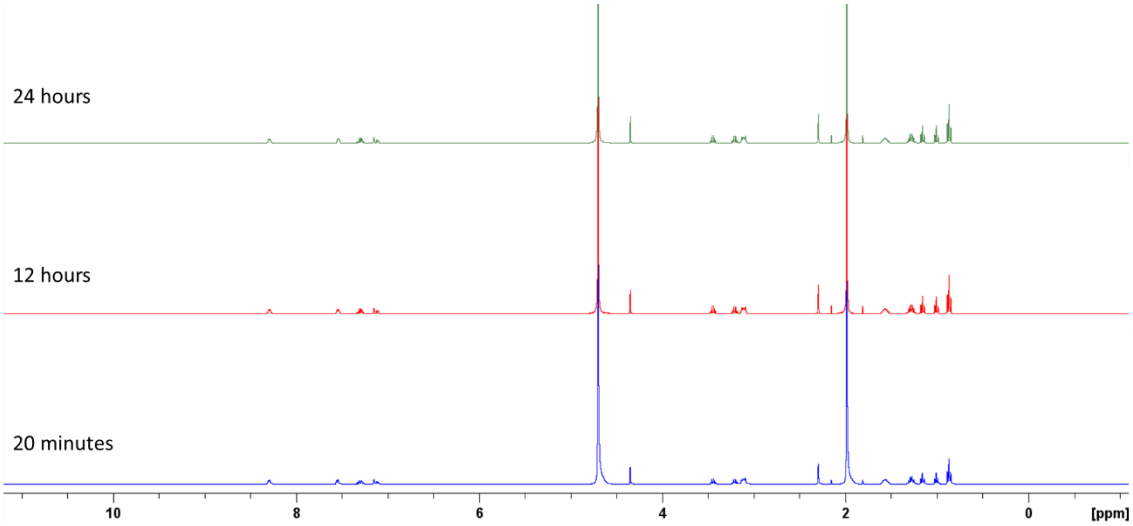

Figure S50 - Zoomed in ^{1}H NMR spectrum with a delay (d_1 = 60 s) of **Co-formulation *k*** (5.56 mM) in D_2O/1.0% CH_3CN. Comparative integration indicated 14% of sample has become NMR silent 20 minutes after the addition of N, N-Diethyl-meta-toluamide, 16% of the sample has become NMR silent after 12 hours and 15% has become NMR silent after 24 hours.

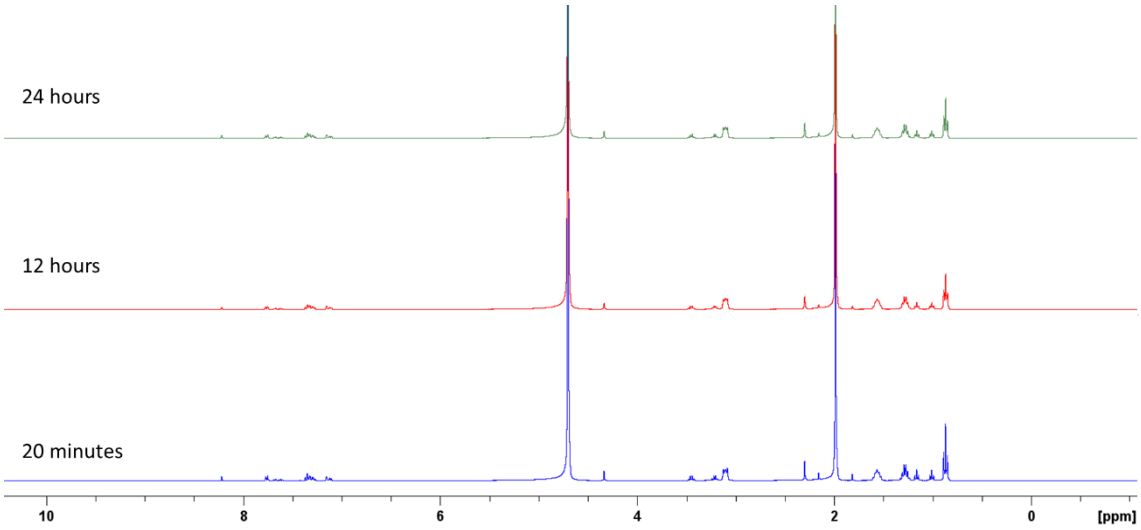

Figure S51 - Zoomed in ^{1}H NMR spectrum with a delay (d_1 = 60 s) of **Co-formulation *l*** (5.56 mM) in D_2O/1.0% CH_3CN. Comparative integration indicated 23% of sample has become NMR silent 20 minutes after the addition of N, N-Diethyl-meta-toluamide, 26% of the sample has become NMR silent after 12 hours and 30% has become NMR silent after 24 hours.

Dynamic light scattering data

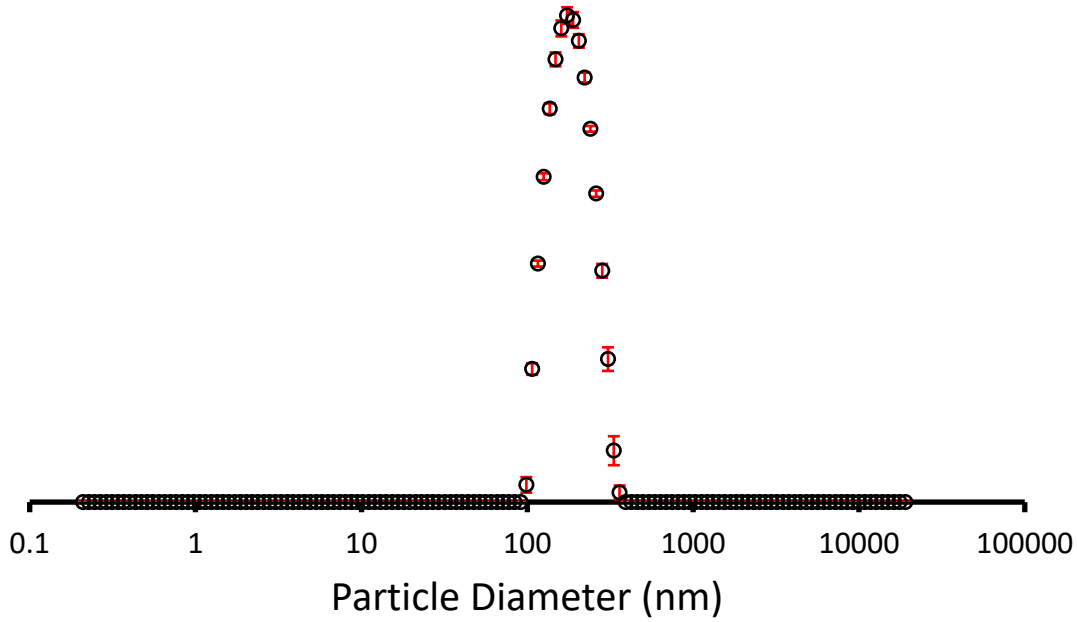

Figure S52 - The average intensity particle size distribution calculated using 10 DLS runs for **4** (5.56 mM) in an EtOH/H_2O 1:19 solution at 298 K.

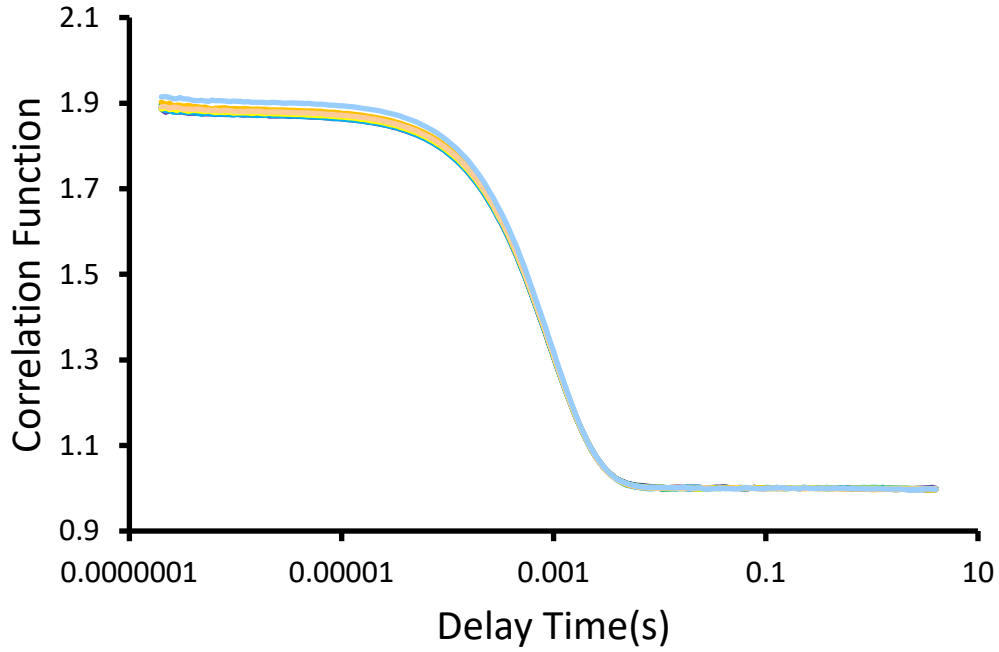

Figure S53 - Correlation function data for 10 DLS runs of **4** (5.56 mM) in an EtOH/H_2O 1:19 solution at 298 K.

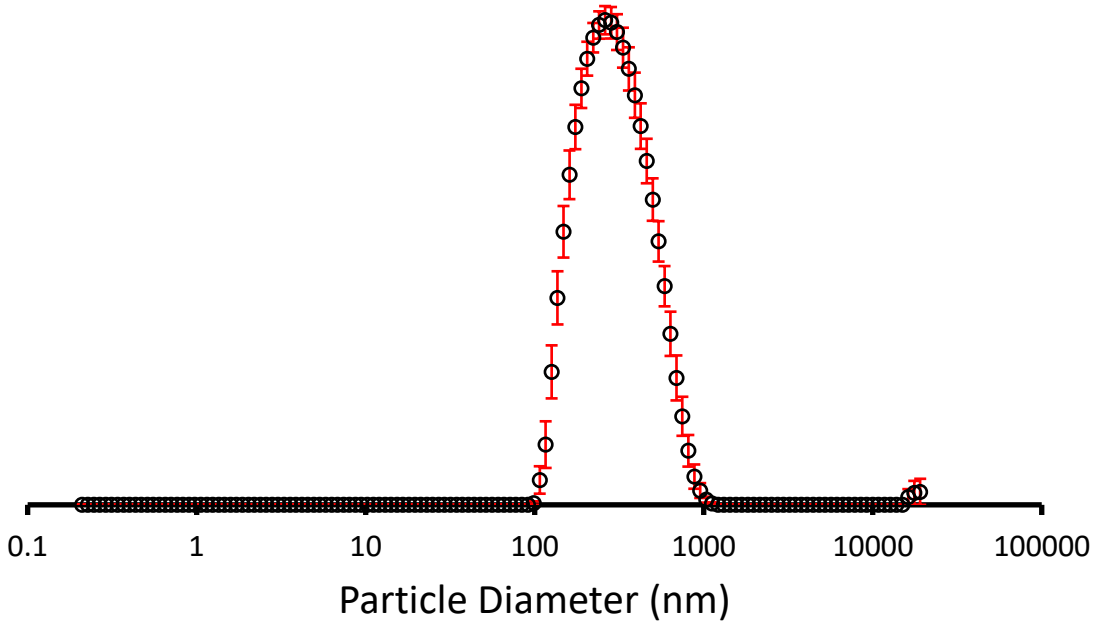

Figure S54 - The average intensity particle size distribution calculated using 10 DLS runs for **5** (5.56 mM) in an EtOH/H_2O 1:19 solution at 298 K.

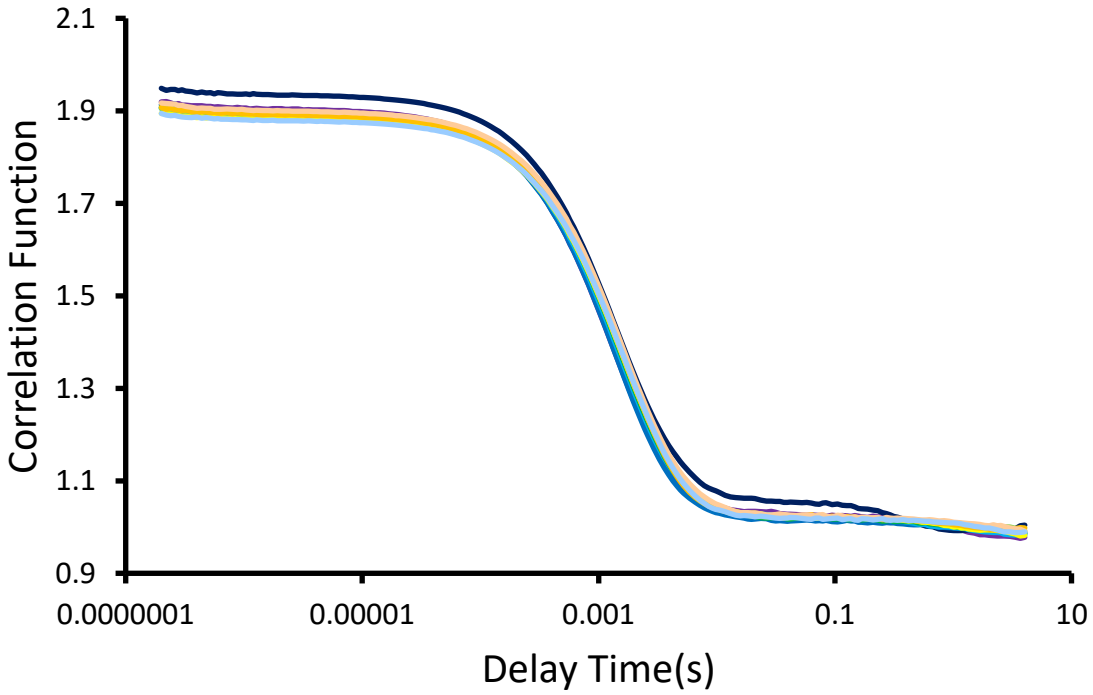

Figure S55 - Correlation function data for 10 DLS runs of **5** (5.56 mM) in an EtOH/H_2O 1:19 solution at 298 K.

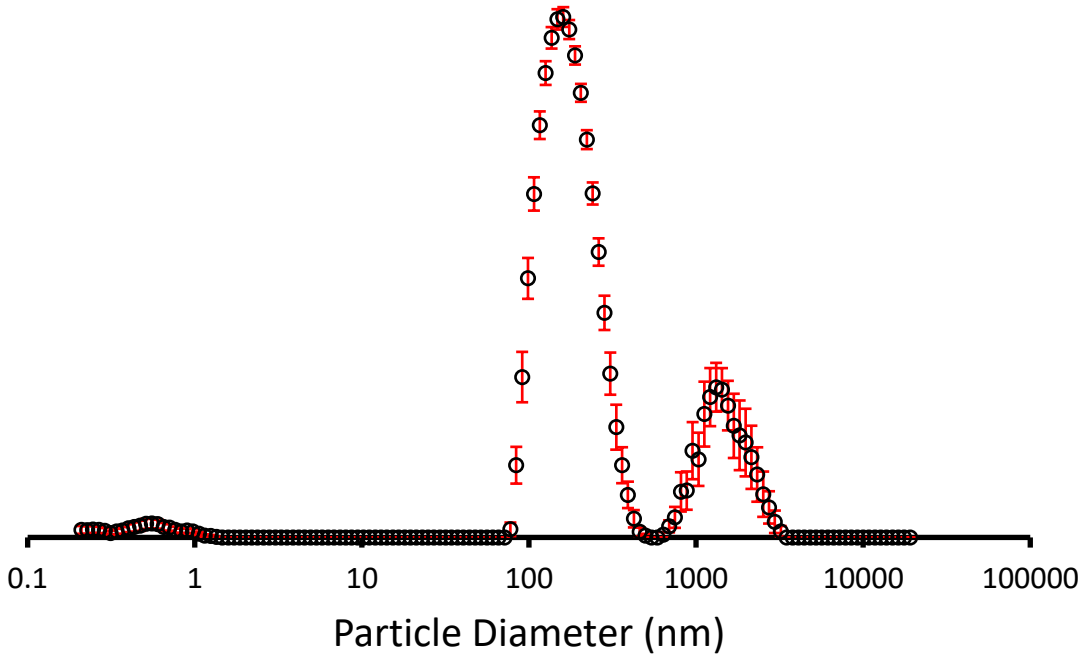

Figure S56 - The average intensity particle size distribution calculated using 10 DLS runs for **3** (5.56 mM) in an EtOH/H_2O 1:19 solution at 298 K.

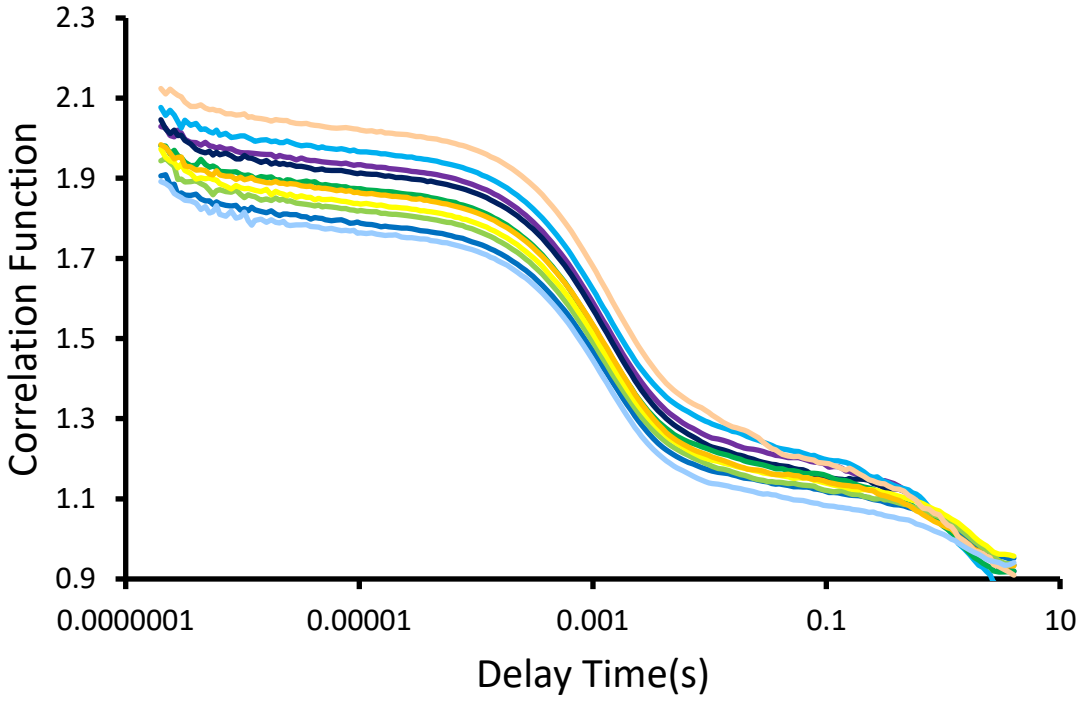

Figure S57 - Correlation function data for 10 DLS runs of **3** (5.56 mM) in an EtOH/H_2O 1:19 solution at 298 K.

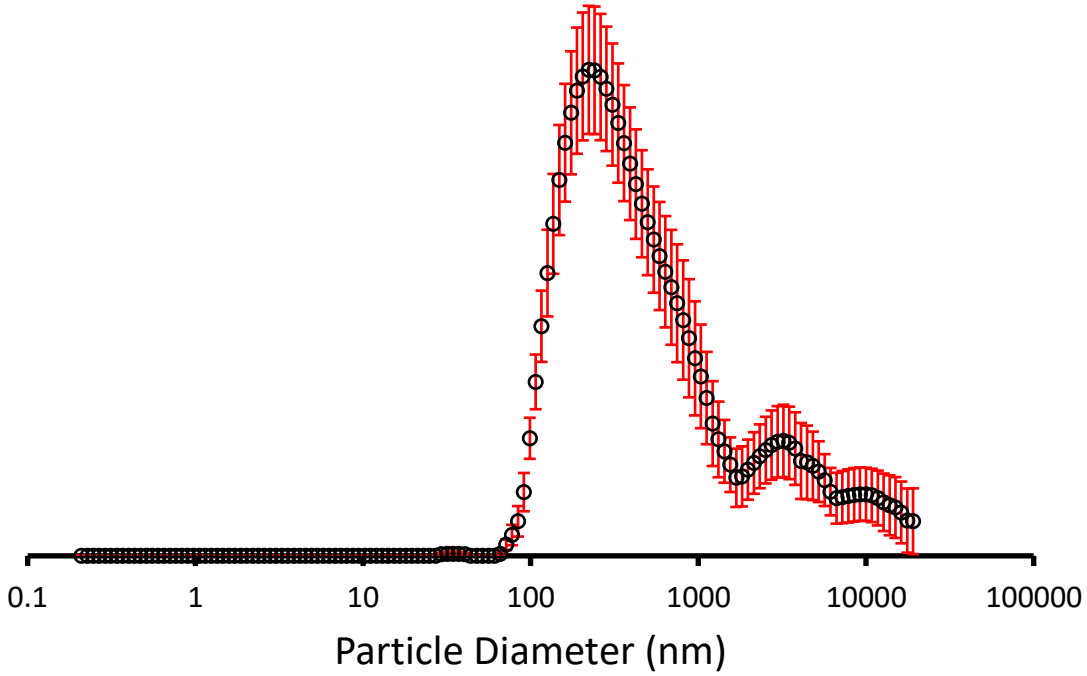

Figure S58 - The average intensity particle size distribution calculated using 9 DLS runs for **Co-formulation *c*** (5.56 mM) in an EtOH/H_2O 1:19 solution at 298 K.

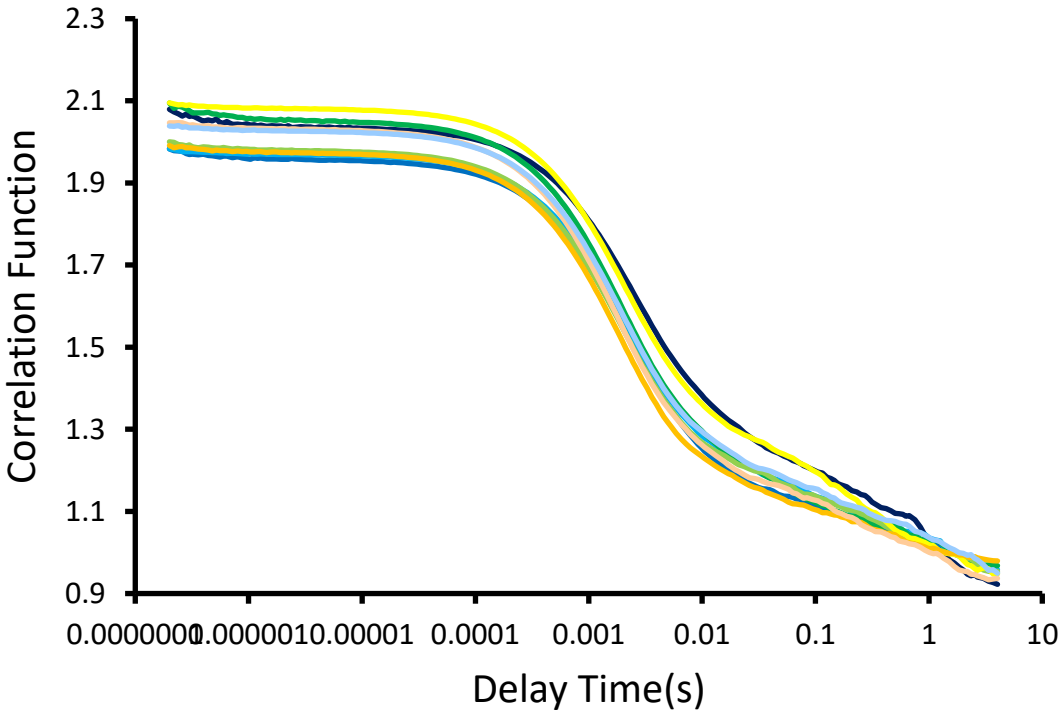

Figure S59 - Correlation function data for 9 DLS runs of **Co-formulation *c*** (5.56 mM) in an EtOH/H_2O 1:19 solution at 298 K.

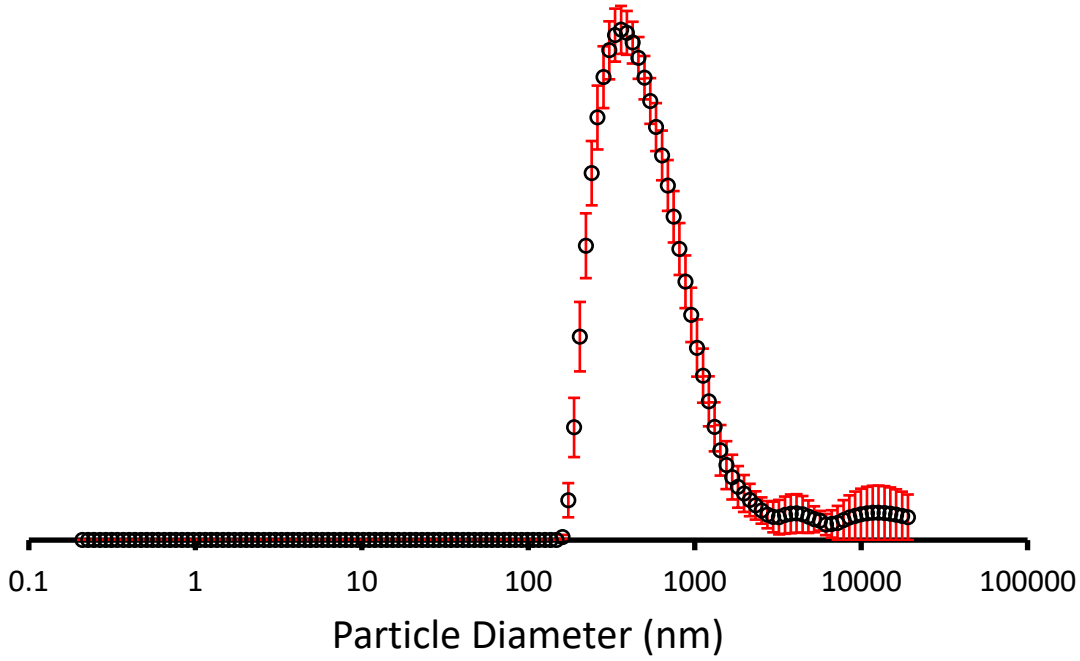

Figure S60 - The average intensity particle size distribution calculated using 10 DLS runs for **Co-formulation *d*** (5.56 mM) in an EtOH/H_2O 1:19 solution at 298 K.

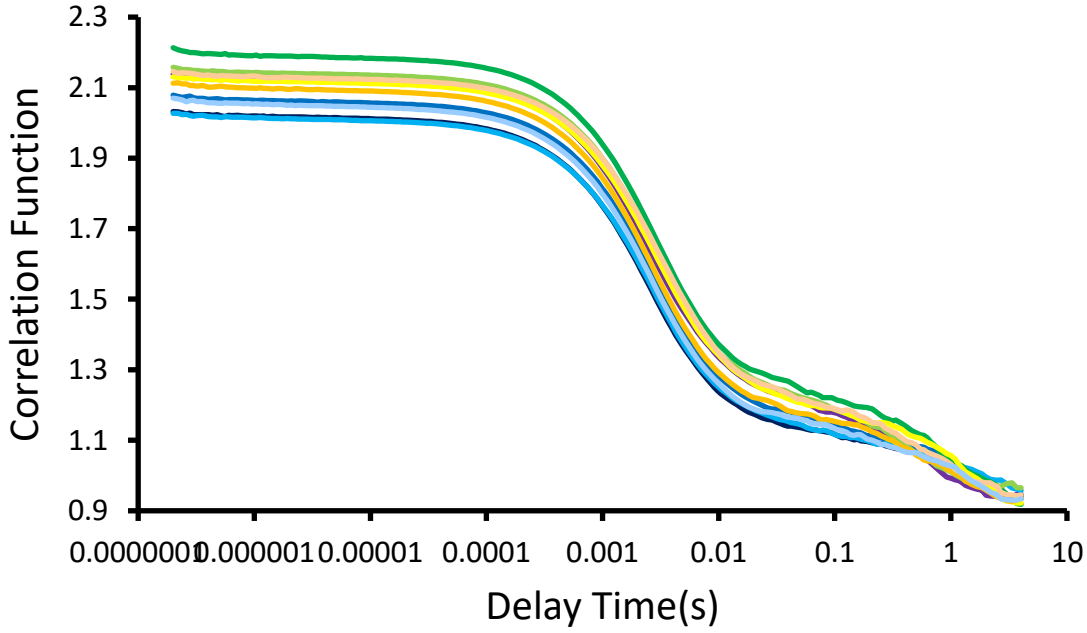

Figure S61 - Correlation function data for 10 DLS runs of **Co-formulation *d*** (5.56 mM) in an EtOH/H_2O 1:19 solution at 298 K.

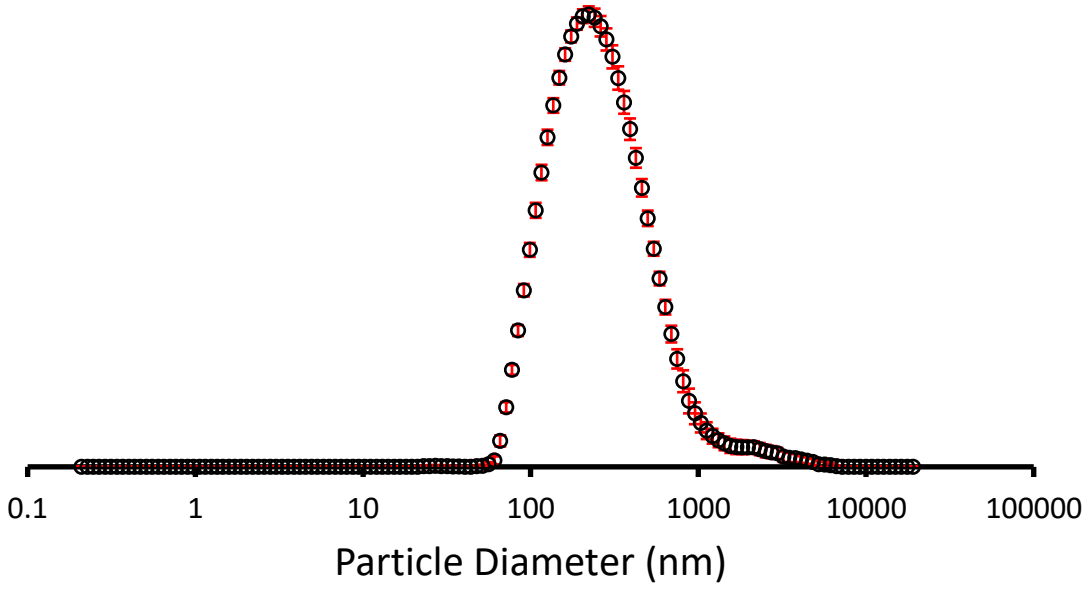

Figure S62 - The average intensity particle size distribution calculated using 10 DLS runs for **Co-formulation *g*** (5.56 mM) in an EtOH/H_2O 1:19 solution at 298 K.

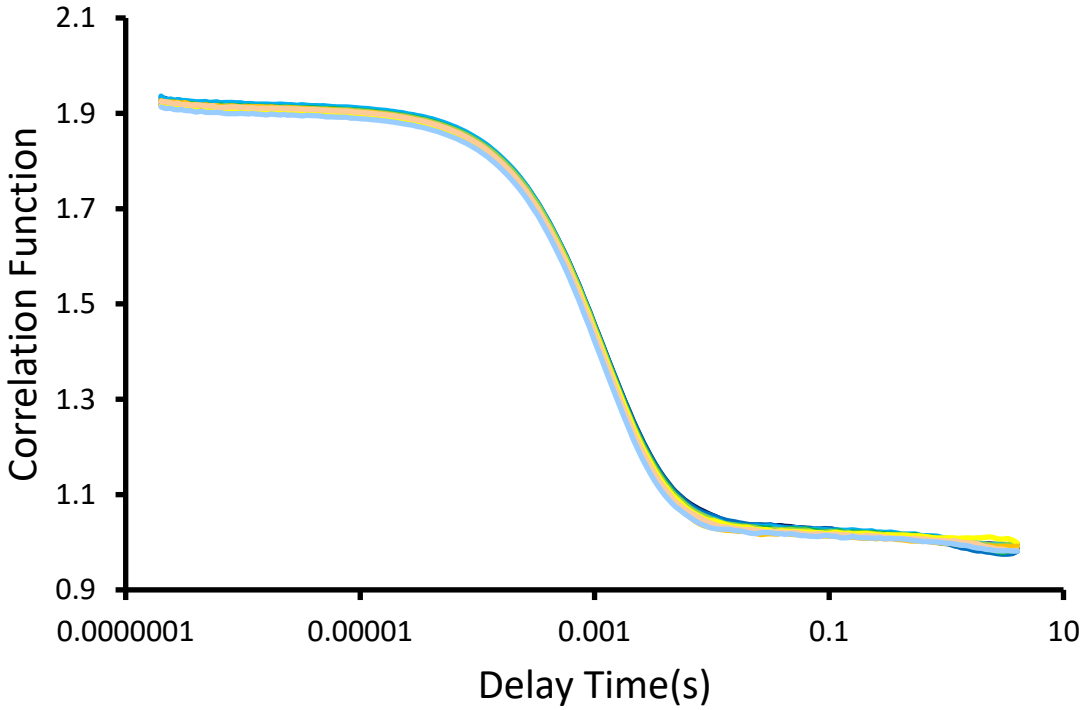

Figure S63 - Correlation function data for 10 DLS runs of **Co-formulation *g*** (5.56 mM) in an EtOH/H_2O 1:19 solution at 298 K.

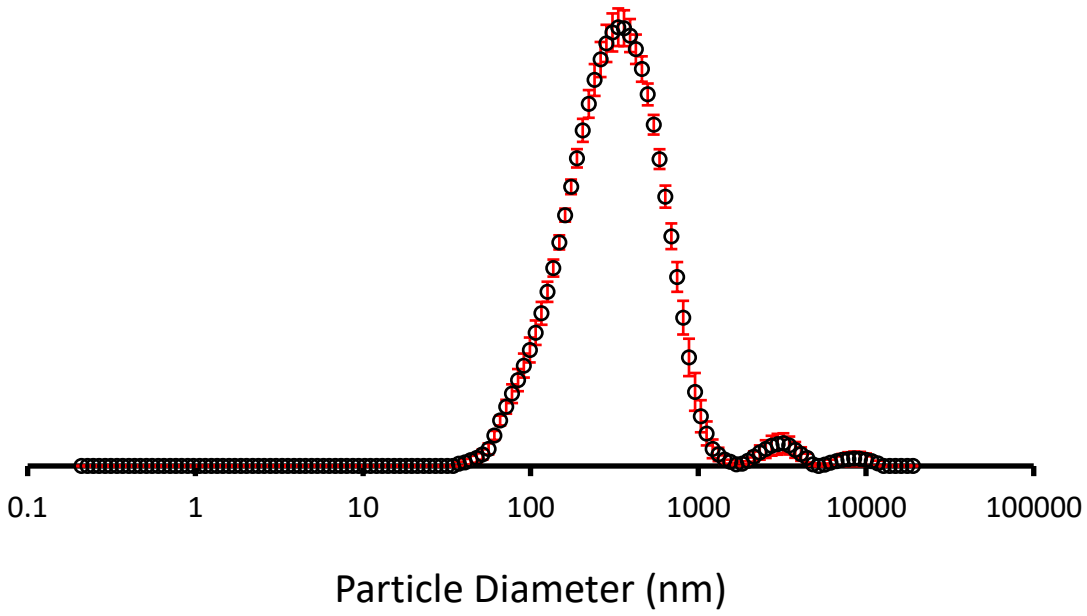

Figure S64 - The average intensity particle size distribution calculated using 10 DLS runs for **Co-formulation *h*** (5.56 mM) in an EtOH/H_2O 1:19 solution at 298 K.

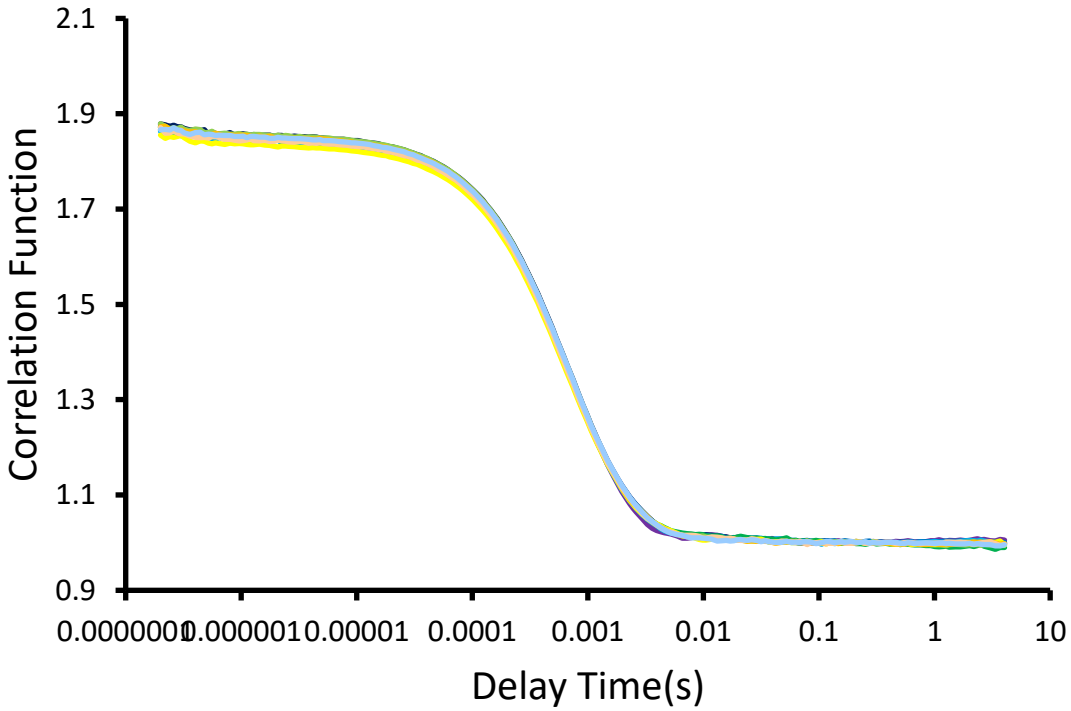

Figure S65 - Correlation function data for 10 DLS runs of **Co-formulation *h*** (5.56 mM) in an EtOH/H_2O 1:19 solution at 298 K.

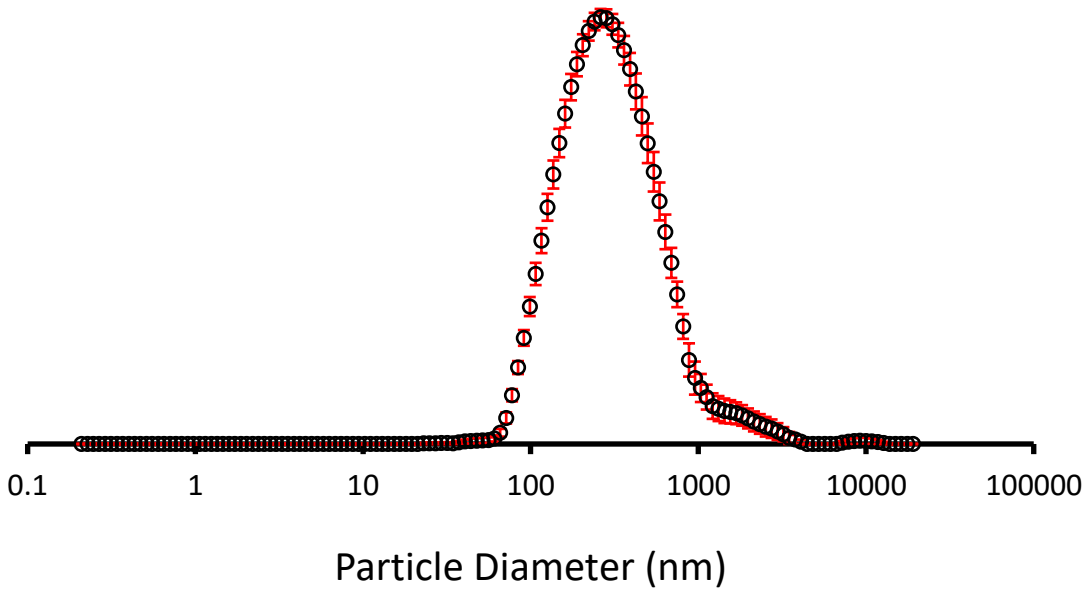

Figure S66 - The average intensity particle size distribution calculated using 10 DLS runs for **Co-formulation *k*** (5.56 mM) in an EtOH/H_2O 1:19 solution at 298 K.

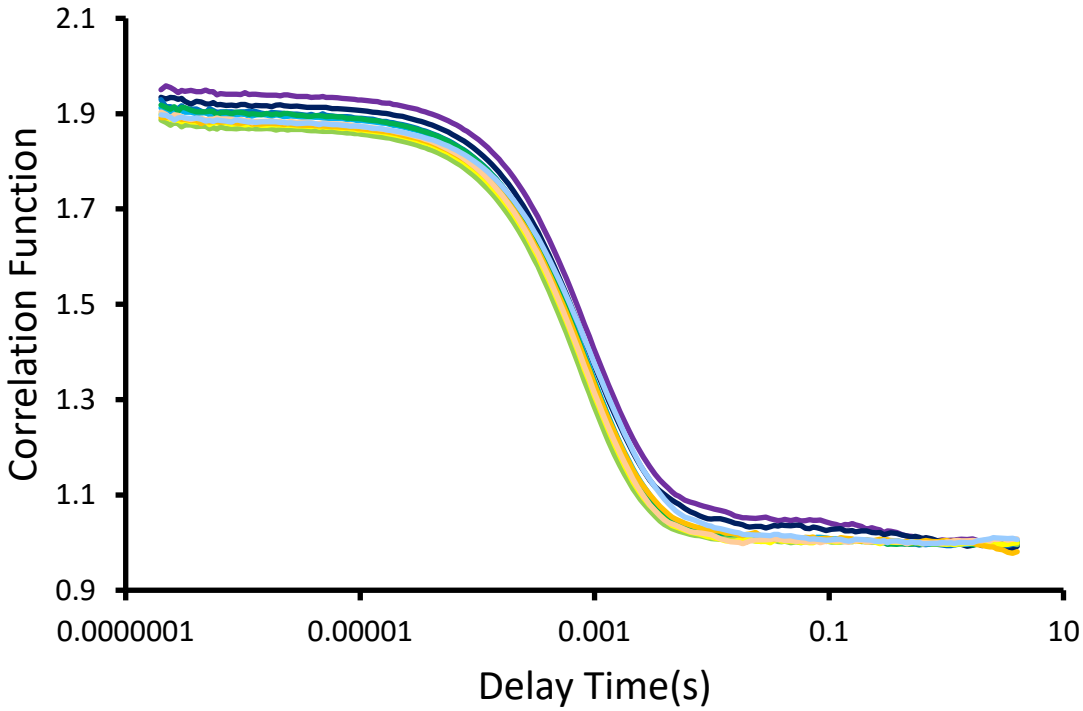

Figure S67 - Correlation function data for 10 DLS runs of **Co-formulation *k*** (5.56 mM) in an EtOH/H_2O 1:19 solution at 298 K.

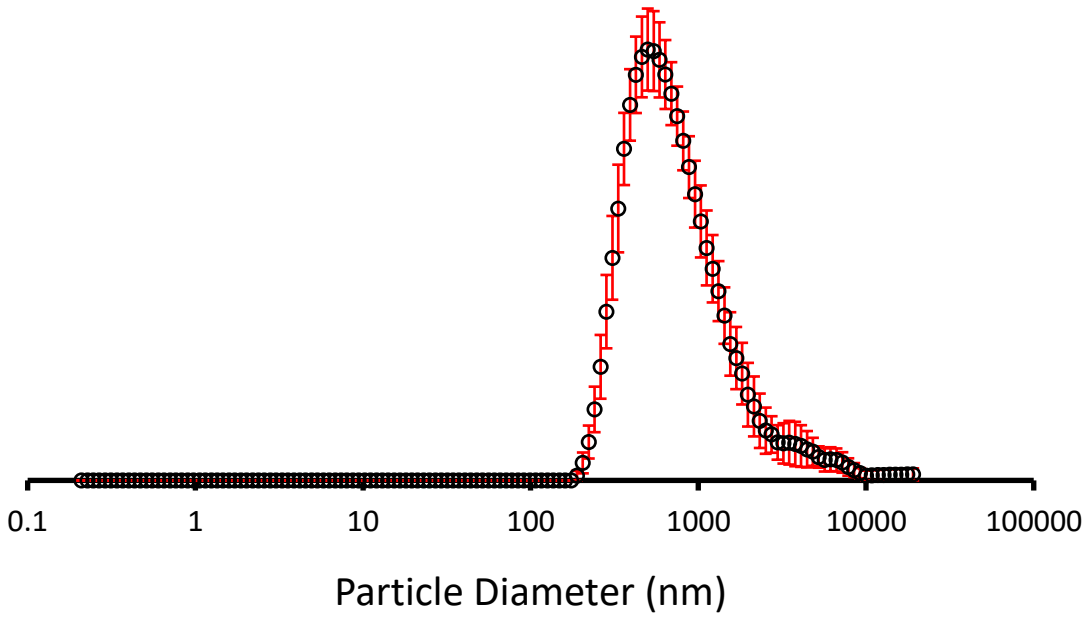

Figure S68 - The average intensity particle size distribution calculated using 10 DLS runs for **Co-formulation *I*** (5.56 mM) in an EtOH/H_2O 1:19 solution at 298 K.

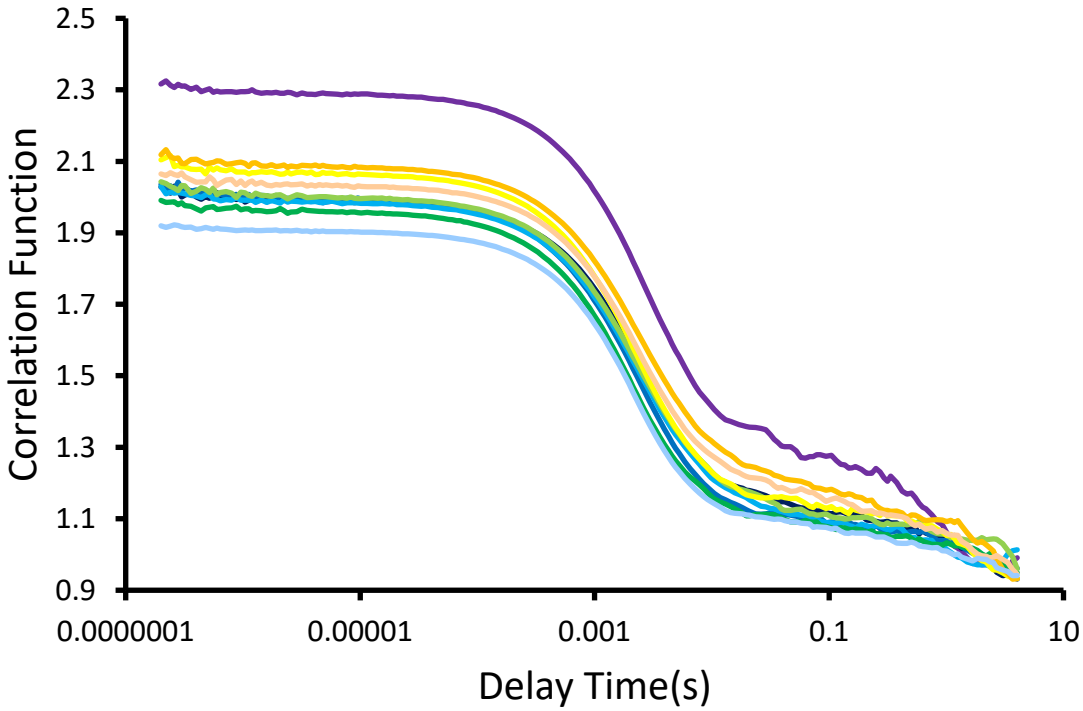

Figure S69 - Correlation function data for 10 DLS runs of **Co-formulation *I*** (5.56 mM) in an EtOH/H_2O 1:19 solution at 298 K.

Dynamic light scattering co-formulant uptake study data (obtained 20 mins post co-formulant addition)

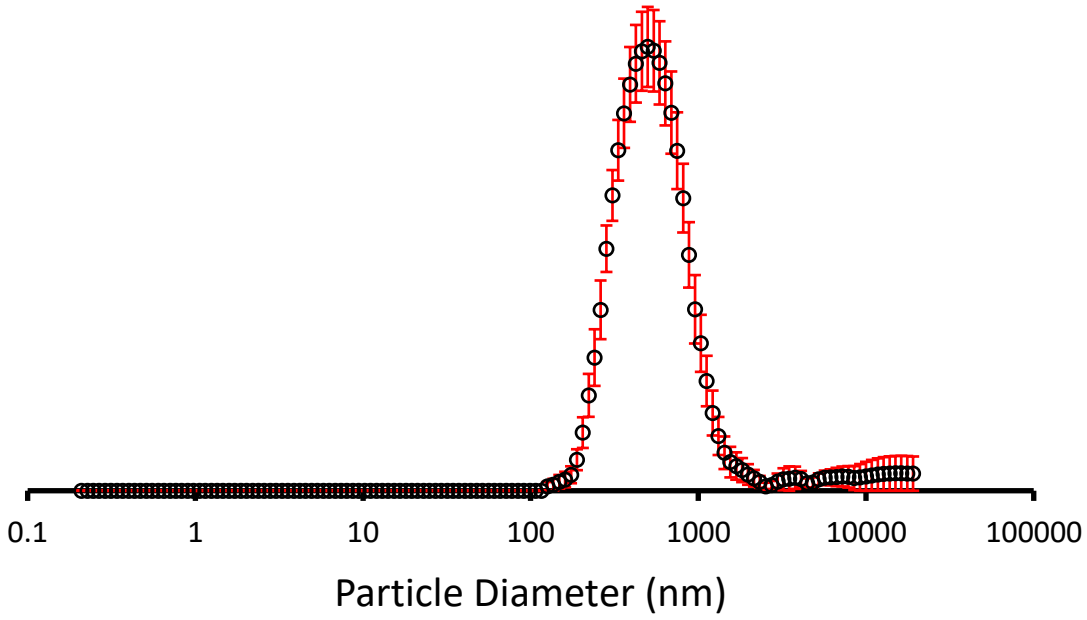

Figure S70 - The average intensity particle size distribution calculated using 9 DLS runs for **1** + **6** (5.56 mM) in a EtOH/H_2O 1:19 solution at 298 K.

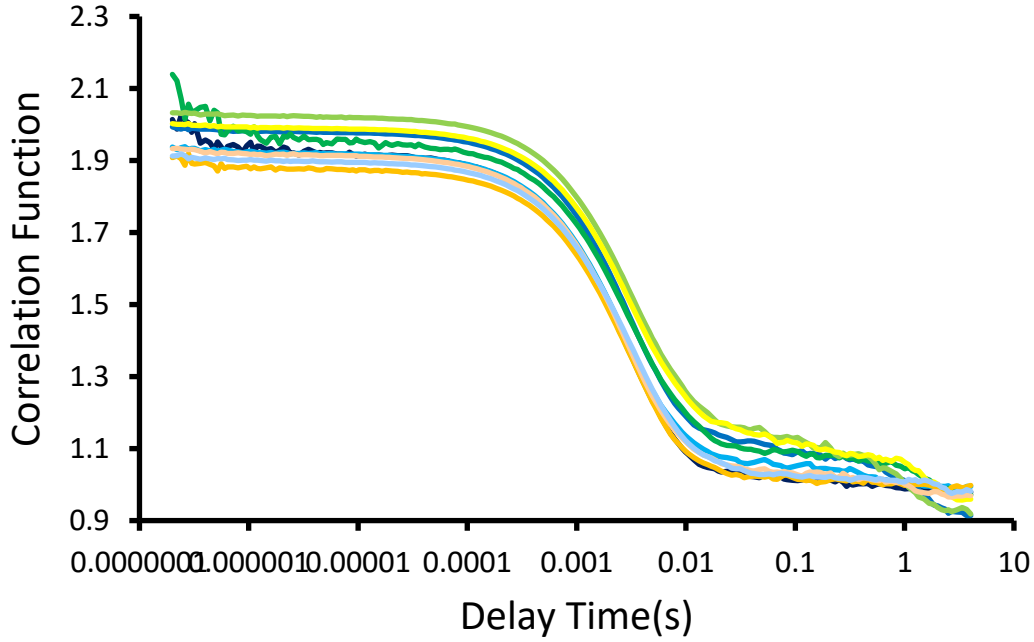

Figure S71 - Correlation function data for 9 DLS runs of **1 + 6** (5.56 mM) in a EtOH/H_2O 1:19 solution at 298 K.

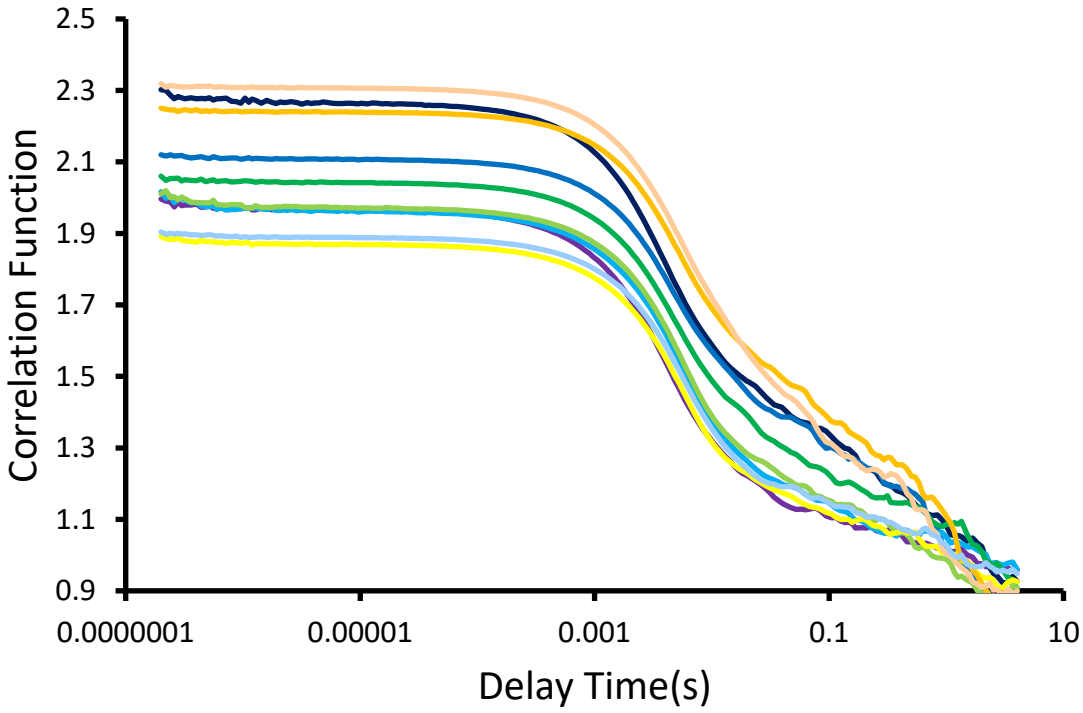

Figure S72 - Correlation function data for 10 DLS runs of **2 + 6** (5.56 mM) in a EtOH/H_2O 1:19 solution at 298 K.

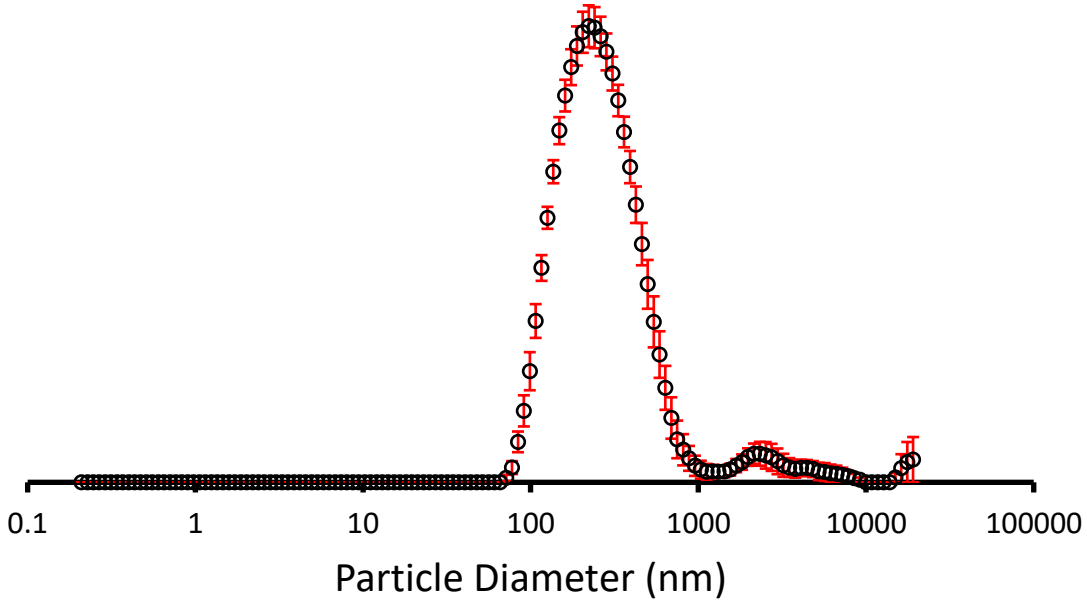

Figure S73 - The average intensity particle size distribution calculated using 10 DLS runs for **3** + **6** (5.56 mM) in a EtOH/H_2O 1:19 solution at 298 K.

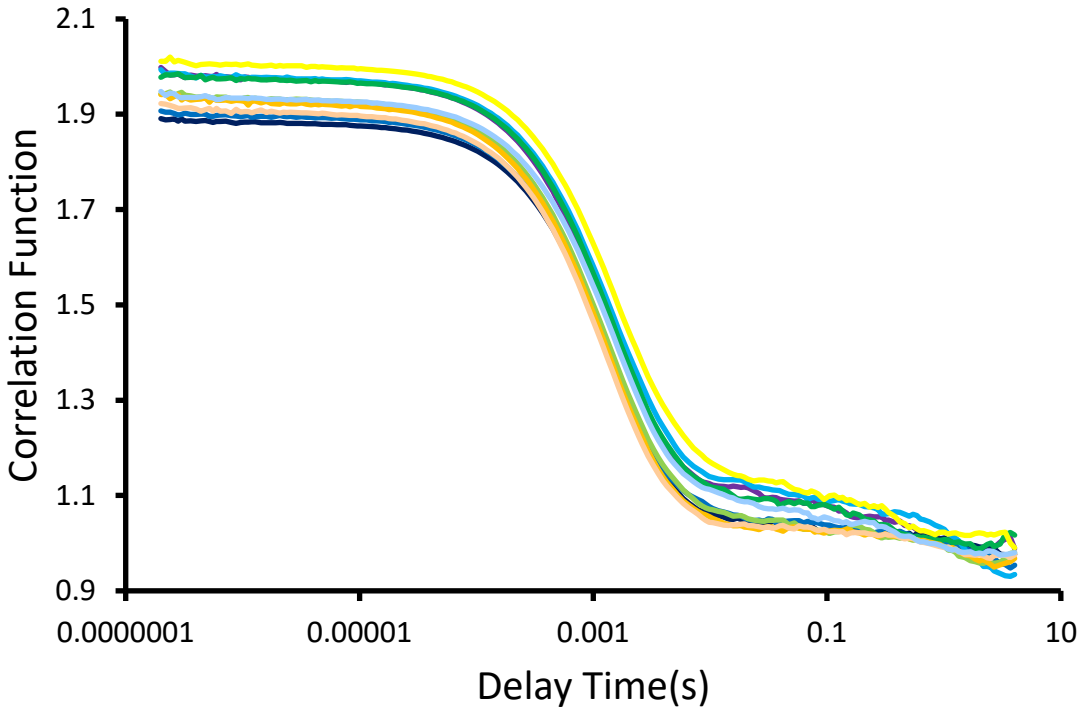

Figure S74 - Correlation function data for 10 DLS runs of **3 + 6** (5.56 mM) in a EtOH/H_2O 1:19 solution at 298 K.

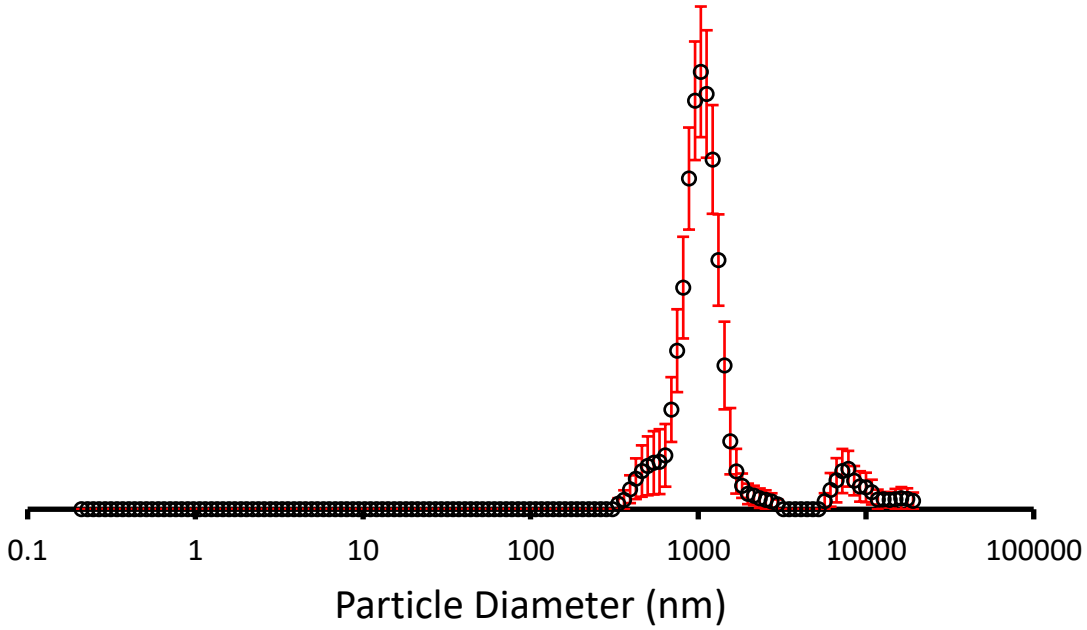

Figure S75 - The average intensity particle size distribution calculated using 8 DLS runs for **5** + **6** (5.56 mM) in a EtOH/H_2O 1:19 solution at 298 K.

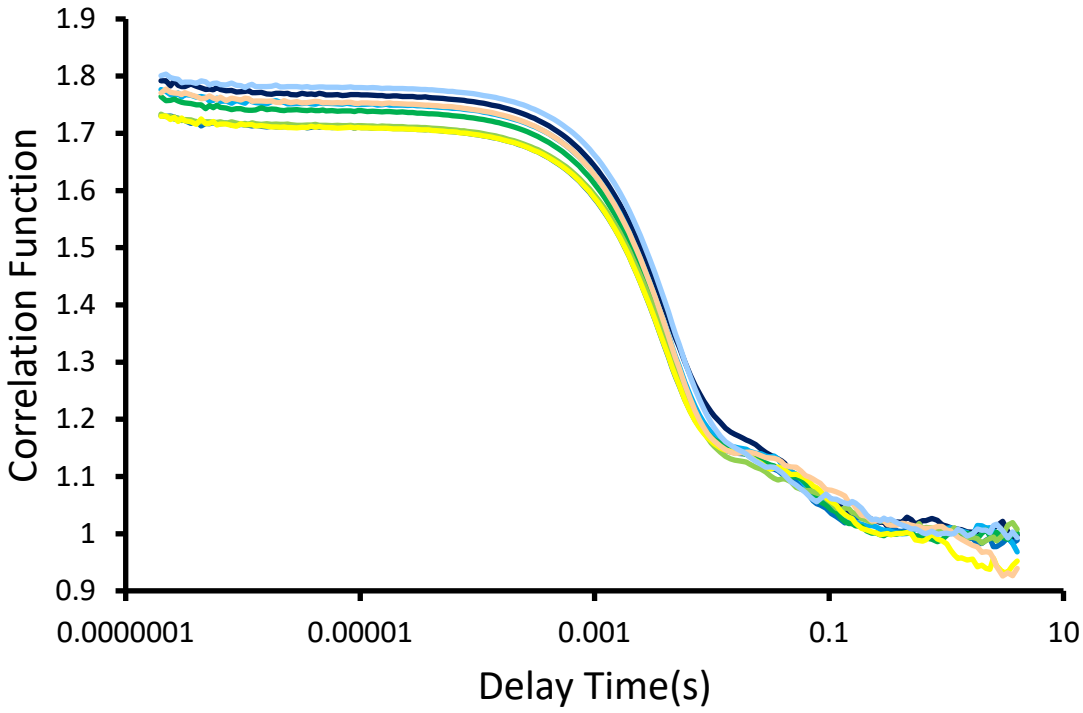

Figure S76 - Correlation function data for 8 DLS runs of **5 + 6** (5.56 mM) in a EtOH/H_2O 1:19 solution at 298 K.

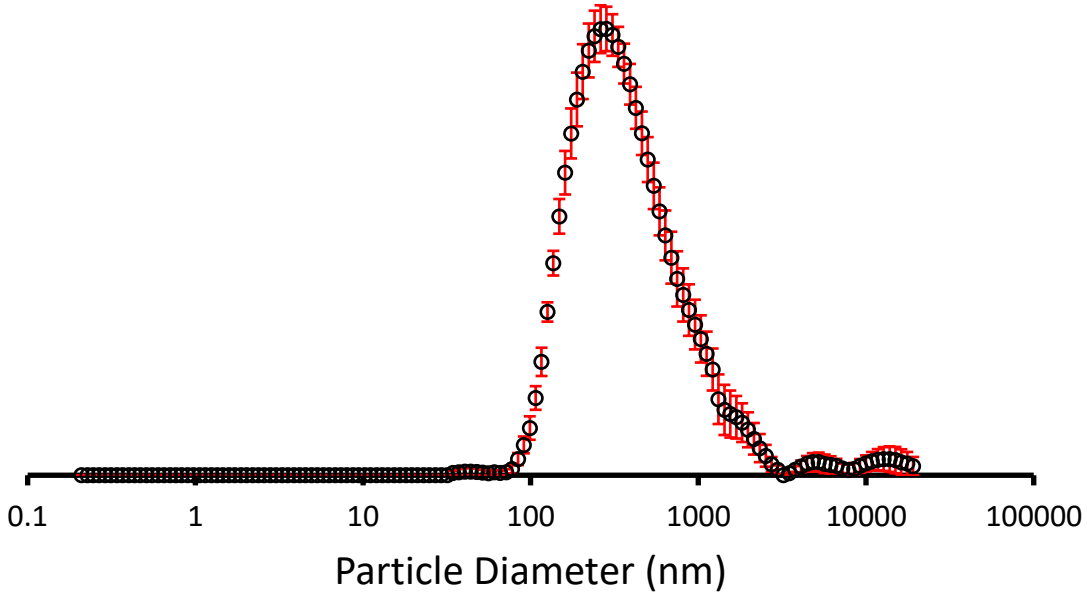

Figure S77 - The average intensity particle size distribution calculated using 10 DLS runs for **1** + **7** (5.56 mM) in a EtOH/H_2O 1:19 solution at 298 K.

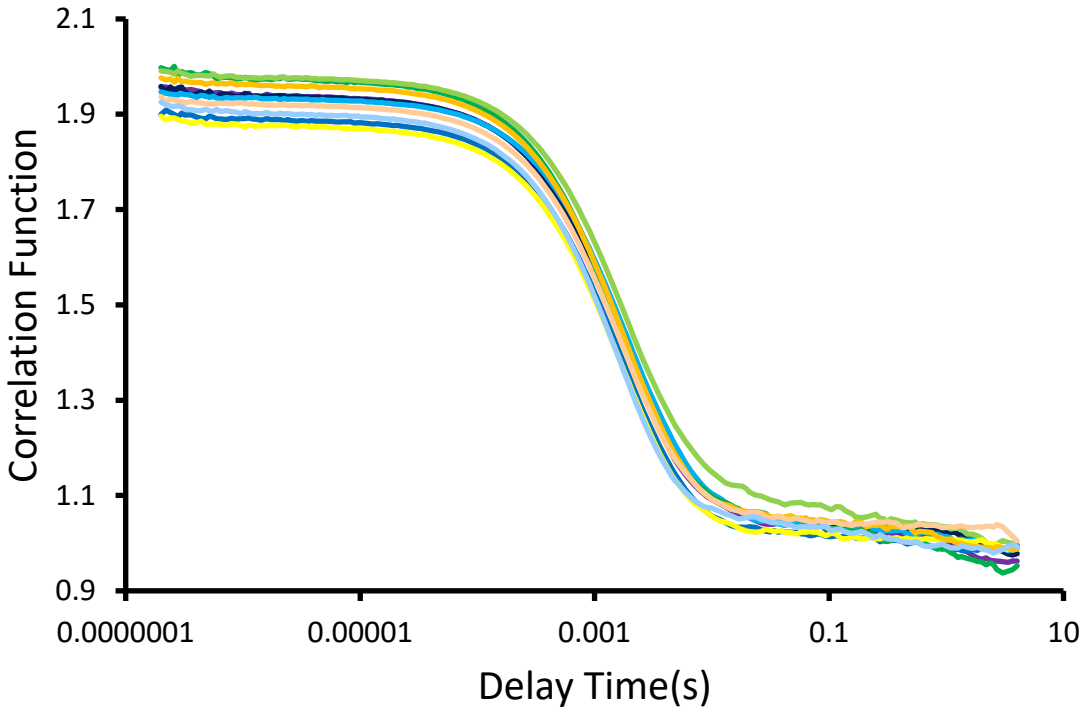

Figure S78 - Correlation function data for 10 DLS runs of **1** + **7** (5.56 mM) in a EtOH/H_2O 1:19 solution at 298 K.

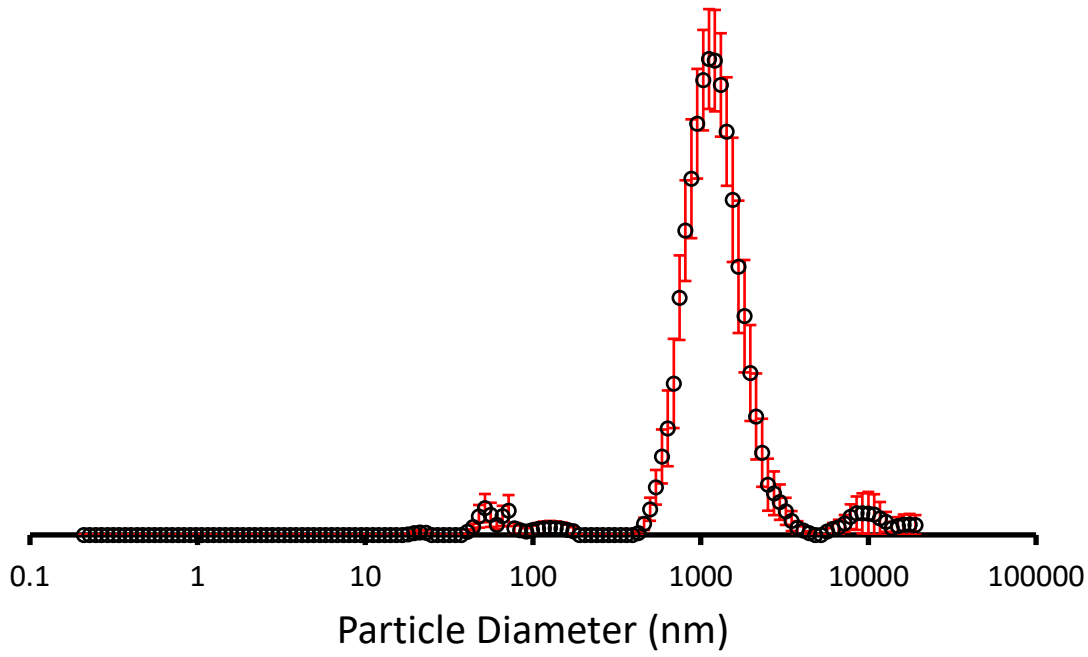

Figure S79 - The average intensity particle size distribution calculated using 10 DLS runs for **2** + **7** (5.56 mM) in a EtOH/H_2O 1:19 solution at 298 K.

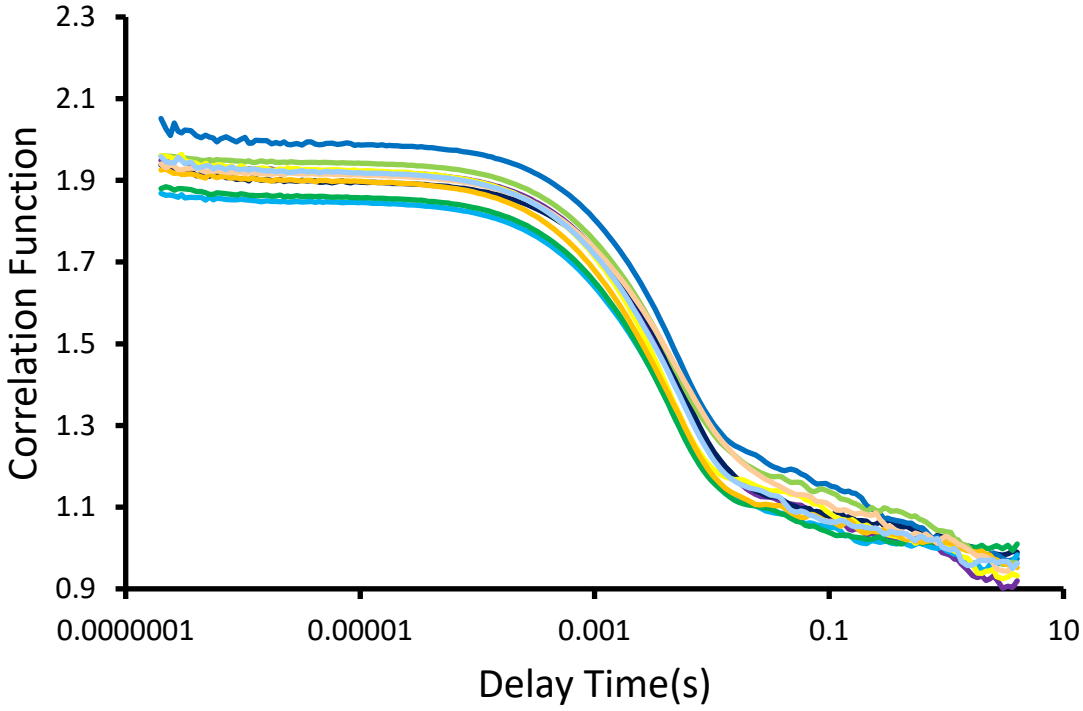

Figure S80 - Correlation function data for 10 DLS runs of **2 + 7** (5.56 mM) in a EtOH/H_2O 1:19 solution at 298 K.

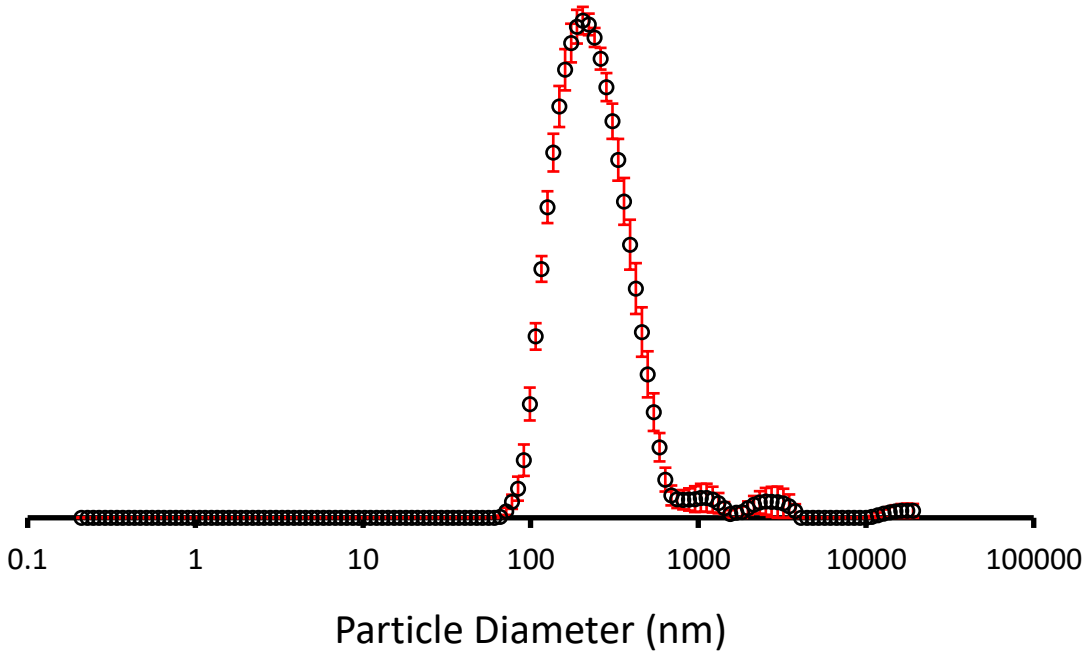

Figure S81 - The average intensity particle size distribution calculated using 10 DLS runs for **3** + **7** (5.56 mM) in a EtOH/H_2O 1:19 solution at 298 K.

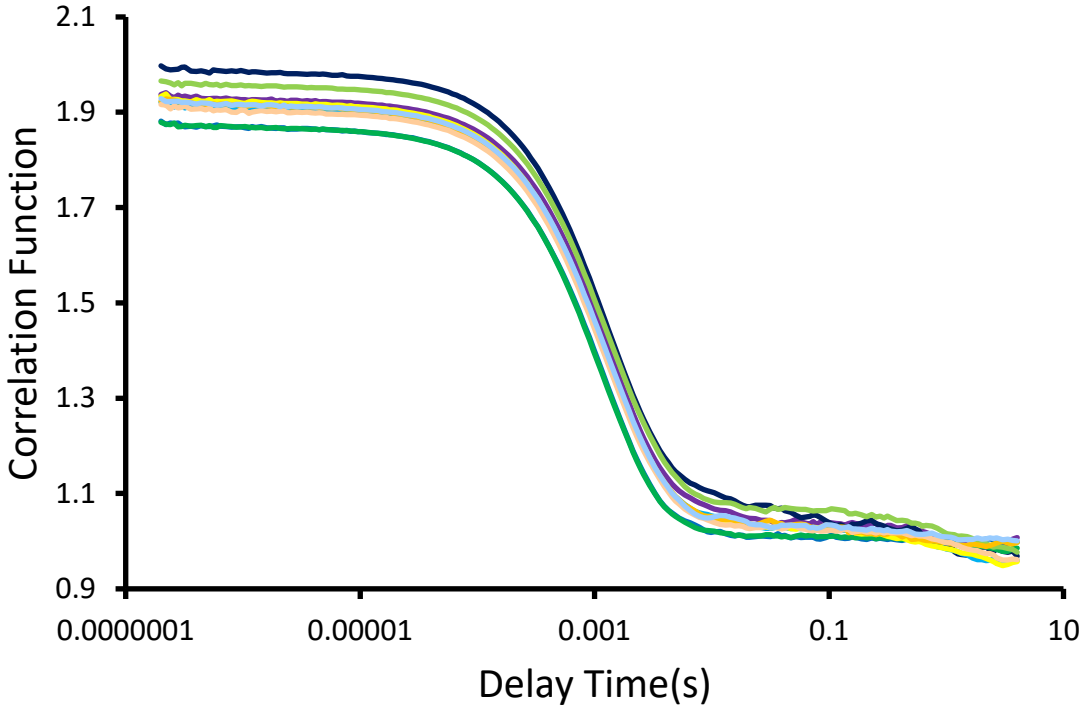

Figure S82 - Correlation function data for 10 DLS runs of **3 + 7** (5.56 mM) in a EtOH/H_2O 1:19 solution at 298 K.

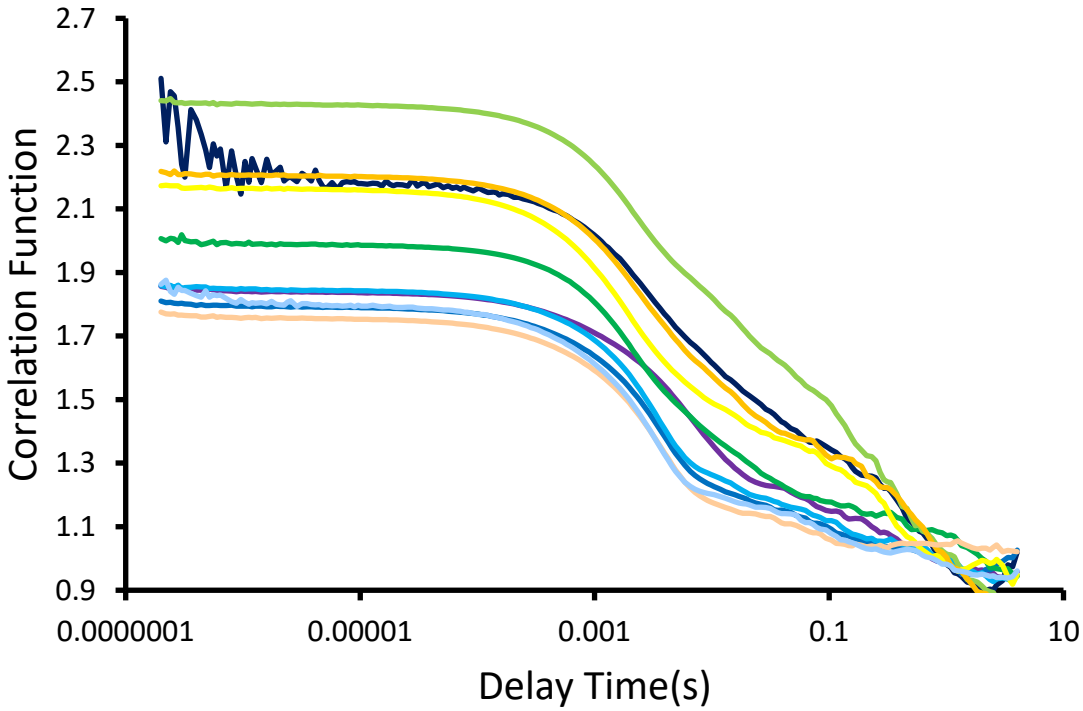

Figure S83 - Correlation function data for 10 DLS runs of **5 + 7** (5.56 mM) in a EtOH/H_2O 1:19 solution at 298 K.

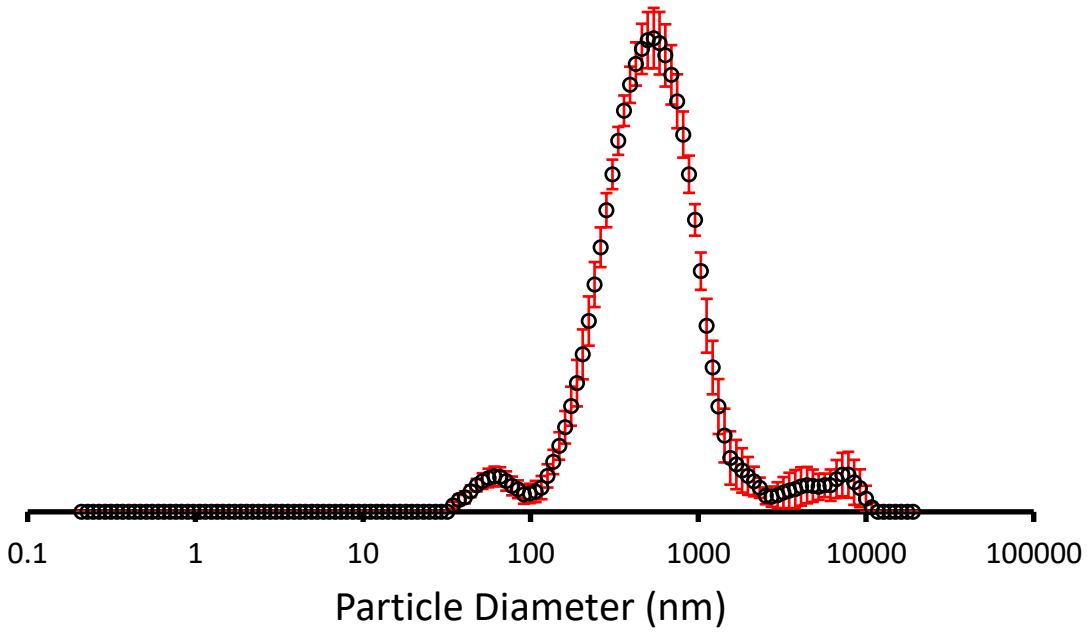

Figure S84 - The average intensity particle size distribution calculated using 10 DLS runs for **1** + **8** (5.56 mM) in a EtOH/H_2O 1:19 solution at 298 K.

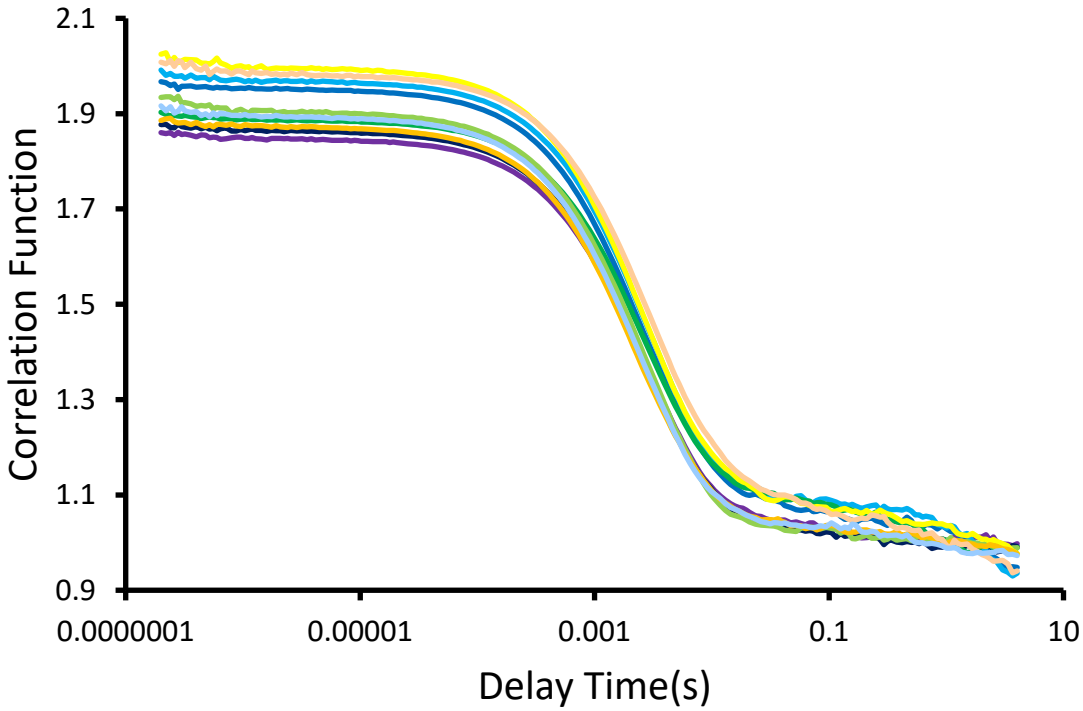

Figure S85 - Correlation function data for 10 DLS runs of **1 + 8** (5.56 mM) in a EtOH/H_2O 1:19 solution at 298 K.

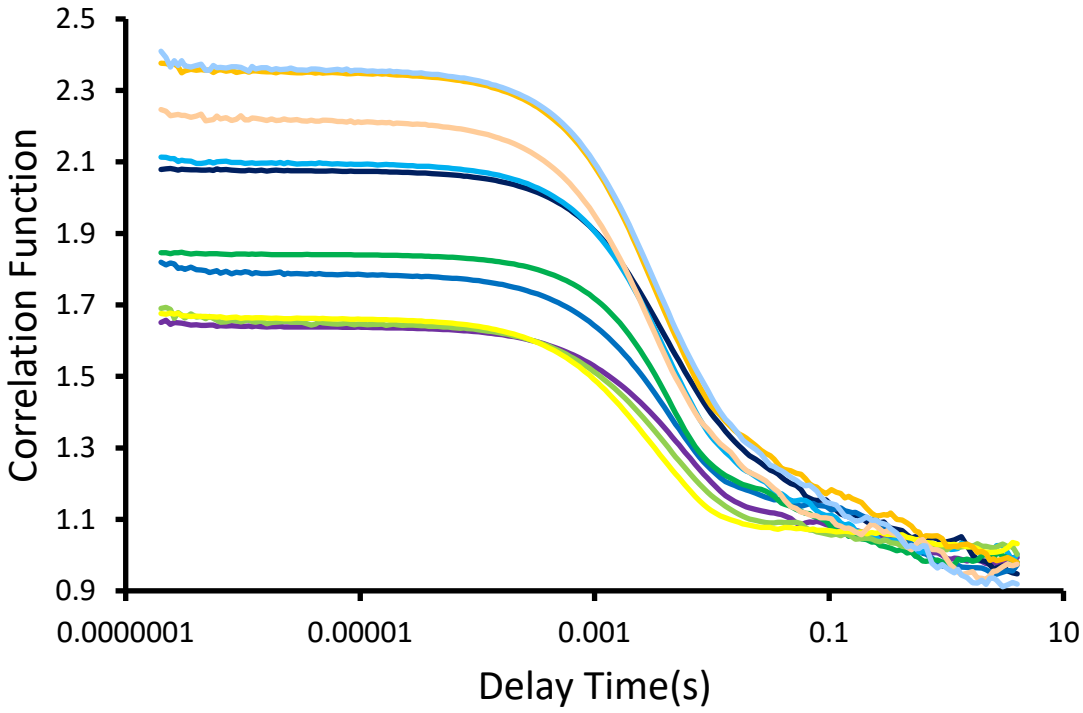

Figure S86 - Correlation function data for 10 DLS runs of **2 + 8** (5.56 mM) in a EtOH/H_2O 1:19 solution at 298 K.

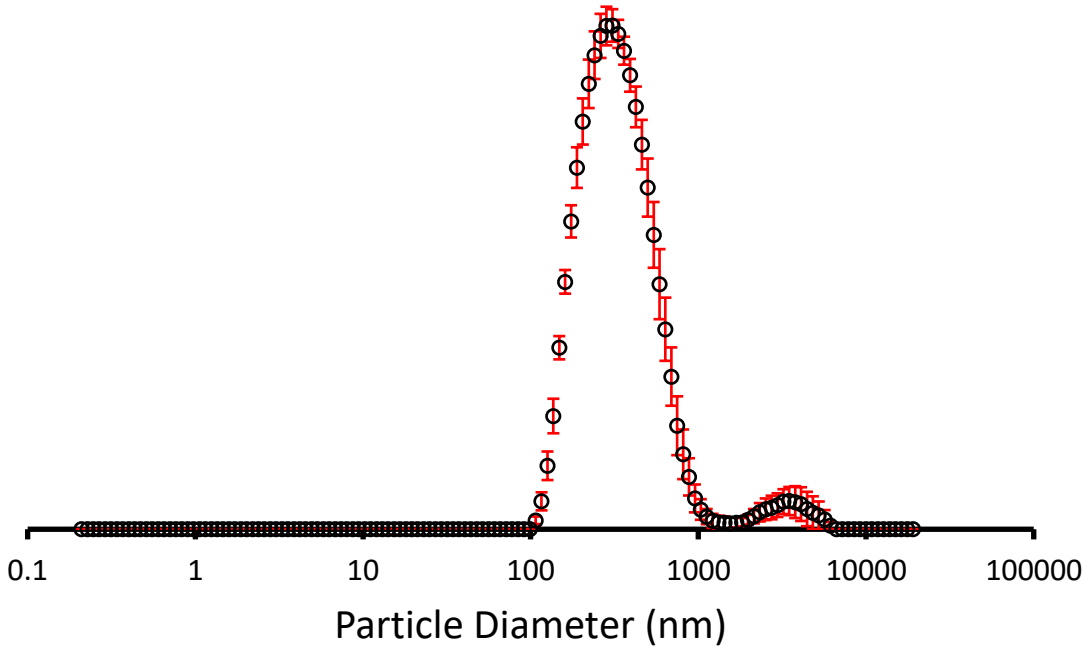

Figure S87 - The average intensity particle size distribution calculated using 10 DLS runs for **3** + **8** (5.56 mM) in a EtOH/H_2O 1:19 solution at 298 K.

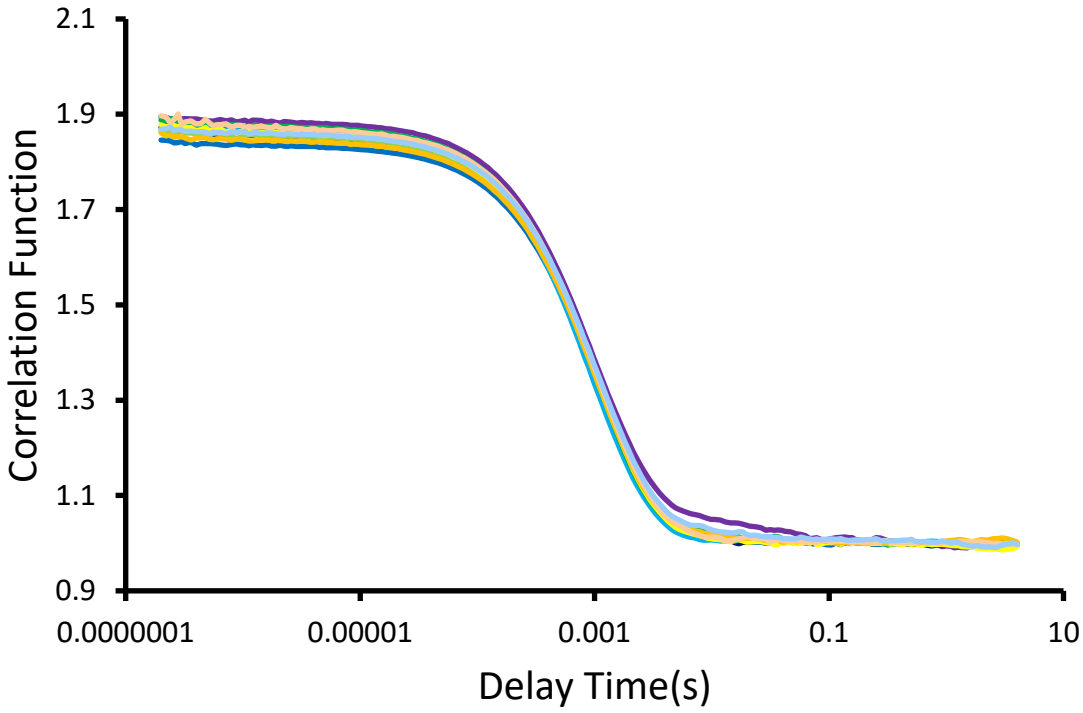

Figure S88 - Correlation function data for 10 DLS runs of **3** + **8** (5.56 mM) in a EtOH/H_2O 1:19 solution at 298 K.

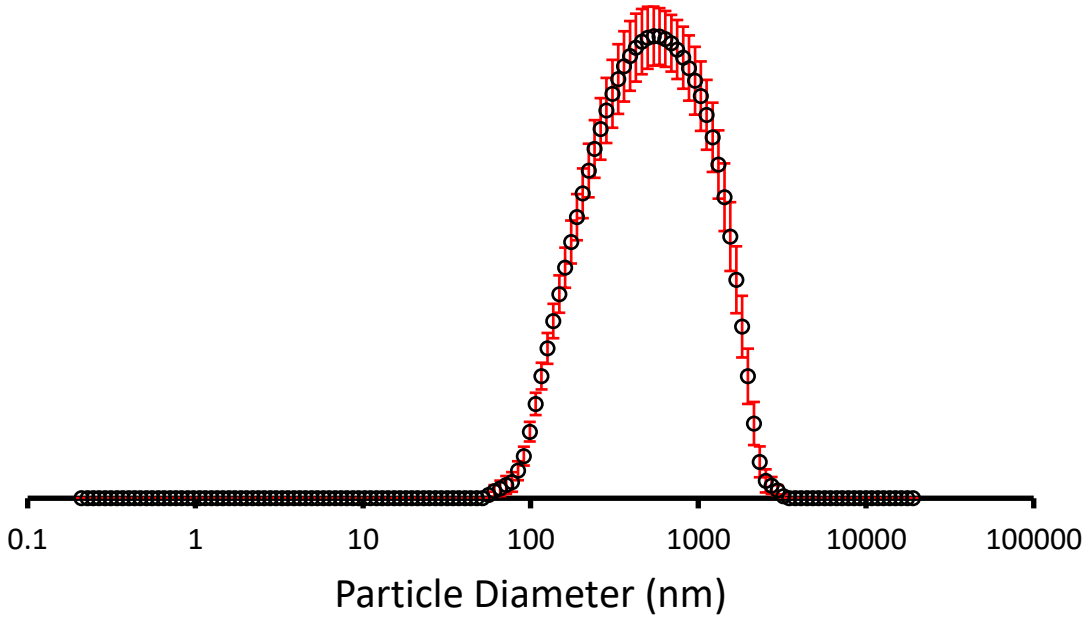

Figure S89 - The average intensity particle size distribution calculated using 10 DLS runs for **5** + **8** (5.56 mM) in a EtOH/H_2O 1:19 solution at 298 K.

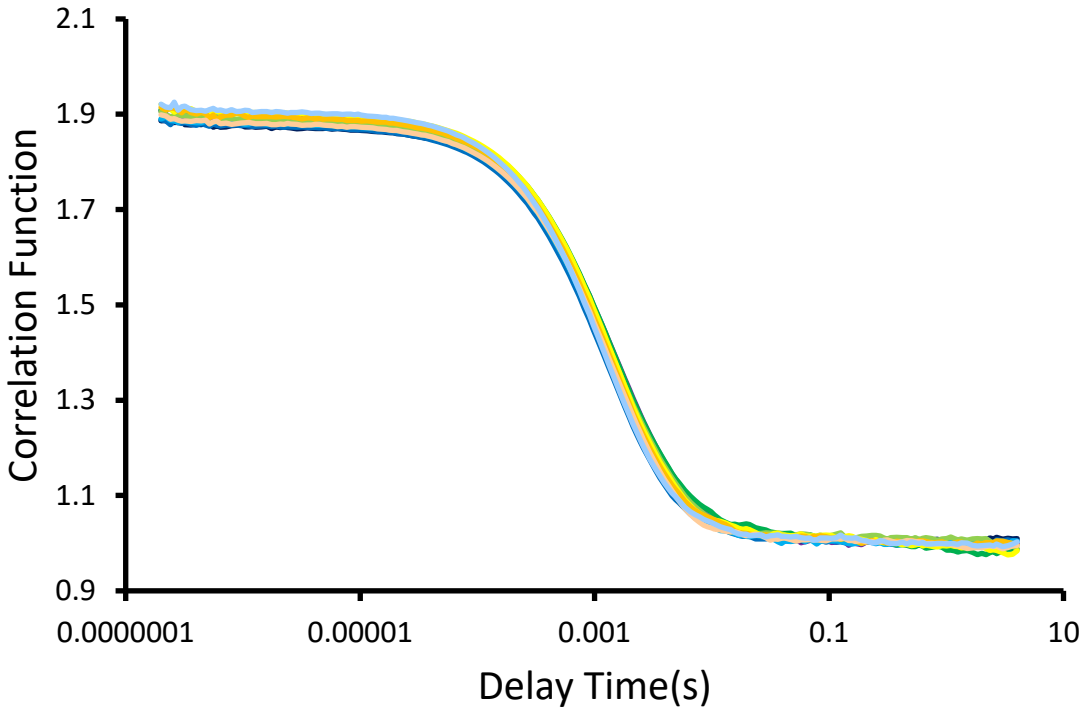

Figure S90 - Correlation function data for 10 DLS runs of **5 + 8** (5.56 mM) in a EtOH/H_2O 1:19 solution at 298 K.

Zeta potential data

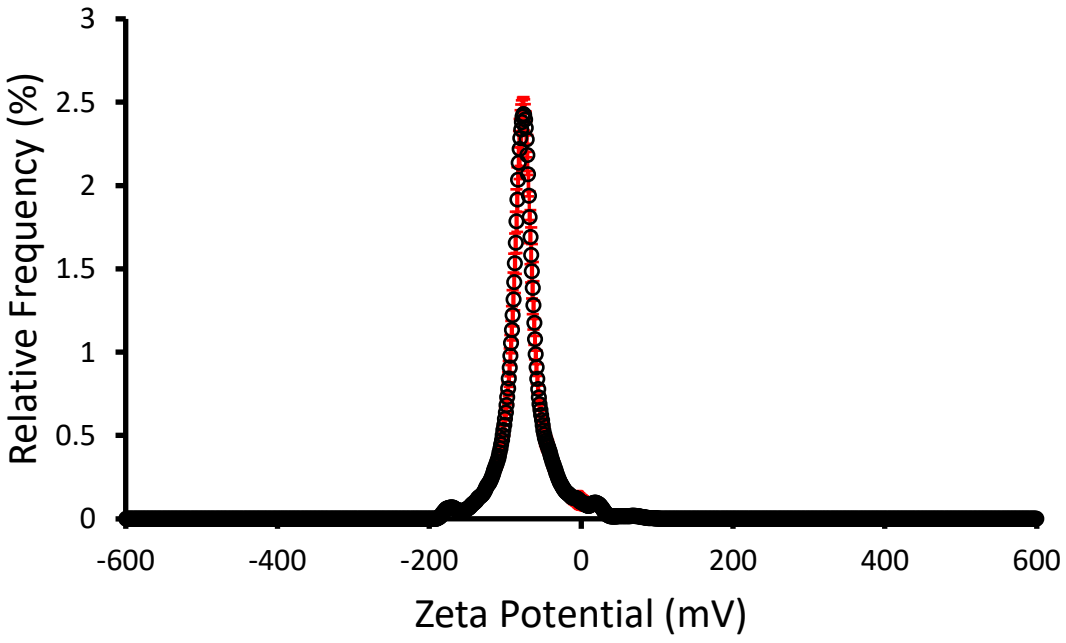

Figure S91 - The average zeta potential distribution calculated using 10 runs for **4** (5.56 mM) in an EtOH/H_2O 1:19 solution at 298 K. Average measurement value -68.16 mV.

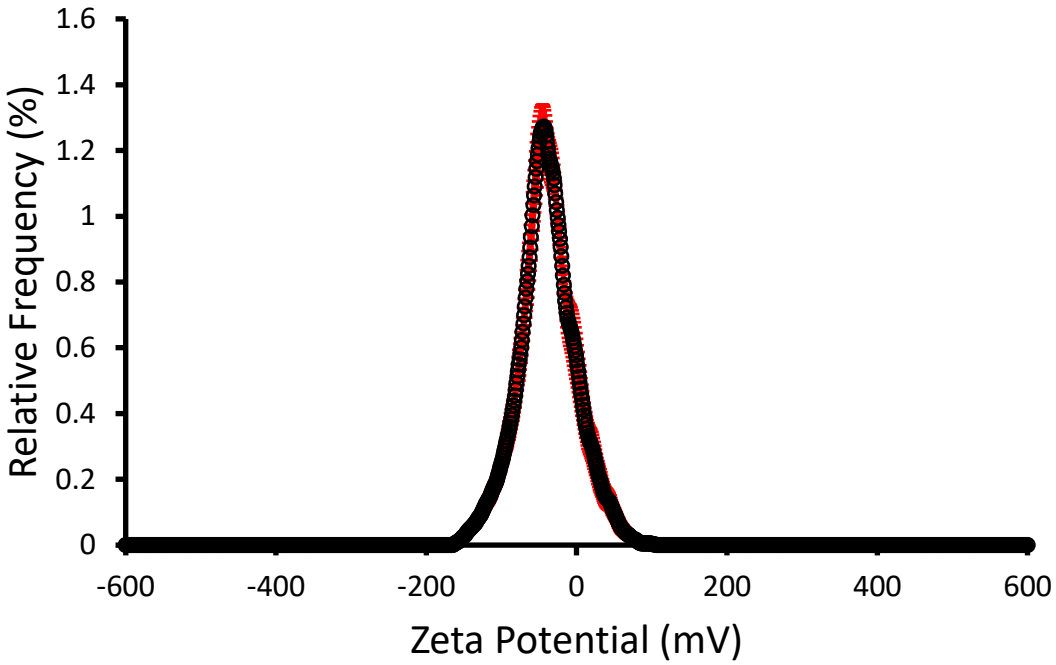

Figure S92 - The average zeta potential distribution calculated using 10 runs for **5** (5.56 mM) in an EtOH/H_2O 1:19 solution at 298 K. Average measurement value -45.45 mV.

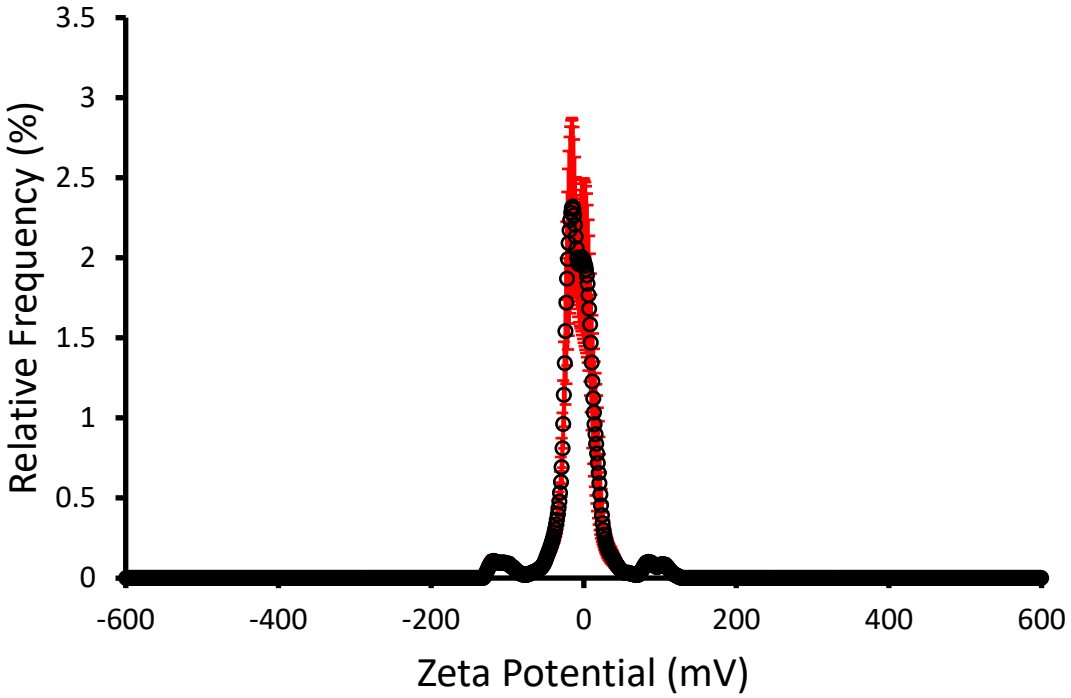

Figure S93 - The average zeta potential distribution calculated using 10 runs for **3** (5.56 mM) in an EtOH/H_2O 1:19 solution at 298 K. Average measurement value -0.95 mV.

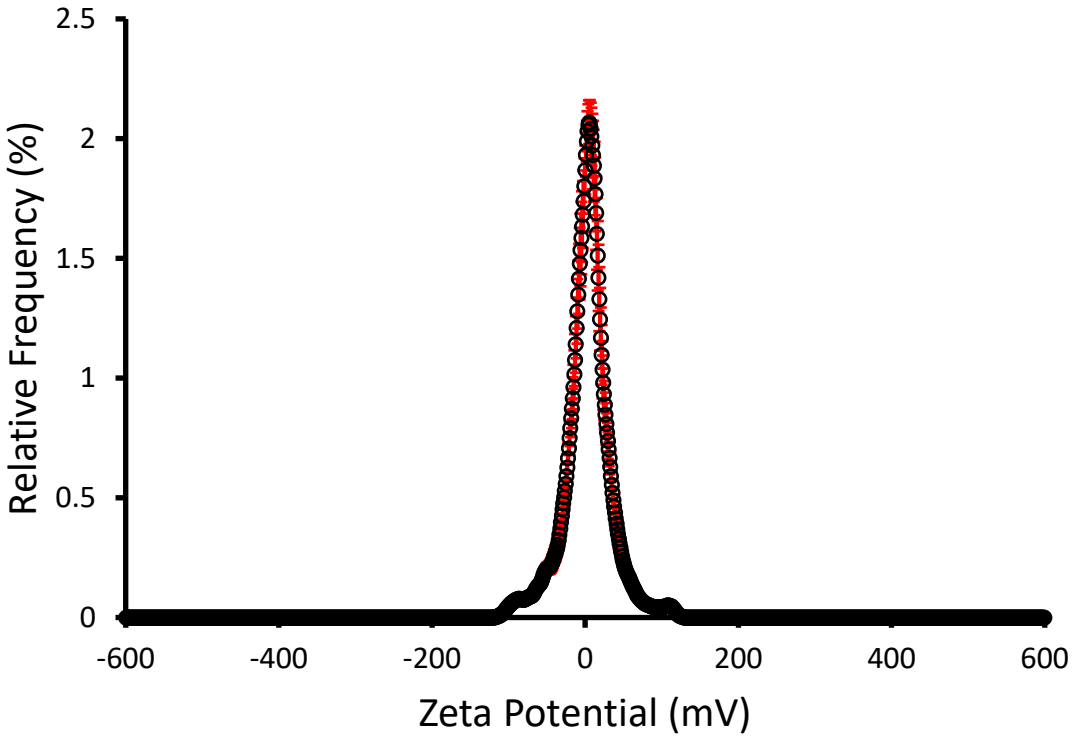

Figure S94 - The average zeta potential distribution calculated using 10 runs for **Co-formulation *c*** (5.56 mM) in an EtOH/H_2O 1:19 solution at 298 K. Average measurement value -11.15 mV.

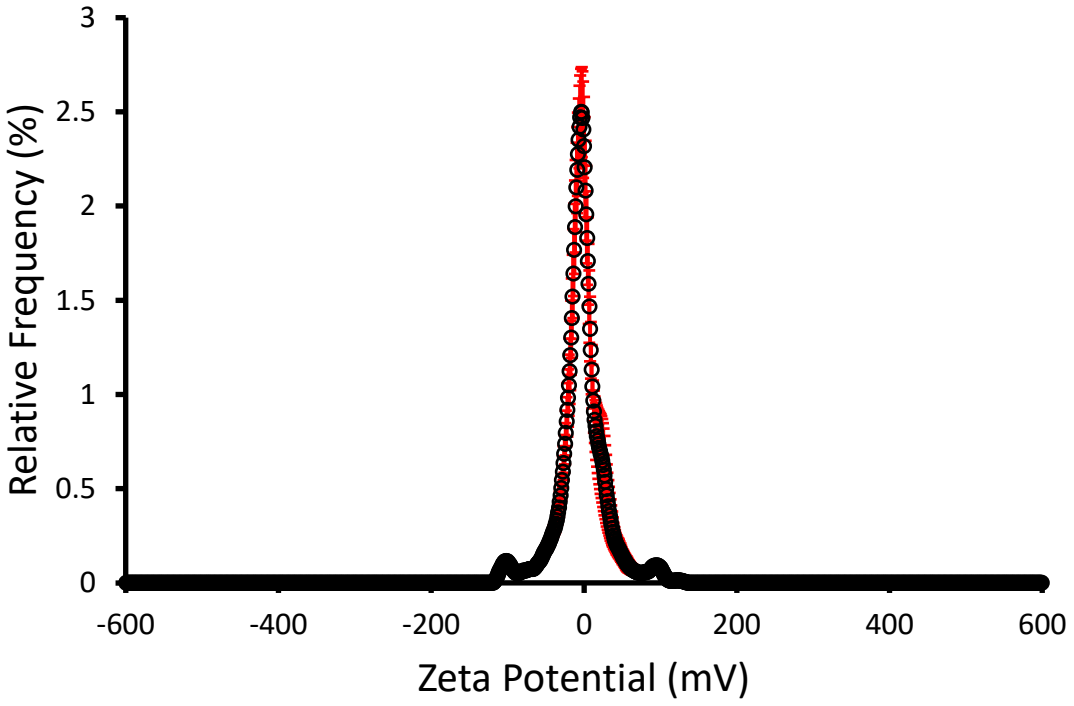

Figure S95 - The average zeta potential distribution calculated using 10 runs for **Co-formulation *d*** (5.56 mM) in an EtOH/H_2O 1:19 solution at 298 K. Average measurement value -7.42 mV.

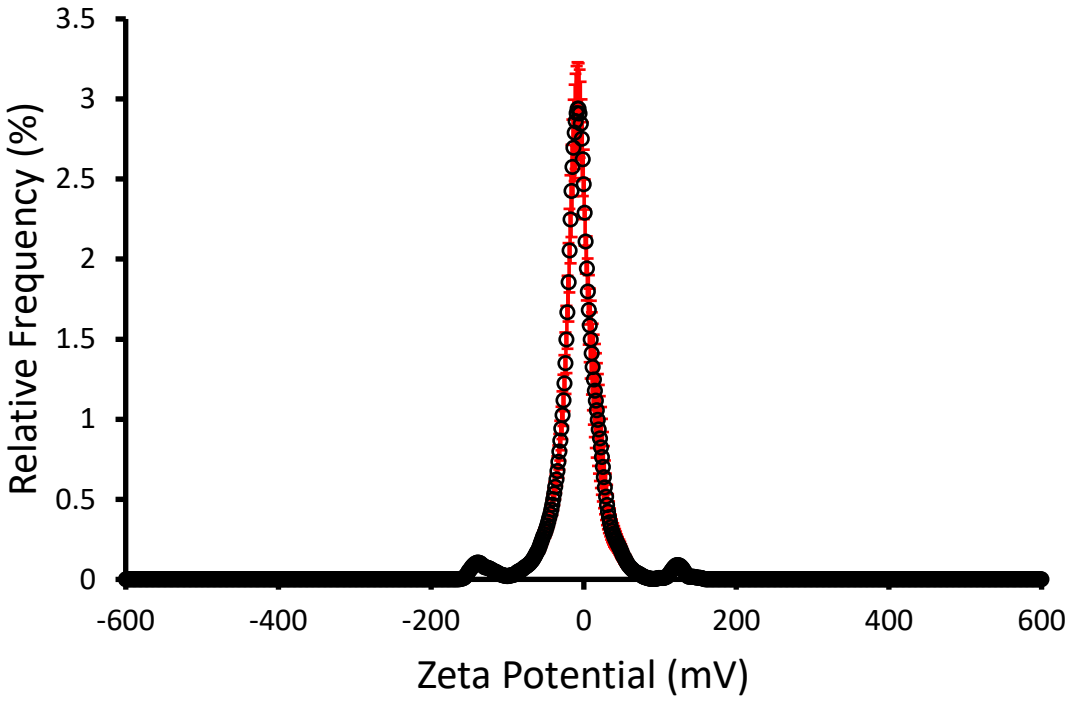

Figure S96 - The average zeta potential distribution calculated using 10 runs for **Co-formulation *g*** (5.56 mM) in an EtOH/H_2O 1:19 solution at 298 K. Average measurement value -5.35 mV.

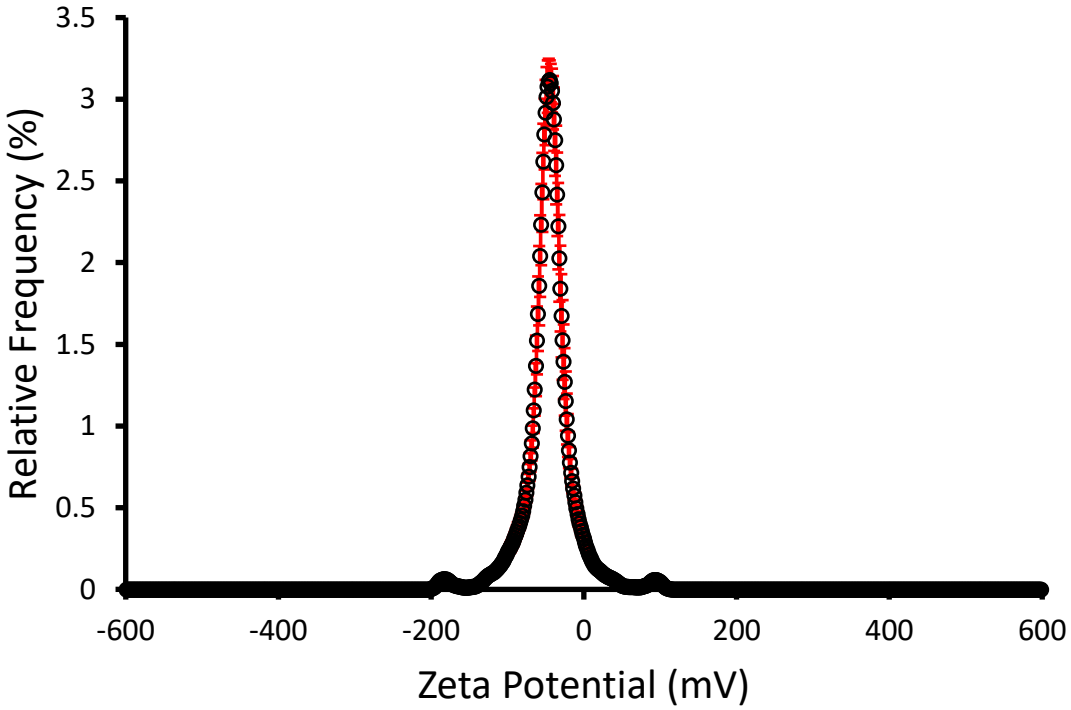

Figure S97 - The average zeta potential distribution calculated using 10 runs for **Co-formulation *h*** (5.56 mM) in an EtOH/H_2O 1:19 solution at 298 K. Average measurement value -39.14 mV.

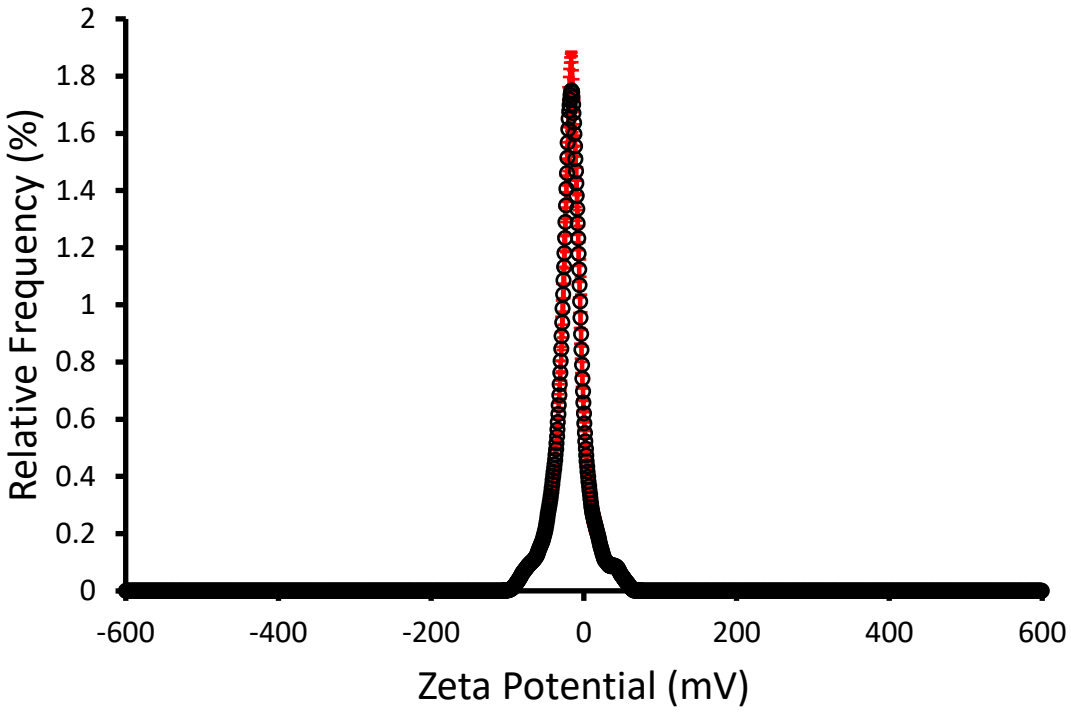

Figure S98 - The average zeta potential distribution calculated using 10 runs for **Co-formulation *k*** (5.56 mM) in an EtOH/H_2O 1:19 solution at 298 K. Average measurement value -18.51 mV.

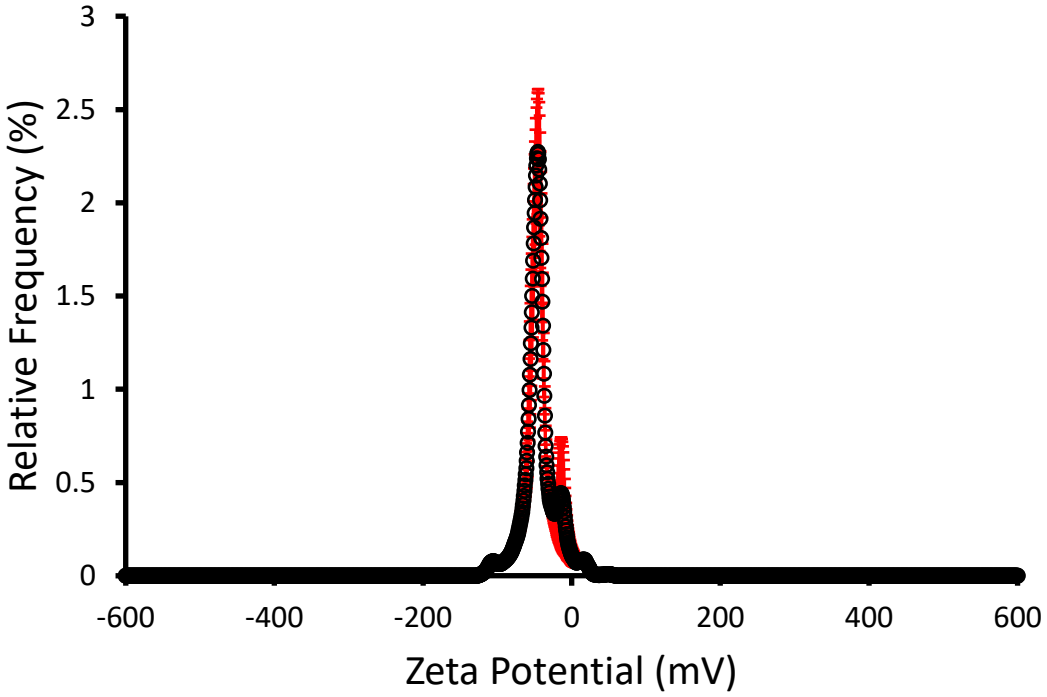

Figure S99 - The average zeta potential distribution calculated using 10 runs for **Co-formulation *l*** (5.56 mM) in an EtOH/H_2O 1:19 solution at 298 K. Average measurement value -15.32 mV.

Zeta potential co-formulant uptake study data (obtained 20 mins post co-formulant addition)

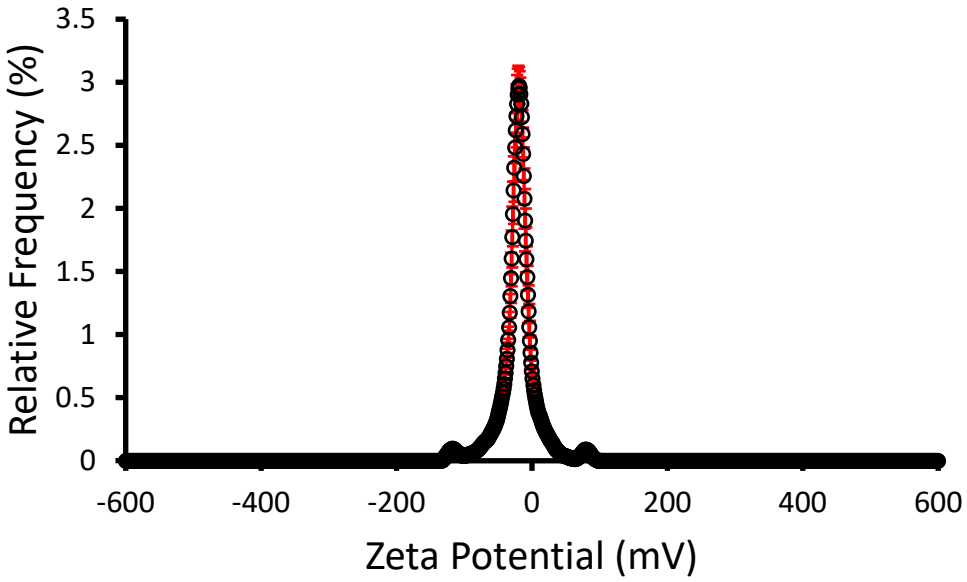

Figure S100 - The average zeta potential distribution calculated using 10 runs for **1 + 6** (5.56 mM) in an EtOH/H_2O 1:19 solution at 298 K. Average measurement value -17.69 mV.

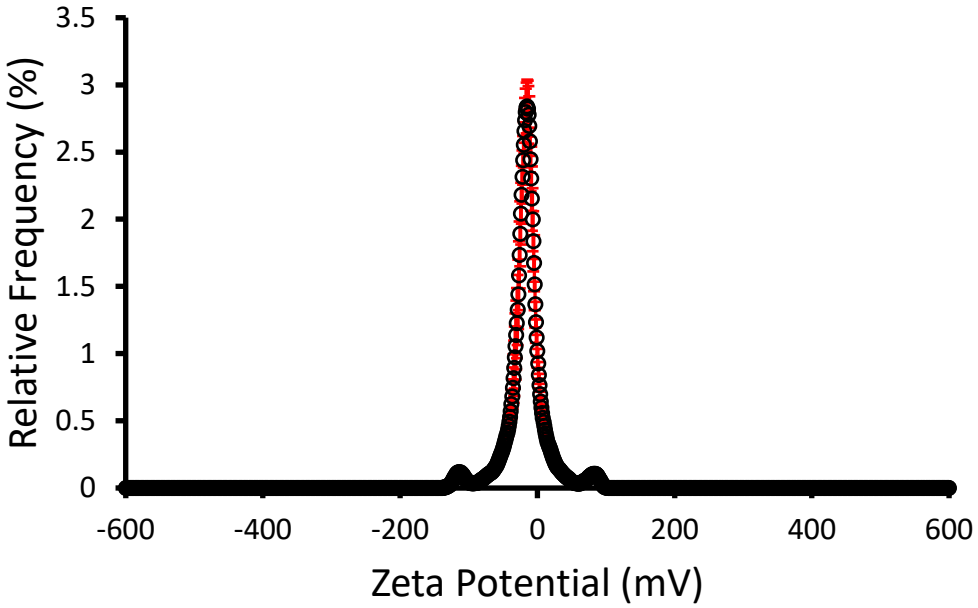

Figure S101 - The average zeta potential distribution calculated using 10 runs for **2 + 6** (5.56 mM) in an EtOH/H_2O 1:19 solution at 298 K. Average measurement value -16.11 mV.

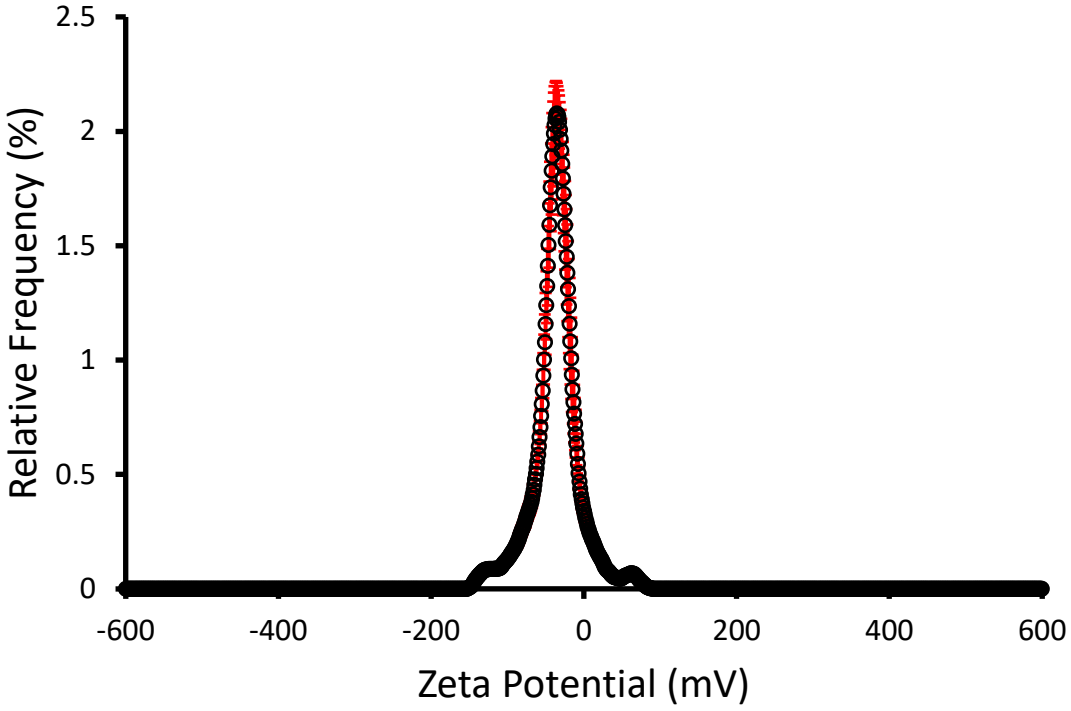

Figure S102 - The average zeta potential distribution calculated using 10 runs for **3 + 6** (5.56 mM) in an EtOH/H_2O 1:19 solution at 298 K. Average measurement value -32.21 mV.

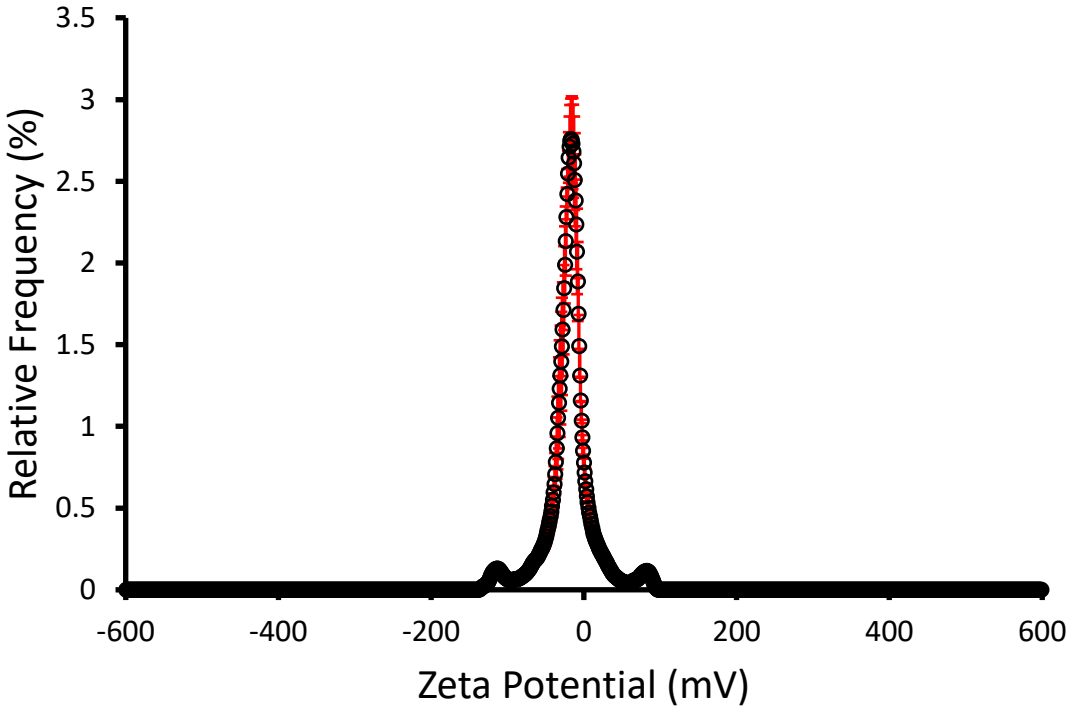

Figure S103 - The average zeta potential distribution calculated using 10 runs for **5 + 6** (5.56 mM) in an EtOH/H_2O 1:19 solution at 298 K. Average measurement value -17.99 mV.

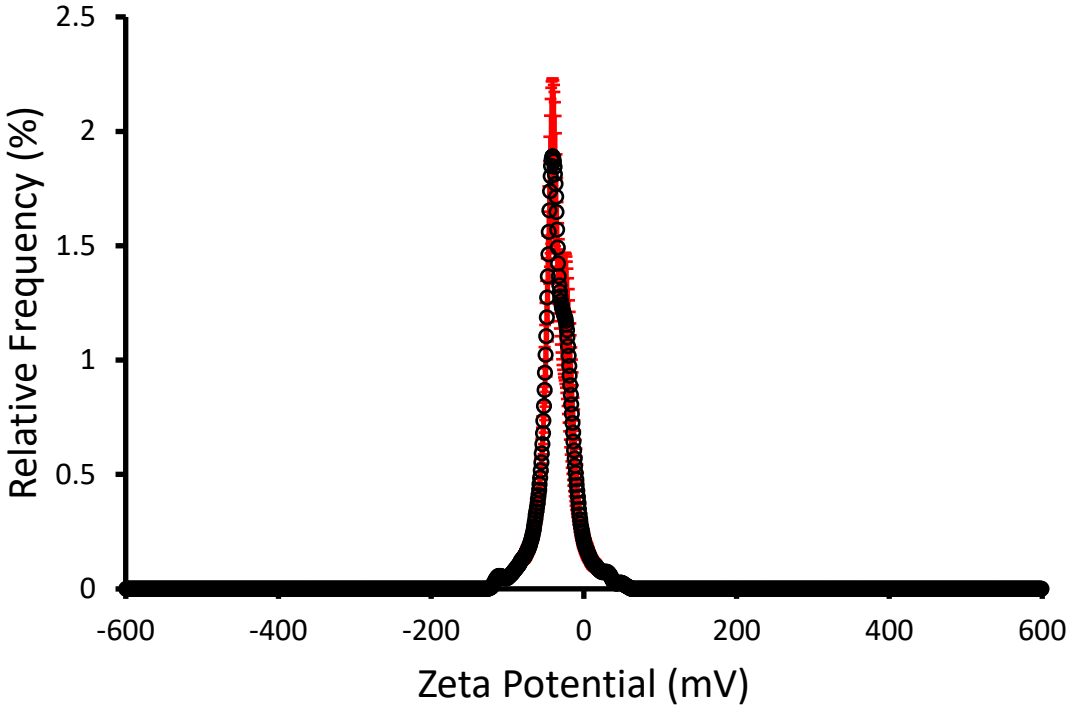

Figure S104 - The average zeta potential distribution calculated using 10 runs for **1 + 7** (5.56 mM) in an EtOH/H_2O 1:19 solution at 298 K. Average measurement value -23.20 mV.

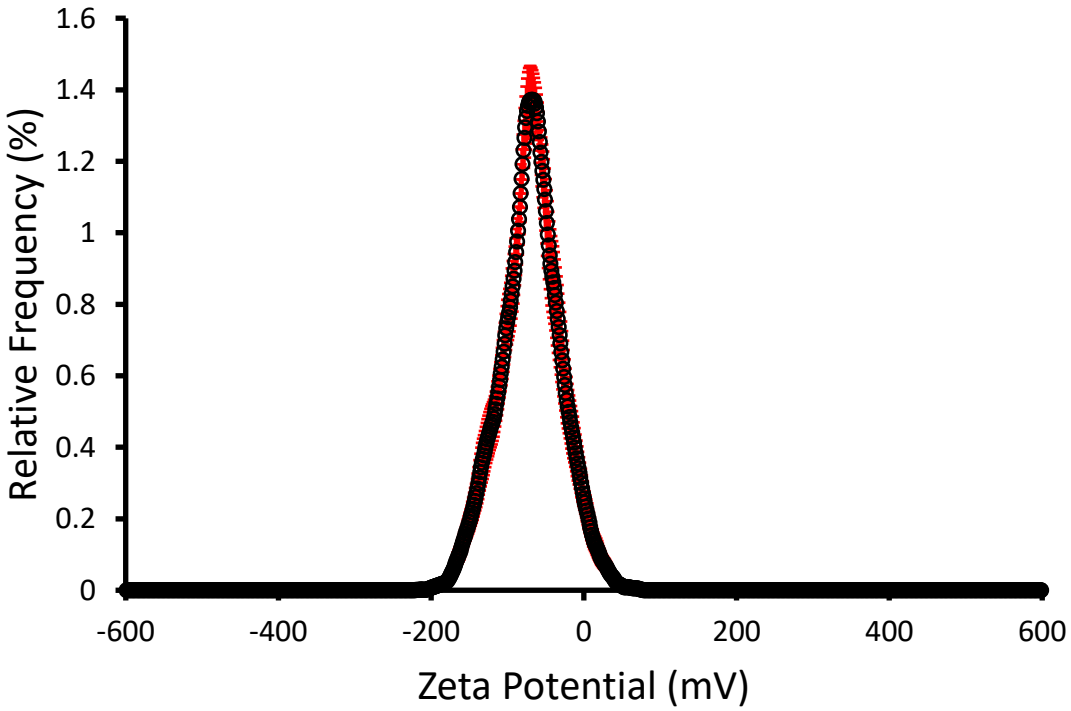

Figure S105 - The average zeta potential distribution calculated using 10 runs for **2 + 7** (5.56 mM) in an EtOH/H_2O 1:19 solution at 298 K. Average measurement value -46.86 mV.

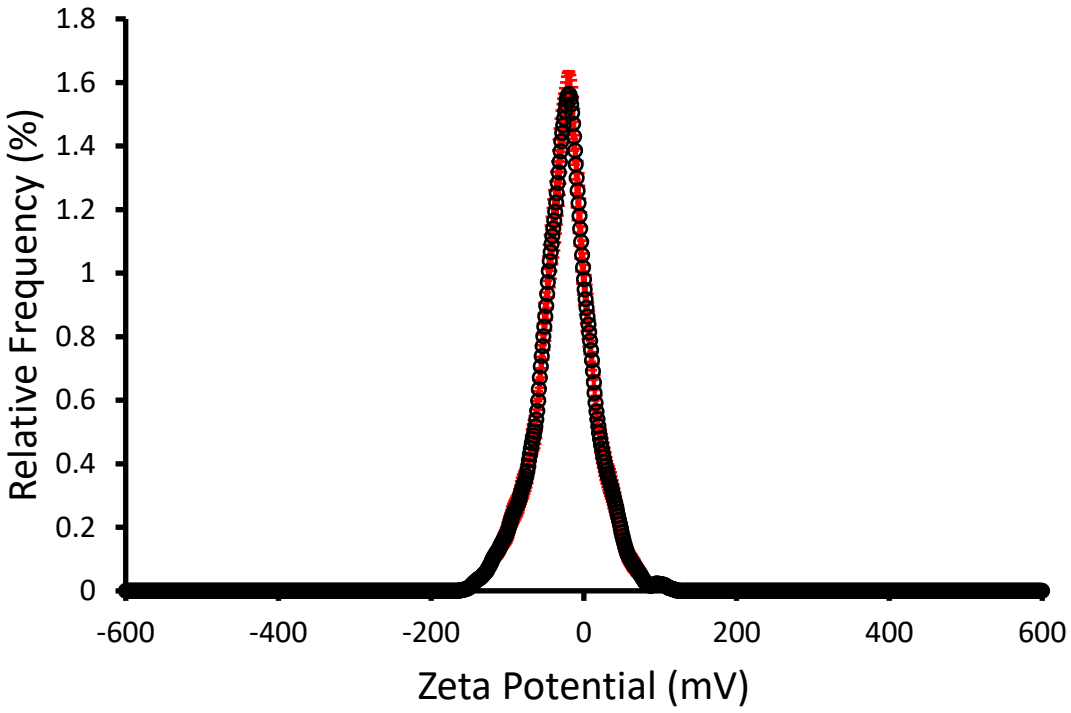

Figure S106 - The average zeta potential distribution calculated using 10 runs for **3 + 7** (5.56 mM) in an EtOH/H_2O 1:19 solution at 298 K. Average measurement value -24.40 mV.

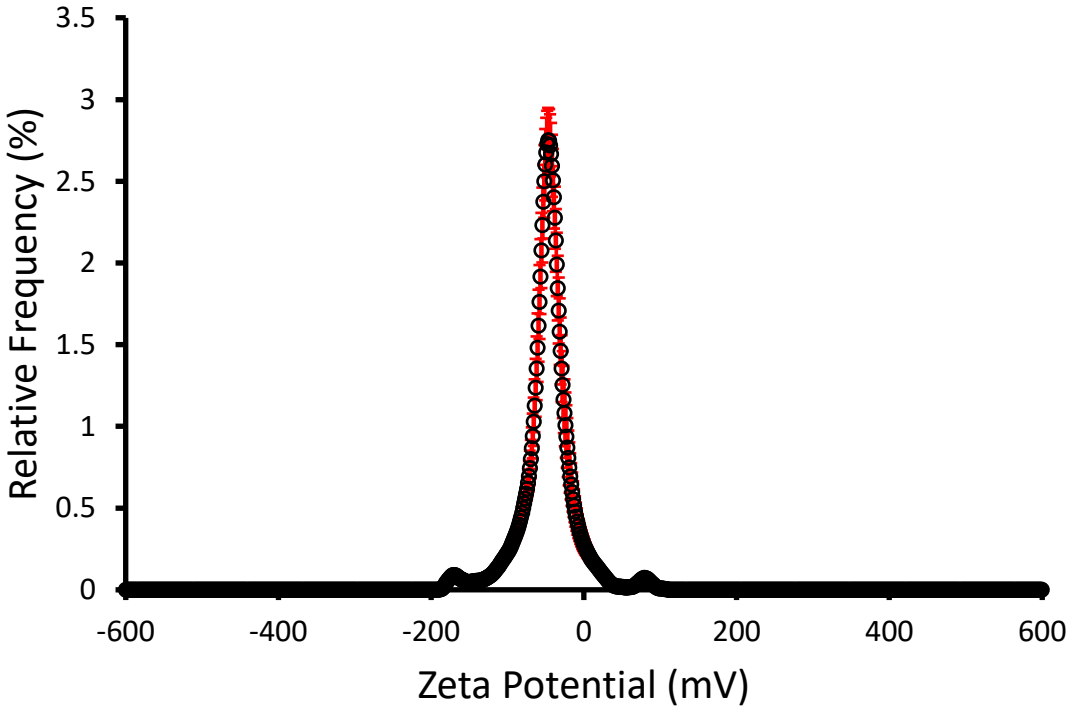

Figure S107 - The average zeta potential distribution calculated using 10 runs for **5 + 7** (5.56 mM) in an EtOH/H_2O 1:19 solution at 298 K. Average measurement value -32.99 mV.

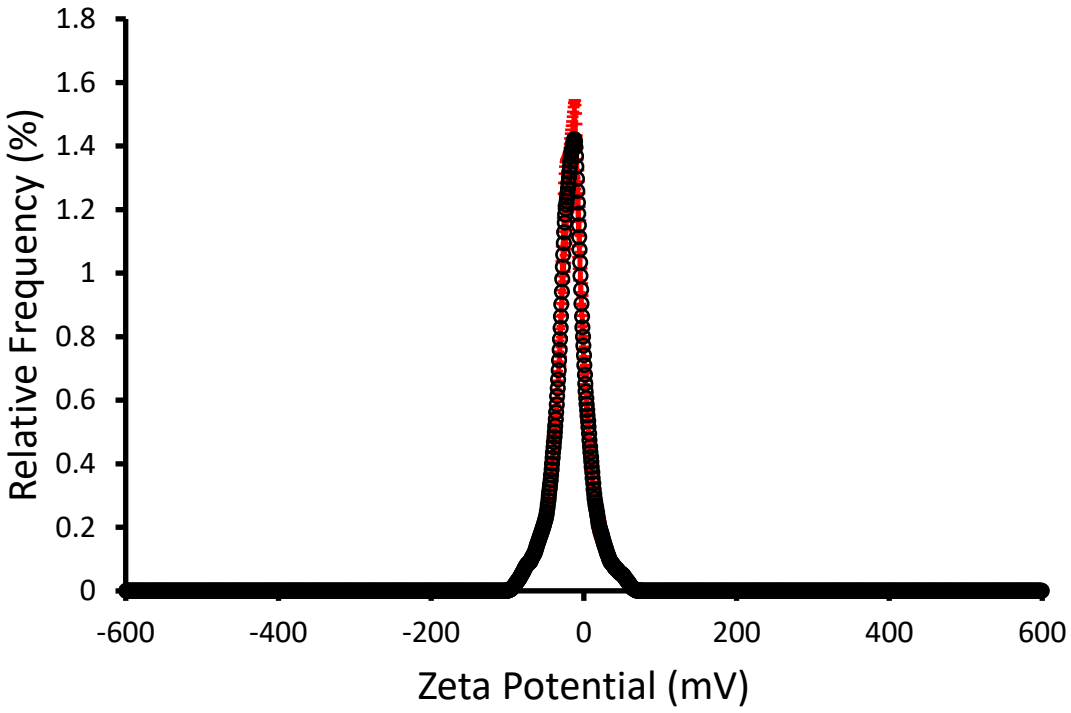

Figure S108 - The average zeta potential distribution calculated using 10 runs for **1 + 8** (5.56 mM) in an EtOH/H_2O 1:19 solution at 298 K. Average measurement value -14.54 mV.

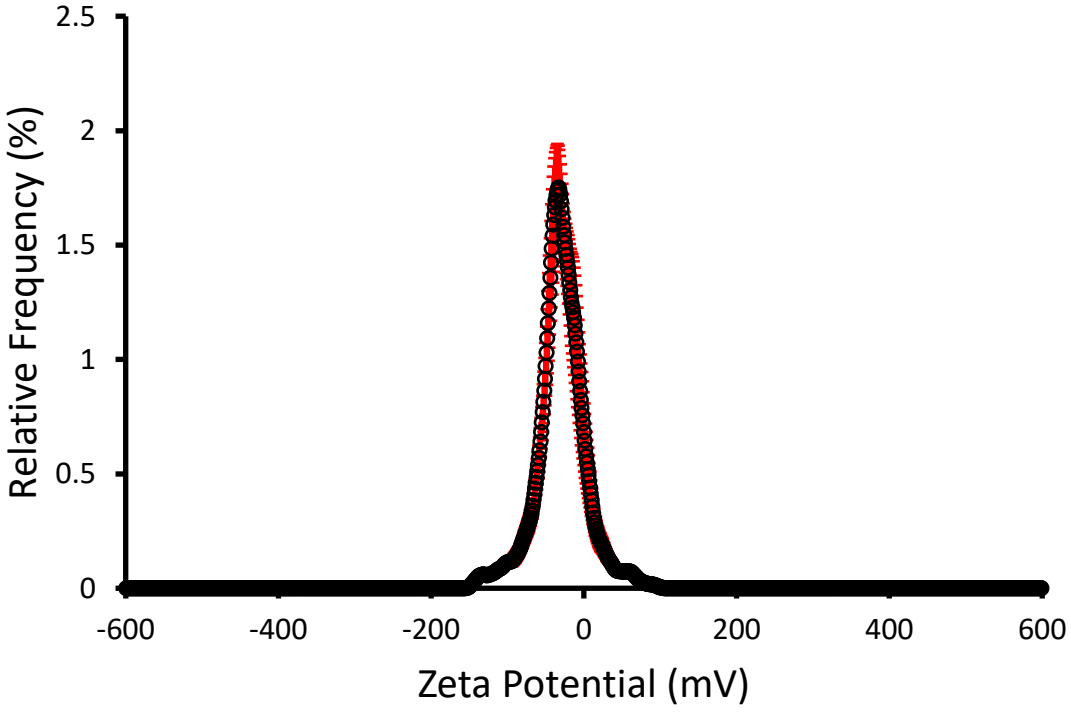

Figure S109 - The average zeta potential distribution calculated using 10 runs for **2 + 8** (5.56 mM) in an EtOH/H_2O 1:19 solution at 298 K. Average measurement value -40.43 mV.

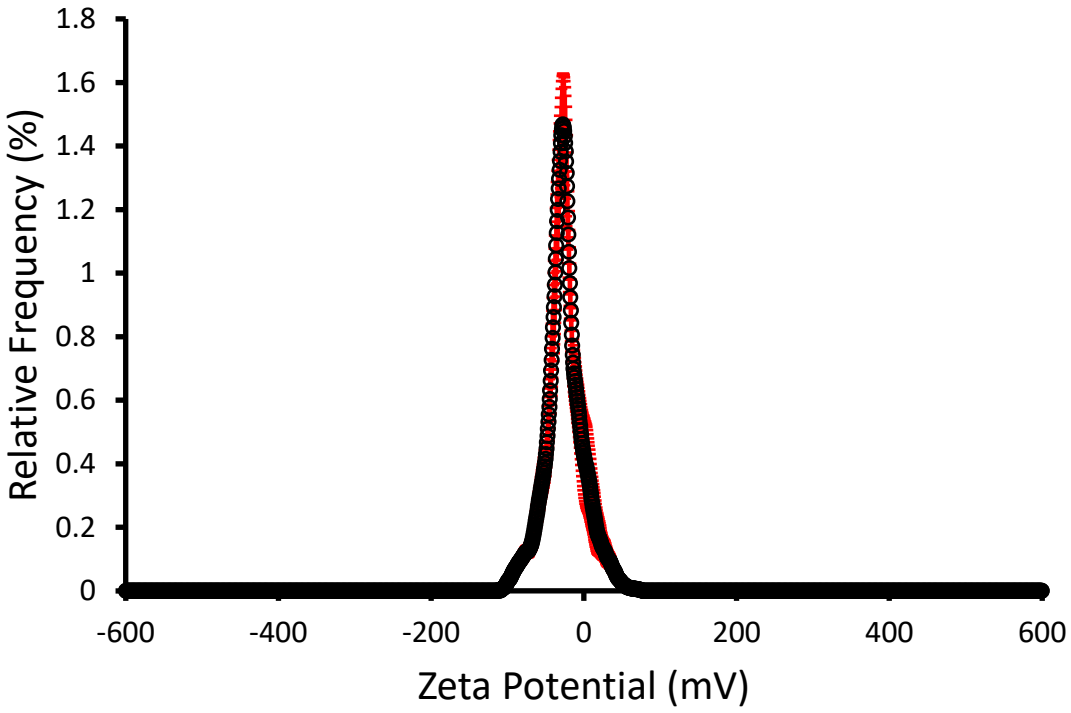

Figure S110 - The average zeta potential distribution calculated using 10 runs for **3 + 8** (5.56 mM) in an EtOH/H_2O 1:19 solution at 298 K. Average measurement value -27.90 mV.

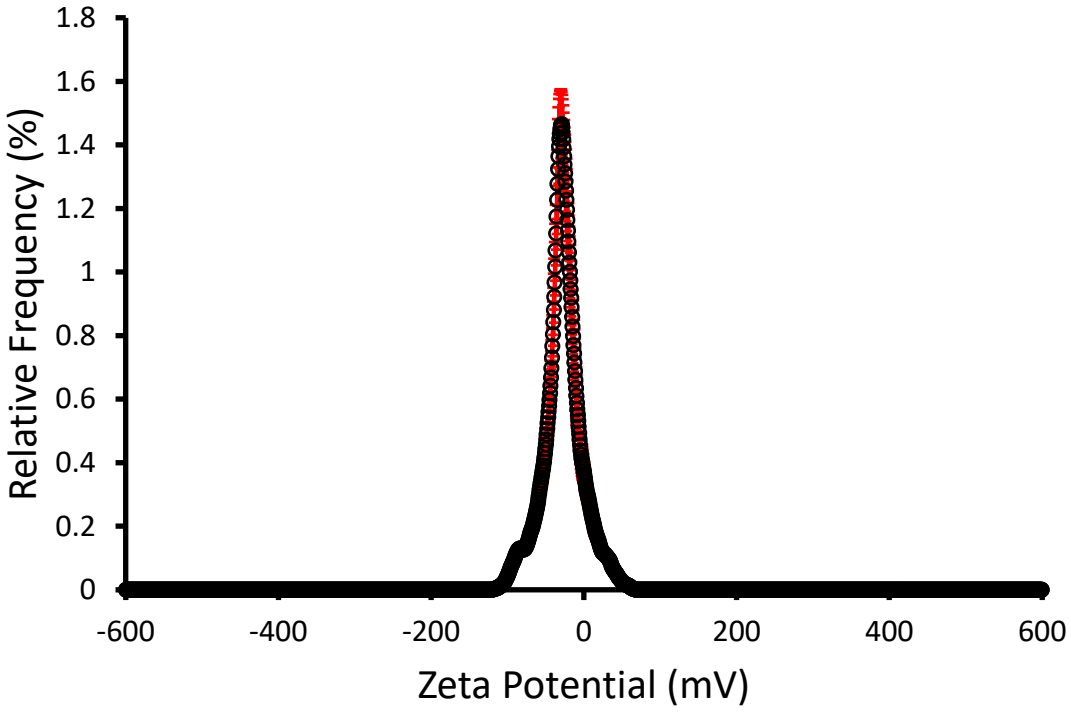

Figure S111 - The average zeta potential distribution calculated using 10 runs for **5 + 8** (5.56 mM) in an EtOH/H_2O 1:19 solution at 298 K. Average measurement value -32.48 mV.

Surface tension and critical aggregation concentration CAC determination

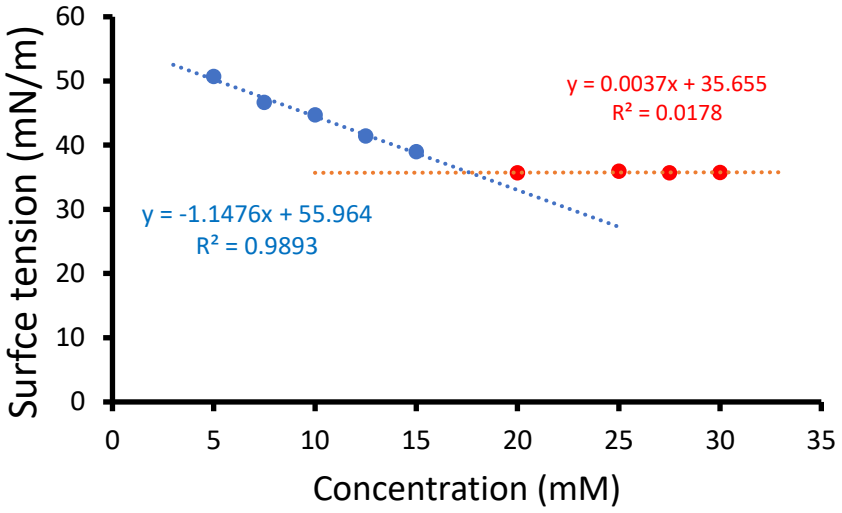

Figure S112 - Calculation of CAC (17.64 mM) for compound **4** in an EtOH/H_2O 1:19 mixture using surface tension measurements.

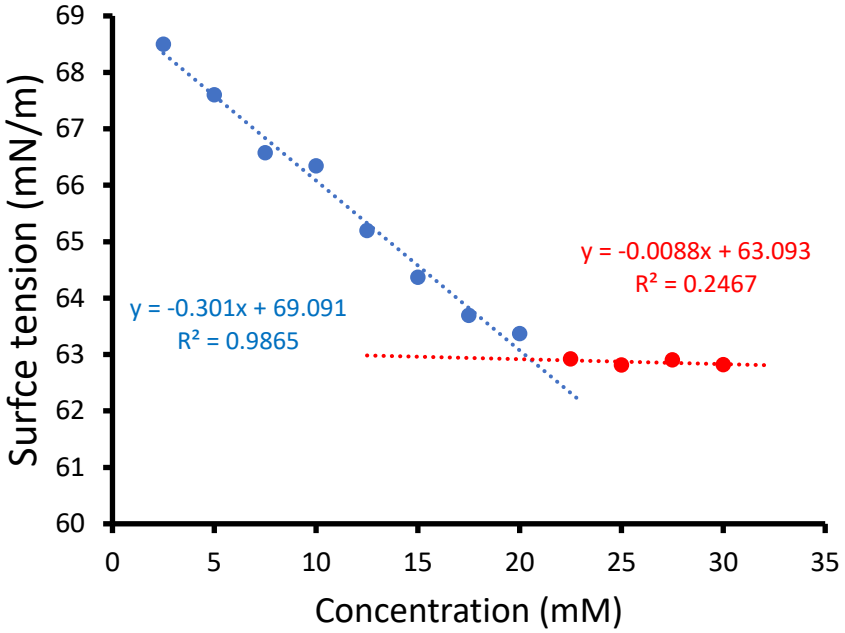

Figure S113 - Calculation of CAC (20.53 mM) for compound **5** in an EtOH/H_2O 1:19 mixture using surface tension measurements.

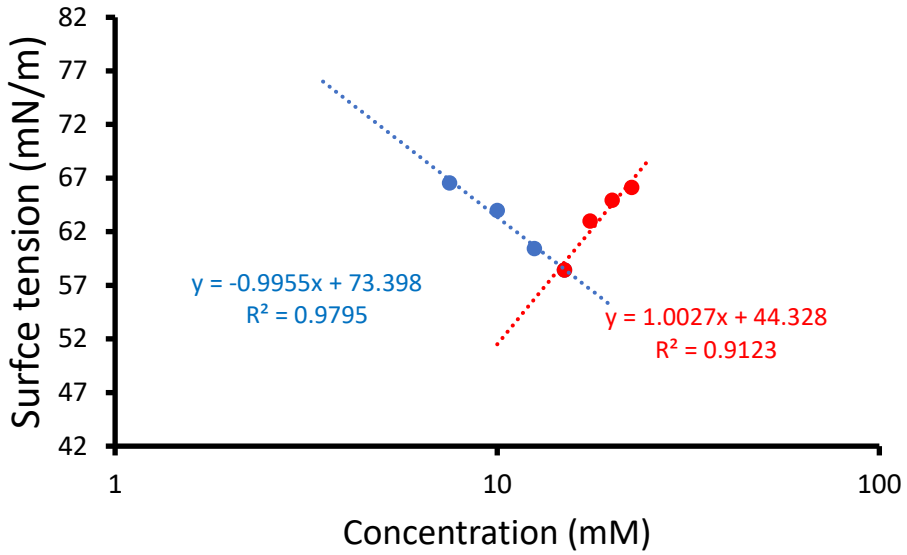

Figure S114 - Calculation of CAC (14.55 mM) for compound **3** in an EtOH/H_2O 1:19 mixture using surface tension measurements.

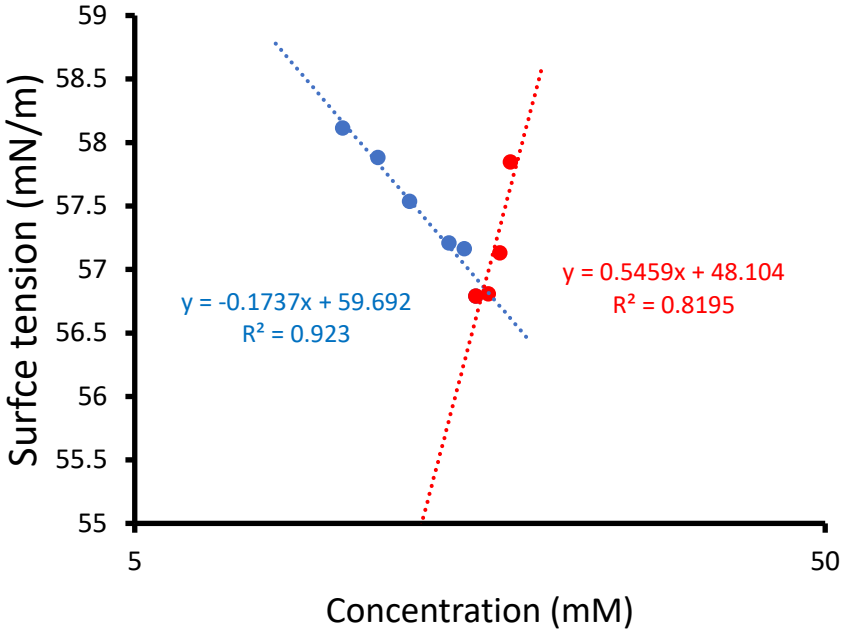

Figure S115 - Calculation of CAC (16.10 mM) for compound **Co-formulation *c*** in an EtOH/H_2O 1:19 mixture using surface tension measurements.

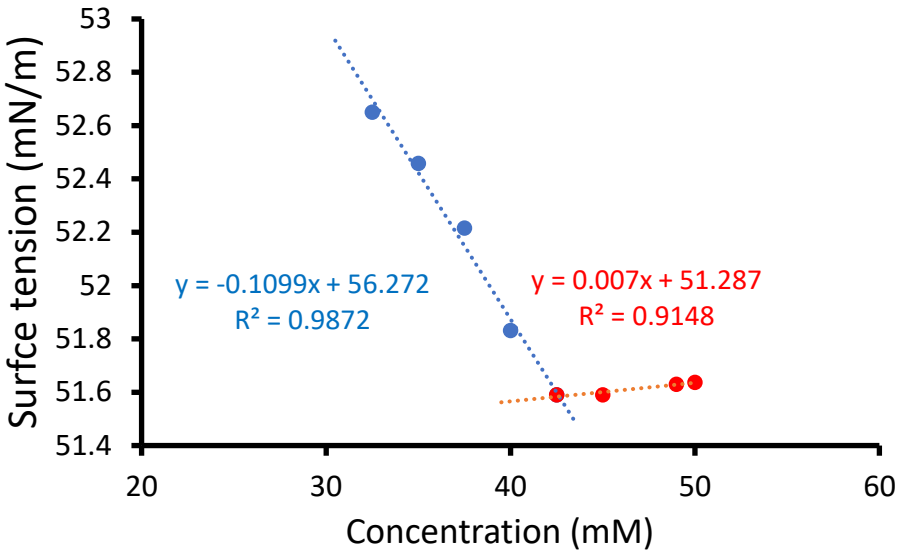

Figure S116 - Calculation of CAC (43.44 mM) for compound **Co-formulation *g*** in an EtOH/H_2O 1:19 mixture using surface tension measurements.

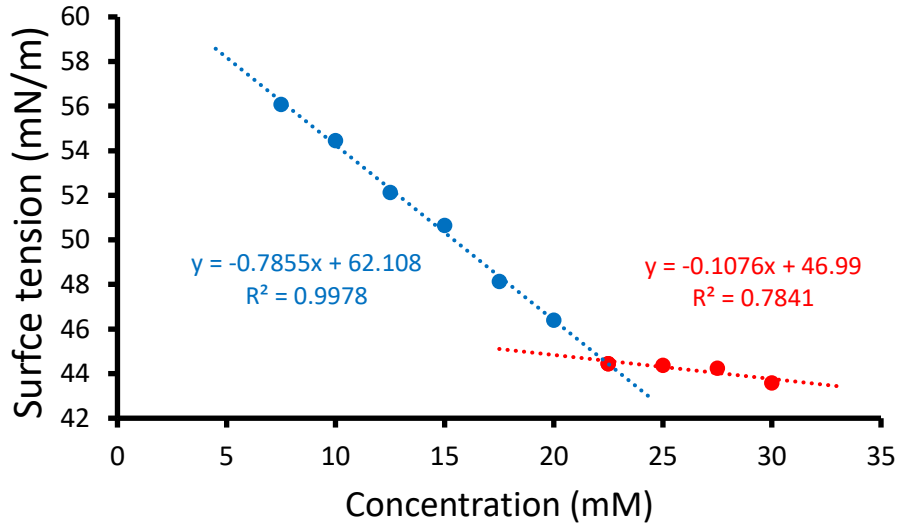

Figure S117 - Calculation of CAC (21.38 mM) for compound **Co-formulation *i*** in a H_2O solution using surface tension measurements.

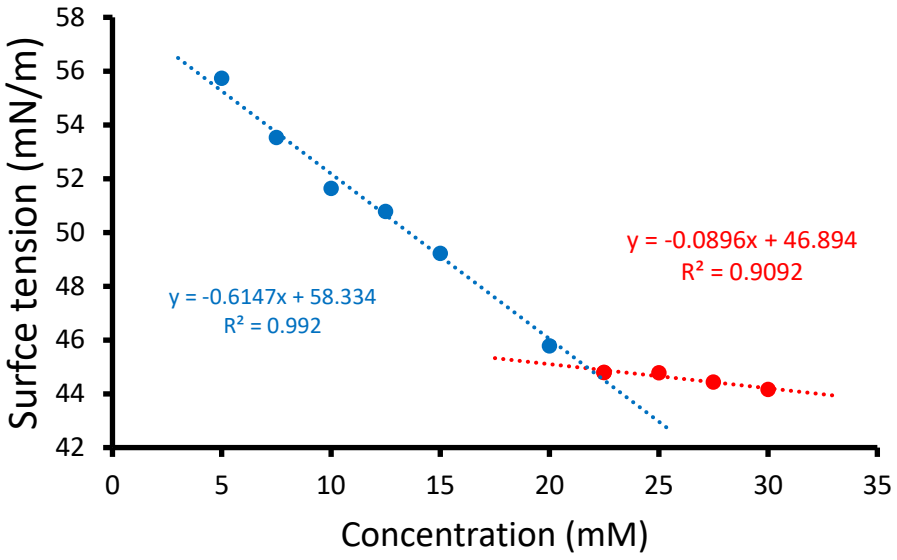

Figure S118 - Calculation of CAC (22.30 mM) for compound **Co-formulation *j*** in a H_2O solution using surface tension measurements.

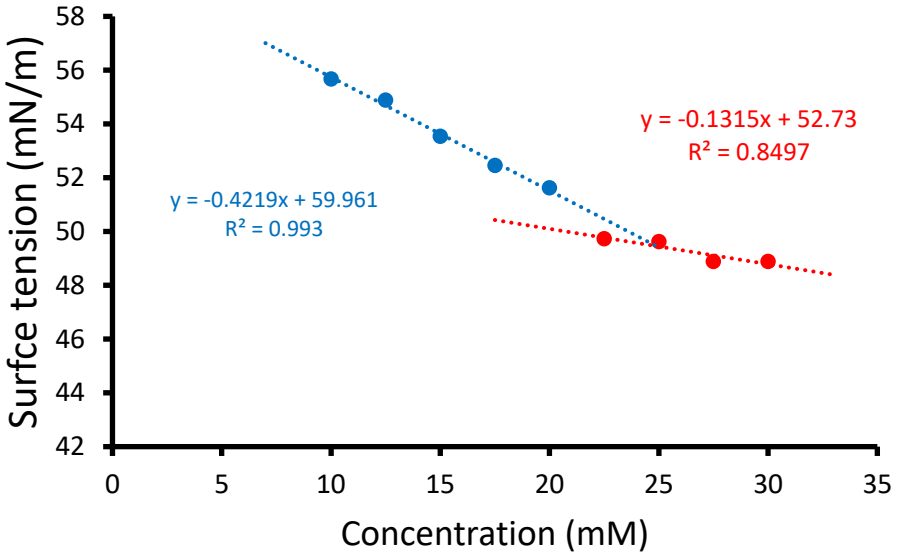

Figure S119 - Calculation of CAC (22.04 mM) for compound **Co-formulation *k*** in a H_2O solution using surface tension measurements.

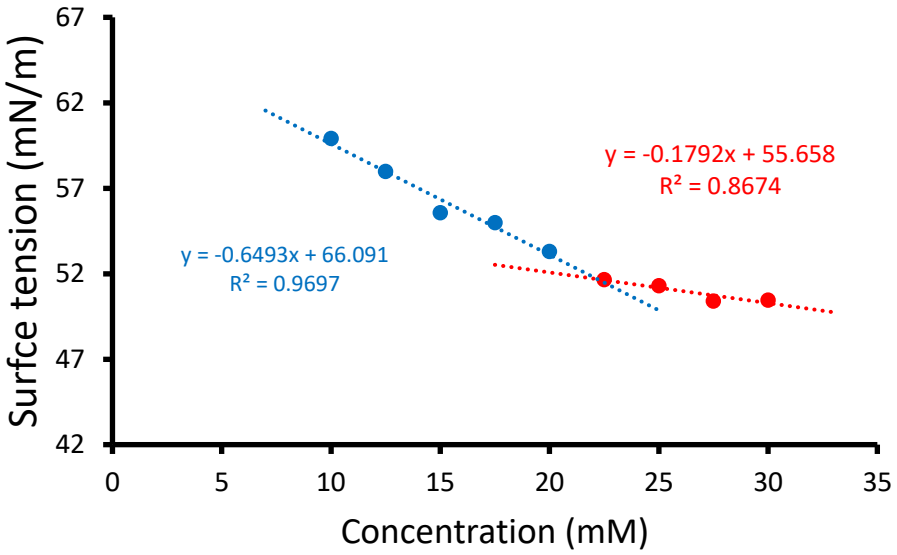

Figure S120 - Calculation of CAC (22.45 mM) for compound **Co-formulation *I*** in a H_2O solution using surface tension measurements.

Table S2 - Summary of zeta potential at 5.56 mM, CAC and surface tension at CAC. Data obtained in an EtOH/H_2O 1:19 solution.

Compound/ Co-formulation	CAC (mM)	Surface tension at CAC (mN/m)
1	a [1]	N/A[1]
2	35.27[2]	32.21[2]
3	14.55	58.92
4	17.64	35.72
5	20.53	62.91
a	a [2]	N/A[2]
b	19.87[2]	37.95[2]
c	16.10	56.89
d	a	N/A
e	a	N/A
f	a	N/A
g	42.64	51.59
h	a	N/A
i	22.30	44.59
j	21.79	44.94
k	24.90	49.46
l	22.19	51.68

a – could not be determined due to compound solubility.

Single crystal X-ray structure data

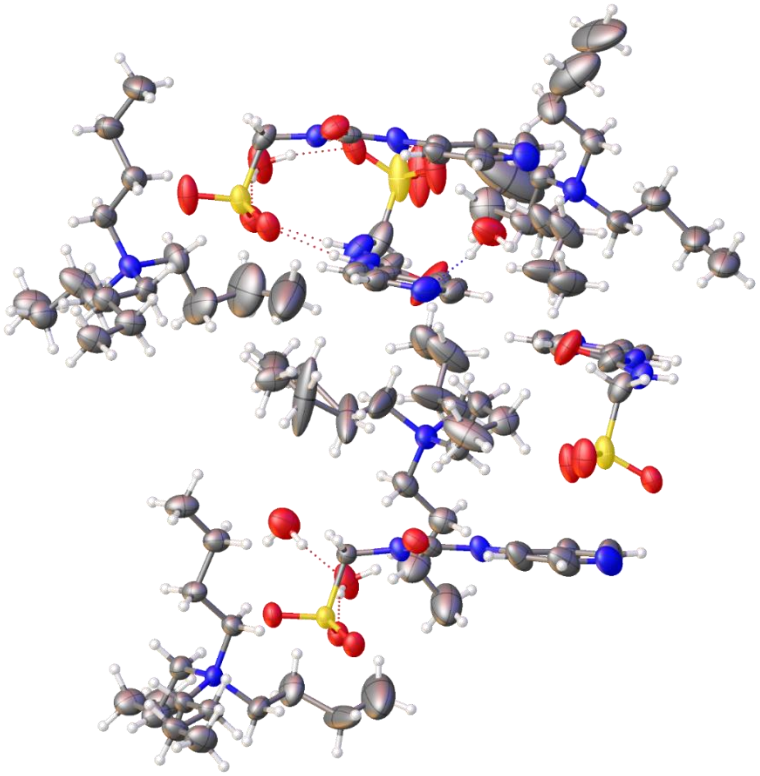

Figure S121 – Single crystal X-ray structure of **3**: red = oxygen; yellow = sulfur; blue = nitrogen; white = hydrogen; grey = carbon. CCDC 2108071, $C_{23}H_{46}N_4O_5S$ (M = 490.70): monoclinic, space group P 21/n, a = 19.4107(3) Å, b = 14.5657(2) Å, c = 38.5152(6) Å, α = 90°, β = 98.1706(15)°, γ = 90°, V = 10778.9(3) $Å^3$, Z = 16, T = 100(1) K, CuK\α = 1.5418 Å, Dcalc = 1.210 g/cm^3, 76889 reflections measured (7.616 ≤ 2Θ ≤ 133.202), 19035 unique (R_{int} = 0.0478**,** R_{sigma} = 0.0372) which were used in all calculations. The final R_1 was 0.1000 (I > 2σ(I)) and wR_2 was 0.2723 (all data).

Internal angle of dimerization: 22.9(3)° and 21.9(2)°.

Table S3 – Hydrogen bond distances and angles observed for **3**, calculated from the single crystal X-ray structure shown in Figure S121.

Hydrogen bond donor	Hydrogen bond acceptor	Hydrogen bond angle (D-H•••A) (°)	Hydrogen bond length (D•••A) (Å)
N1	O5	171.1(3)	2.941(5)
N2	O7	156.2(3)	2.868(6)
N4	O2	171.0(3)	2.985(6)
N5	O3	167.6(3)	2.812(6)
N7	O13	168.2(3)	3.013(5)
N8	O15	165.3(3)	2.839(5)
N10	O9	172.3(3)	2.943(5)
N11	O11	156.9(3)	2.872(6)
O17	O2	162.4(3)	2.825(5)
O17	O5	158.3(3)	2.689(5)
O18	O17	176.5(4)	2.805(6)
O18	N6	154.9(3)	2.929(6)
O19	O13	165.2(4)	2.866(5)
O19	O9	157.4(3)	2.713(5)
O20	O19	168.7(3)	2.817(6)
O20	N9	173.6(3)	2.900(6)

References

1 L. J. White, S. N. Tyuleva, B. Wilson, H. J. Shepherd, K. K. L. Ng, S. J. Holder, E. R. Clark and J. R. Hiscock, *Chem. Eur. J.*, 2018, **24**, 7761.

2 L. J. White, J. E. Boles, K. L. F. Hilton, R. J. Ellaby and J. R. Hiscock, *Molecules*, 2020, **25**, 4126.